UNIVERSITY OF CALIFORNIA, SAN DIEGO

The role of ATP release and autocrine/paracrine P1/P2 receptor signaling in the modulation of neutrophil chemotaxis

A dissertation submitted in partial satisfaction of the requirement for the degree Doctor of Philosophy

in

Biomedical Sciences

by

Ross Corriden

Committee in charge:

Professor Paul A. Insel, Chair
Professor Timothy D. Bigby
Professor James R. Feramisco
Professor Tracy M. Handel
Professor Victor Nizet

2008

The Dissertation of Ross Corriden is approved, and it is acceptable in quality and form for publication on microfilm and electronically:

Chair

University of California, San Diego

2008

DEDICATION

This dissertation is dedicated to my parents and brother, who have provided me invaluable support during the last five plus years of my life.

TABLE OF CONTENTS

LIST OF FIGURES

LIST OF TABLES

ACKNOWLEDGEMENTS

I would like to thank the chair of my committee, Professor Paul Insel, for all of his support and guidance over the last few years. His advice has been invaluable and has undoubtedly contributed to my success. I'd also like to thank Dr. Wolfgang Junger for hosting me in his lab and enabling me to work on this project. In addition I want to thank my thesis committee members, Professors Timothy Bigby, James Feramisco,, Tracy Handel and Victor Nizet for all of their help during this process.

Finally I'd like to thank my friends and family, in particular my parents, for all of their support over the years. Without them, this wouldn't have been possible.

Chapter 4, in full, is a reprint of the material as it appears in the American Journal of Physiology – Cell Physiology, October 2007, Corriden, Ross; Insel, Paul A.; Junger, Wolfgang G.; 293(4):C1420-5. The dissertation author was the primary investigator and author of this paper.

Chapter 5, in full, is a reprint of the material as it appears in Science, December 2006, Corriden, Ross*; Chen, Yu*; Inoue, Yoshiaki; Yip, Linda; Hashiguchi, Naoyuki; Zinkernagel, Annelies; Nizet, Victor; Insel, Paul A.; Junger, Wolfgang G.; Dec 15;**314**(5816):1792-5. The dissertation author was one of two co-primary investigators and authors of this paper (*co-first author credit given).

Chapter 6, in full, is a reprint of the material as it appears in the Journal of Biological Chemistry, August 2008, Corriden, Ross; Chen, Yu; Inoue, Yoshiaki; Beldi, Guido; Robson, Simon; Insel, Paul A.; Junger, Wolfgang G. (Epub ahead of print) . The dissertation author was the primary investigator and author of this paper.

VITA

2001	Bachelor of Science, Biochemistry and Molecular Biology, University of California, Santa Cruz
2002-2008	Research Assistant, University of California, San Diego
2008	Teaching Assistant, Department of Biology University of California, San Diego
2008	Doctor of Philosophy, Biomedical Science, University of California, San Diego

PUBLICATIONS

Corriden , Ross*; Chen, Yu*; Inoue, Yoshiaki; Yip, Linda; Hashiguchi, Naoyuki; Zinkernagel, Annelies; Nizet, Victor; Insel, Paul A.; Junger, Wolfgang G.. "ATP release guides neutrophil chemotaxis via P2Y2 and A3 receptors", *Science*. 2006 Dec 15;**314**(5816):1792-5. (*both authors contributed equally to this work)

Corriden, Ross; Insel, Paul A.; Junger, Wolfgang G.. "A novel method using fluorescence microscopy for real-time assessment of ATP release from individual cells", *Am J Physiol Cell Physiol*. 2007 Oct; **293**(4):C1420-5.

Corriden R, Chen Y, Inoue Y, Beldi G, Robson S, Insel PA, Junger WG. ECTO-nucleoside triphosphate-diphosphohydrolase 1 (E-NTPDASE1/CD39) regulates neutrophil chemotaxis by hydrolyzing released ATP to adenosine. *J Biol Chem*. 2008 Aug 19. [Epub ahead of print]

FIELDS OF STUDY

Major Field: Biomedical Sciences (Pharmacology/Immunology)

Studies in Pharmacology
Professor Paul A. Insel

Studies in Immunology
Professor Wolfgang G. Junger

ABSTRACT OF THE DISSERTATION

The role of ATP release and autocrine/paracrine P1/P2 receptor signaling in the modulation of neutrophil chemotaxis

by

Ross Corriden

Doctor of Philosophy in Biomedical Sciences

University of California, San Diego, 2008

Professor Paul. A. Insel, Chair

Polymorphonuclear leukocytes (neutrophils) utilize an extremely sensitive chemosensory system to detect and migrate towards invading pathogens and damaged

tissues in many species, including humans. Chemoattractants, chemical compounds released by such targets, bind to receptors on the neutrophil cell membrane and activate signal transduction cascades that promote directional migration. Neutrophils are capable of correctly orienting themselves in fields of chemoattractant as shallow as 1% across the length of the cell body. To maintain correct polarity in such shallow chemoattractant fields, the cells must be able to amplify these external signals.

In this dissertation, ATP is identified as an autocrine/paracrine modulator of neutrophil chemotaxis. In response to stimulation with chemoattractants, neutrophils release ATP into the extracellular space. A novel assay for extracellular ATP was developed and reveals that ATP is released predominantly at the leading edge of stimulated neutrophils. Neutrophils rapidly metabolize released ATP, ultimately to adenosine. Elimination of extracellular ATP or adenosine inhibits chemotaxis, revealing that both compounds play a critical role in this process. Release of ATP at the leading edge establishes polarity in chemoattractant fields through the activation of P2Y2 receptors. Extracellular adenosine drives forward movement by activating A3 adenosine receptors, which localize at the leading edge of migrating cells. The hydrolysis of ATP (and generation of adenosine) is facilitated by ecto-nucleoside triphospho-dihydrolase 1 (E-NTPDase1/CD39), which is also localized at the leading edge. Inhibition of any of these steps leads to aberrant cell migration, revealing a novel autocrine/paracrine signal amplification system in neutrophils that is critical for chemotaxis.

Chapter 1: Thesis Synopsis

Background/Significance

The ability of neutrophils to infiltrate through the vascular endothelial layer of blood vessels and migrate to infected or damaged tissues is critical for their function in the inflammatory process (1). The process by which neutrophils detect, and direct their movements in response to, chemical compounds released by pathogens and damaged tissues (chemoattractants) is called chemotaxis. Neutrophils utilize an extremely sensitive chemosensory system in this process that enables them to respond to chemoattractant gradients as shallow as 1% from the leading edge to the trailing edge of the cell body (2). In order to effectively migrate in such shallow gradients, neutrophils must possess mechanisms that amplify chemoattractant signals and define intracellular polarity (3). However, until recently no such mechanisms have been definitively identified.

Hypertonic saline, a resuscitation solution that improves organ function and recovery following trauma, causes a release of ATP from neutrophils (4). The released ATP stimulates neutrophil function, which can be blocked by treatment with P2 nucleotide receptor antagonists, suggesting that these receptors regulating neutrophil physiology. Other studies reveal that neutrophils release ATP in response to treatment with the chemoattractant formyl-Met-Leu-Phe and that neutrophils hydrolyze released ATP to generate adenosine, which has been implicated as a regulator of neutrophil

function via the activation of P1 receptors (5). Taken together, these data suggested that release of ATP, ATP conversion to adenosine, and autocrine/paracrine activation of P1 and P2 receptor, signaling contribute to neutrophil chemotaxis and provide a mechanism for polarity in neutrophils and for amplification of chemoattractant gradients to which neutrophils respond.

Hypothesis: Extracellular ATP and adenosine facilitate chemotaxis and activation of polymorphonuclear leukocytes (PMN) by stimulation of P2 receptors and P1 receptors, respectively, such that receptors that stimulate migration and activation of PMN are trafficked to the leading edge.

Specific Aims

1) **Develop and optimize an assay that allows real-time detection and quantification of ATP release from migrating PMN.**
2) **Determine the expression levels, distribution and functional roles of key P1 and P2 receptors in migrating PMN.**
3) **Determine which ecto-ATPases are responsible for the hydrolysis of extracellular ATP (to adenosine) and evaluate their expression levels, distribution and functional role in chemotaxis.**

Overview/Brief summary of data chapters

There are three main parts to this work, presented in chapters 4-6, which were published at the time of writing this thesis. Chapters 2 and 3 are reviews of literature in the fields of neutrophils chemotaxis and autocrine/paracrine nucleotide signaling, respectively. Chapter 7 is a discussion of the results that were a product of work on this

thesis project. The key ideas and results from the data chapters (chapters 4-6) are summarized below.

Chapter 4

Chapter 4 describes the development of a NADPH-based assay for the visualization of extracellular ATP, The assay utilizes the Hexokinase/Glucose 6-phosphate dehydrogenase reaction that consumes ATP and produces NAPDH, a fluorophore. When these two enzymes plus NADP are added to media in which cells are bathed, released ATP drives production of NADPH, which thus acts as a probe for ATP. Using the correct optical filters, one can visualize NADPH using a microscope. When treated with known stimulants of ATP release, extracellular regions of increased fluorescence intensity can be visualized, quantified and correlated to known ATP concentrations.

Chapter 5

Chapter 5 elucidates the role of ATP release and P1/P2 receptor activation in neutrophil chemotaxis. Using the NADPH-based visualization assay described in chapter 4, polarized release of ATP can be detected at the leading edge of neutrophils in a chemoattractant gradient. Elimination of extracellular ATP with the enzyme apyrase or removal of extracellular adenosine with the enzyme adenosine deaminase inhibits cell migration. Treatment of neutrophils with a specific antagonist of the A3 adenosine receptor also inhibits chemotaxis. This receptor localizes at the leading edge of migrating, neutrophil-like HL-60 cells transfected with an A3-EGFP construct. Microscope-based studies reveal that inhibition of the A3 receptor does not affect directionality but greatly reduces cell speed. Disruption of P2Y2 ATP receptor signaling, however, impairs directionality. Extracellular ATP therefore modulates neutrophil migration in an

autocrine fashion, establishing polarity by activating P2Y2 receptors and, after conversion to adenosine, promoting forward movement by activating A3 receptors.

Chapter 6

Chapter 6 identifies which ecto-ATPase that is expressed by neutrophils is responsible for hydrolysis of extracellular ATP. Neutrophils rapidly hydrolyze extracellular ATP. Through inhibitor studies and analysis of the kinetics of ATP breakdown, I determined that the primary ecto-ATPase responsible for this action is E-NTPDase1 (CD39). Inhibition of E-NTPDase1 prevents this hydrolysis and impairs neutrophil migration. HL-60 cells transfected with a E-NTPDase1-EGFP construct localize this ecto-ATPase at the leading edge of migrating cells. Neutrophils isolated from E-NTPDase1/CD39 knockout mice show impaired migration, which confirms the role of this ecto-ATPase in migration.

Chapter 2: Background: Neutrophil Chemotaxis

Introduction and History

Chemotaxis is the process by which cells direct their movement based on chemical cues detected in their environment. A wide variety of cell types exhibit chemotactic activity and a diverse array of mechanisms are utilized that facilitate movement (1). Review of the literature reveals that the chemotactic activity of polymorphonuclear leukocytes (neutrophils), the primary phagocytic leukocyte of the innate immune system, is one of the most extensively studied examples of this process. Neutrophils rapidly migrate towards bacteria and can move at speeds ranging from 15-30 um per minute (i.e, up to several-times greater than their diameter (2,3)). In addition to being able to migrate at rapid speeds, neutrophils utilize an extremely sensitive chemosensory system that allows them to detect and correctly polarize in chemical gradients as shallow as 1% across the length of the cell (4).

Advances in our understanding of neutrophil chemotaxis have closely paralleled improvements in technology. The first time-lapse images of neutrophils migrating towards bacteria were captured by Jean Comandon in 1919 (5), providing visual evidence of directed cell migration. A lack of cost-effective, facile, reproducible methods hampered the field until the introduction of the Boyden Chamber technique, which is still

in use today (6). This technique, in which neutrophils are placed in one of two chambers separated by a porous filter that actively migrating cells must penetrate, enabled the identification of chemoattractants, including the bacteria-derived N-formyl peptides (7,8,9). Subsequent advances in molecular biology led to the cloning of receptors for the formyl peptide (FRP) and other chemoattractants, e.g. C5a (C5AR), and IL-8 (10-16). More recently the introduction of fluorescent protein technology enabled the study of signaling molecule/protein localization in migrating cells (17); however, the relatively short lifespan of isolated neutrophils limits their usefulness in these types of experiments. For this reason, HL-60 cells, a human leukemia cell line that can be differentiated into neutrophil like cells that migrate towards chemoattractants, have emerged as a highly useful system for studies of neutrophil function and of subcellular localization of components involved in cell migration (18). These advances have all helped further understanding of the molecular machinery and events that drive chemotaxis. The mechanisms by which neutrophils respond to changing environments and are properly polarized in extremely shallow chemoattractant gradients (i.e. the 'compass'), however, has remained unidentified. In this chapter I will review what is known about the mechanisms that drive chemotaxis and introduce the idea of an extracellular compass guided by autocrine/paracrine ATP signaling.

The formation of a cell 'front' and 'back' during chemotaxis

Neutrophils respond to chemoattractant gradients by rapidly adopting a 'front' or 'leading edge' (pseudopod) and a 'back' or 'trailing edge' (uropod) (4,19-22) These

polarized ends are characterized by an accumulation of F-actin at the leading edge and contractile actin-myosin complexes at the trailing edge, effects achieved by polarized activation of Rho small GTPases, which promote actin polymerization or formation of actin-myosin complexes (23,24). The following section reviews the signaling events that drive these two pathways. Since there is often a considerable difference in chemotaxis signaling cascades between different cell types, I have only included pathways that have been clearly demonstrated in neutrophils or the neutrophil-like HL-60 cells.

Signaling at the leading edge

At the leading edge of neutrophils, localized activation of PI3Kγ is the primary mechanism that facilitates actin polymerization/forward movement (25). Activation of heterotrimeric G protein-coupled chemoattractant receptors leads to dissociation of G proteins into G_i and Gβγ subunits. The Gβγ subunit binds to and activates PI3Kγ, which in turn leads to the conversion of PtdIns(4,5)P3 to PtdIns(3,4,5)P3 (26) at the leading edge of PMN. Proteins that contain Plekstrin homology (PH) domains can bind to the PtdIns(3,4,5)P3 lipids with high affinity (27,28), In neutrophil chemotaxis, one of the most important PH domain containing proteins is the cdc42 guanine exchange factor (GEF) PIX (27). PtdIns(3,4,5)P3 binding activates PIX, which facilitates the exchange of GTP for GDP on cdc42.

Cdc42 promotes actin polymerization at the leading edge through a pathway that involves Arp2/3 (Actin related protein 2/3), a complex of those two proteins (30). Arp2/3 binds to the slow polymerizing, pointed ends of actin filaments, stabilizing them and

thereby inducing polymerization (31). Though uniformally distributed in the cell under basal conditions, Arp2/3 are redistributed to the leading edge in response to chemoattractant stimulation (32). Cdc42 stimulates the actin polymerization activity of Arp2/3 via a third protein, N-Wasp (33). Cdc42GTP binds to and activates N-Wasp, which in turn binds to and activates Arp2/3 (34). Continual generation of PtdIns(3,4,5)P3 during chemotaxis drives this process and results in forward movement of the leading edge.

Signaling at the trailing edge

In order to facilitate retraction of the uropod in migrating cells and promote net forward movement, the cytoskeletal composition of the sides and trailing edge of the cells must differ significantly from the leading edge. The mechanism involves the contraction of localized actin/myosin II complexes, which pull the back portion of the cell forward (35, 36). Perhaps as importantly as retraction of the uropod, cells must have a system in place that prevents the formation of multiple pseudopods. Based on evidence found in the slime mold Dictyostelium discoideum (a model for studying cell migration), the phosphate and tensin homolog (PTEN) was the primary candidate for establishing 'back-ness' in human neutrophils (37). PTEN, an inositolphosphate dephosphorylase, has the opposite effect of PI3K, converting PtdIn(3,4,5)P3 to PtdIns(4,5)P2 (38). This action would prevent the localized activation of PH domain-containing GEFs until a sufficient level of chemoattractant stimulation and PI3K activation overcome the inhibition to form a leading edge. Studies performed on neutrophils isolated from PTEN-knockout mice,

however, have produced conflicting results with some reports showing significant decreases in migration efficiency in the knockouts compared to wild-type cells (37) while others show negligible differences (39). Other data demonstrate either a polarized distribution of PTEN (37) or no distinguishable polarization (40) at the trailing edge of migrating cells. In addition, a recent study demonstrated that PtdIns(4,5)2, the product of PTEN dephosphorylation, localizes to the leading edge of HL60 cells in a manner similar to that of PtdIns(3,4,5)P3, suggesting that PTEN activity may not be the sole or dominant mechanism of polarization (41). Thus, while PTEN is likely involved in neutrophil chemotaxis, the extent of its role in determining cell polarity is a source of controversy.

Some recent studies suggest that the Src homology 2-containing inositol 5' phosphate 1 (SHIP1) is the neutrophil analog of Dictyostelium discoideum PTEN. SHIP 1 dephosphorylates PtdIns(3,4,5)P3 to PtdIns(3,4)P2 (42,43,44), which results in inhibition of PH domain-containing proteins (45). A study using GFP-tagged PH domain fusion proteins demonstrated that SHIP1 activity can selectively degrade PtdIns(3,4,5)P3 at the trailing edge and sides of neutrophils (39). The same study showed that neutrophils isolated from SHIP1-KO mice have significantly impaired polarization in response to chemoattractant stimulation. While such data imply that SHIP1 is a critical modulator of cell polarity, the cellular distribution of SHIP1 during chemotaxis is not known.

In addition to inhibiting PtdIns(3,4,5)P3-stimulated actin polymerization, neutrophils preferentially activate actin/myosin complex formation and contraction at the trailing edge. RhoA, a Rho GTPase that regulates the actin cytoskeleton via the Rho-dependent kinase p160-ROCK (46,47), is highly expressed in neutrophil-like HL-60 cells (48). RhoA is activated by the G_{12} subunit, in a pathway which requires the guanine

exchange factor p115-GEF (50). RhoA localizes to the trailing edge of HL-60 cells (40). The latter study showed that inhibition of either p160-ROCK or myosin II results in the formation of multiple pseudopods in chemoattractant-stimulated cells, suggesting the existence of a self-potentiating feedback loop to prevent pseudopod formation and promote retraction of the trailing edge.

The cAMP/PKA pathway is another regulator of chemotaxis. Chemoattractant stimulation can increase intracellular cAMP levels (50-55) and increases in cAMP levels inhibit neutrophil migration (56-58). Chemoattractant-stimulated regulation of adenylyl cyclase activity seems to be G_i mediated (55). The cAMP signaling pathway has been directly connected to cell polarization by evidence indicating that PKA activity is necessary for chemoattractant-induced polarization, and that even in the absence of chemoattractant a PKA inhibitor gradient can induce polarization in human neutrophils (59). The mechanisms that mediate such effects remain to be elucidated.

Uncovering an extracellular compass for neutrophil migration

The preceding section summarized the machinery involved in promoting actin polymerization at the leading edge and actin/myosin contraction at the trailing edge of migrating neutrophils (summarized in figure 1). It is clear that the two poles of a migrating cell show drastically different localized physiologies. How does a cell determine, though, where each of these two different poles should form when activated by a single type of receptor (i.e. the chemoattractant receptor)? When considering the answer to this question, two important facts must be kept in mind:

1) Chemoattractant receptors are uniformly distributed on the neutrophil cell membrane, even when cells are polarized and migrating (60).
2) Neutrophils that are exposed to a uniform concentration of chemoattractant (i.e. no gradient) are still capable of forming a leading and trailing edge.

In the presence of a uniform concentration of chemoattractant, why do the cells not form multiple pseudopods? Similarly, what prevents the formation of multiple pseudopods when the cells are moving within a chemoattractant gradient even though the sides and back of the cell are exposed to continually increasing concentrations of chemoattractant? In other words, how is polarity both established and maintained during chemotaxis?

Of all the messengers/effectors involved in neutrophil chemotaxis, the evidence pointing to PtdIns(3,4,5)P3 as an intracellular regulator of polarity is strongest (26). Based on the importance of localized PtdIns(3,4,5)P3 signaling in neutrophils, a simple model can be proposed to explain migration in a chemoattractant gradient (figure 2a). In this model, stimulation of chemoattractant receptors on one side of the cell leads to polarized activation of PI3Kγ and accumulation of PtdIns(3,4,5)P3, a local activator of migration. If only a small concentration of chemoattractant is present, such a cell could probably migrate, but in the presence of a higher concentration of chemoattractant, the formation of multiple pseudopods resulting from chemoattractant receptor activation on the sides and back of the cell might occur. Additionally, in the absence of a mechanism to

inhibit psuedopod formation, exposure to a uniform concentration of chemoattractant could potentially cause the cell to pull itself apart (figure 2b).

Such ideas emphasize how a global inhibitor of pseudopod formation might be necessary to help explain the specificity and directionality of chemotaxis in neutrophils. The global inhibitor could be represented by SHIP1, which converts PtdIns(3,4,5)P3 to PIP2, which would have an inhibitory effect on pseudopod formation (figure 2c). In the "global inhibition/local stimulation" model, PI3Kγ activity would have to achieve a local level sufficient to overcome the inhibition of SHIP1 inhibition in order to facilitate pseudopod formation (a notion similar to what occurs for the generation of action potentials, figure 2d). Such a mechanism might help prevent the formation of multiple pseudopods in the presence of a gradient of chemoattractant. If exposed to a high, uniform concentration of chemoattractant, however, the cells might damage themselves if the entire membrane were to seek to overcome inhibition of SHIP1 (figure 2e). Alternatively, if PI3Kγ activity was too 'dilute', no pseudopods would form and no migration would occur (figure 2f). However, a simple "global inhibition/local stimulation" model does not match with what is known about neutrophil behavior.

One potential way that cells could use to circumvent this problem is to polarize their chemosensory system. Such polarization would be consistent with observations that neutrophils usually turn to re-orient themselves in response to sudden changes in chemoattractant gradients rather than stopping and forming a new leading edge (61). Since chemoattractant receptors do not polarize even in migrating cells (60), for this model to be correct cells must secrete their own modulator of autocrine/paracrine chemotaxis that would activate receptors distinct from the chemotactic receptor (figure

2g).Ideally such a modulator would be readily available (e.g., plentiful in the cytosol to allow for sustained release), rapidly cleared to allow for fast adaptation to changing chemotactic signals, and have multiple receptor targets to activate the contrasting cytoskeletal components at the leading or trailing edge of the cells. A candidate molecule that fits all of these criteria is ATP, which work to be shown in this thesis will demonstrate is released from neutrophils upon chemoattractant stimulation. The following chapter provides background regarding autocrine/paracrine ATP signaling.

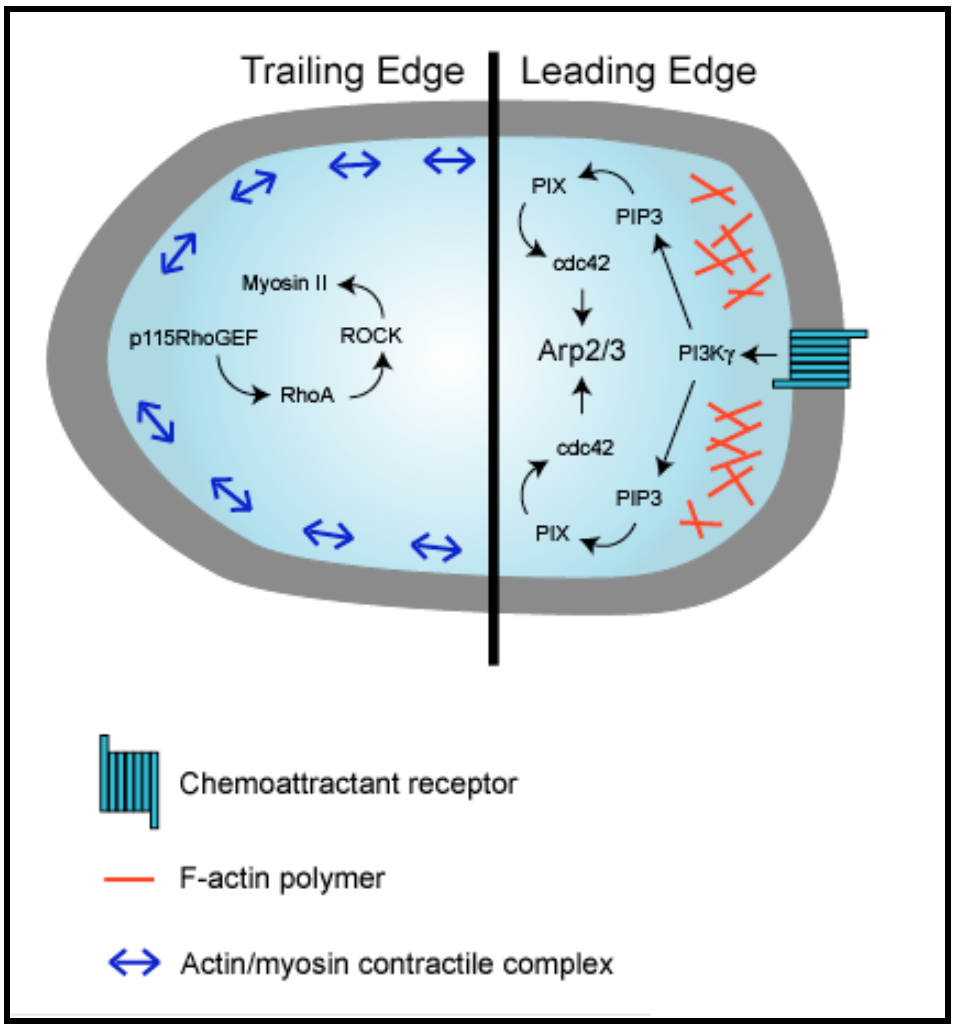

Figure 1: Overview of signaling events that occur at the leading edge and trailing edge of migrating cells.

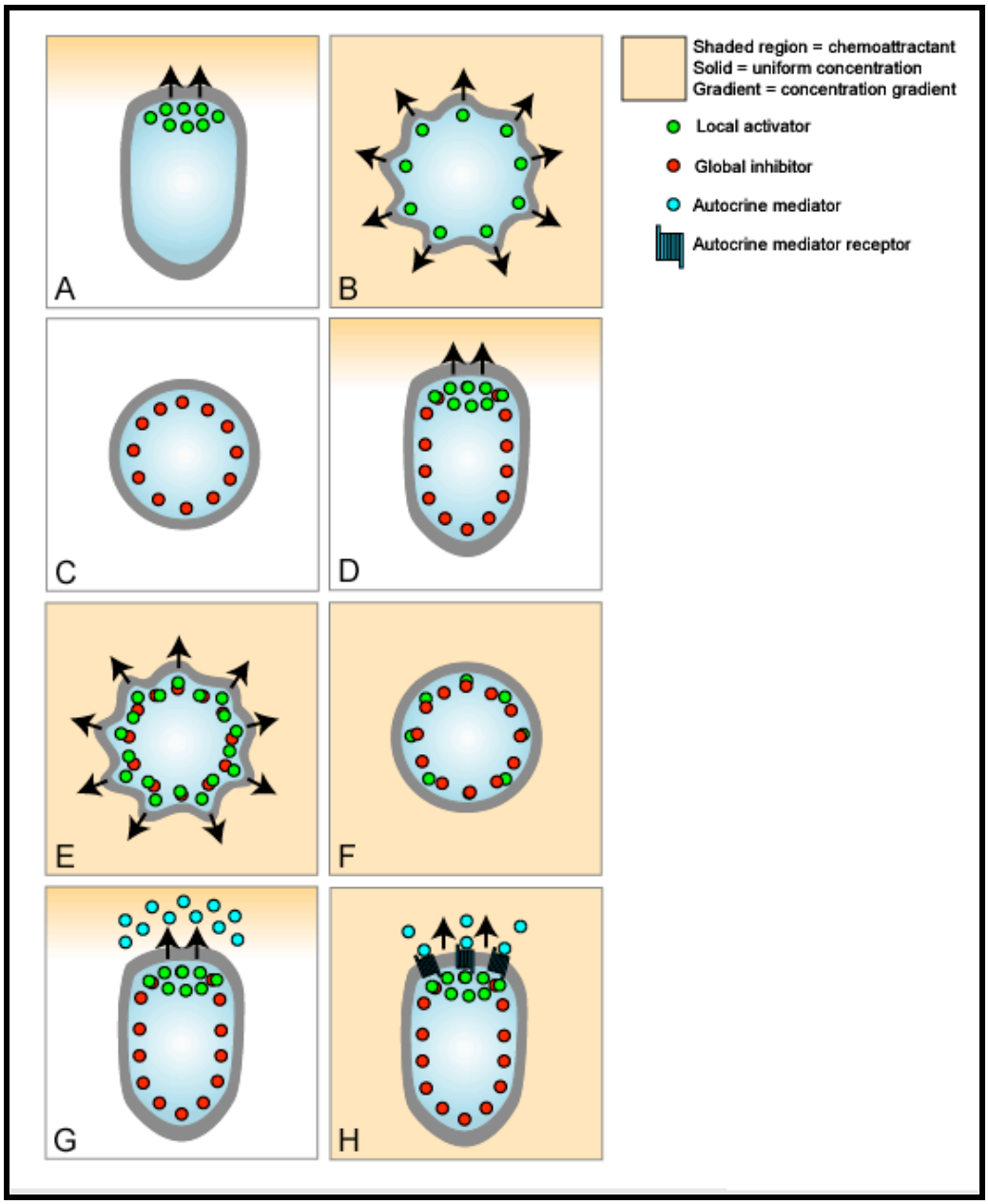

Figure 2: Models of neutrophil chemotaxis. In a simple local activator model, cells can migrate in a clear gradient (A) but will form opposing pseudopods around the entire cell body in the presence of a uniform concentration of chemoattractant (B). In a global inhibitor/local activator model the presence of a global inhibitor blocks migration (C) until sufficient activity of a local activator can overcome the inhibition (D). Uniform chemoattractant concentrations will still either create opposing pseudopods (E) or, if the local activator is too diluted will block chemotaxis entirely (F). Release of an autocrine mediator (G) and subsequent polarization of sensory machinery, however, could allow for polarization in uniform concentrations of chemoattractant (H).

Chapter 3

Background: Autocrine/Paracrine ATP Signaling

Introduction

The idea that ATP is released from cells as an extracellular signaling molecule was first proposed by Geoffrey Burnstock in the 1970's (1). Initially, the notion that cells intentionally release the primary unit of energy storage was met with much skepticism. Over the years, however, the discovery of multiple mechanisms for cellular release of ATP and the widespread expression of nucleotide-activated (P2) receptors in various cell types has helped to bring the concept into the scientific mainstream (3,4).

Many types of cells release ATP when stimulated biochemically or mechanically (2, table 3). Extracellular ATP exerts a diverse array of effects on cells by activating one of two classes of nucleotide receptors: G protein-coupled P2Y and ion channel P2X. There are eight known G protein-coupled P2Y receptors expressed in mammalian cells, two of which are preferentially activated by ATP (P2Y2 and P2Y11) (3) (table 1). These receptors couple to downstream signaling pathways via the heterotrimeric G-proteins Gi, Gq/11, or Gs. There are seven different P2X ion channel isoforms expressed in mammalian cells, all of which are activated by ATP (4). In addition, extracellular ATP can be hydrolyzed by a variety of ecto-ATPases expressed on the cell surface (5,6), and adenosine, formed by the action of those ATPases can activate P1 adenosine receptors

(7). Through the activation of P2 receptors (or the indirect activation of P1 receptors) extracellular ATP can alter cellular levels of second messengers and has the potential to modulate cellular function.

While there is extensive evidence for autocrine/paracrine ATP signaling in many different cell types (table 2), the actual mechanism for ATP release remains ill defined. Early studies suggested that the cystic fibrosis transmembrane regulator (CFTR) was responsible for releasing ATP but later work revealed that it was likely acting as a mediator of release rather than an ATP conductor itself (8,9,10). Regulated exocytotic release of ATP has been shown to occur in some non-excitatory cell types upon biochemical and mechanical stimulation (11,12,13). Currently, connexin and pannexin hemichannels (14,15), maxi anion channels (16,17), volume-regulated anion channels (VRAC, 18,19) and even the P2X7 receptor (20) have been proposed as putative sites of ATP release. It is likely that multiple mechanisms may be operative, perhaps differentially utilized by different cell types.

Both exogenous ATP and endogenous release of ATP can alter cell physiology. One important example is the "basal" release of ATP, via autocrine/paracrine stimulation of P2 receptors, that contributes to the 'set point' of second messengers in cells (21). In the following chapters of this thesis I present evidence for an autocrine ATP signaling pathway that contributes to the establishment of polarity in migrating neutrophils. To illustrate the broad applicability of this signaling mechanism, I have compiled all of the published examples of autocrine/paracrine ATP signaling in table 2. Below I briefly discuss some of the more commonly observed regulatory pathways to highlight the

diverse roles and important cellular regulation that occurs by autocrine/paracrine ATP signaling.

Regulation of calcium signaling

Many cell types appear to utilize ATP and its receptors to modulate intracellular calcium levels and calcium waves between cells. Indeed, paracrine signaling by ATP has been proposed as an alternative mechanism to mechanically-stimulated, predominantly gap junction-mediated calcium wave propagation between cells (23,43,53,54,56,79,83). One study attributed this effect to activation of P2Y2 receptors and proposed that heterogeneous expression of these receptors is responsible for the observed variation in response among cells in a population (53). Given the variety of stimulants that result in ATP-mediated changes to intracellular calcium levels, it seems likely that many investigators have unknowingly observed autocrine/paracrine ATP signaling in their studies, in particular when they mechanically stimulate cells by adding drugs, hormones, growth factors, etc. since such addition almost certainly stimulates the release of ATP and autocrine/paracrine activation of receptors that respond to ATP or its metabolites.

Regulatory volume decrease (RVD)

Epithelial cells in some organs are often subject to changes in their osmotic environment ("osmotic stress"). Liver hepatocytes, which show uptake of substrates and electrolytes and excretion of bile and various metabolic products, are one example. To

maintain a normal cell volume under hypo-osmotic conditions, hepatocytes must be able to rapidly adjust by increasing ionic secretion (94). Many cell types, including hepatocytes, release ATP in response to osmotic stress, and this release of ATP and subsequent activation of P2 receptors can play an important role in maintaining cell volume (75-78,87,88). Hypotonicity-induced release of ATP leads to the activation of volume-sensitive chloride channels, allowing cells to dynamically regulate their volume. Similar mechanisms likely exist in renal epithelial cells, where ATP release and P2 receptor activation also can activate ion channels and change cellular transport of constituents (69,70).

Response to Pathogens

Autocrine/paracrine ATP signaling can contribute to several different modes of pathogen response. In some cases, activation of P2 receptors leads to the production/release of inflammatory mediators. For example, treatment of microglia with the bacterially-derived endotoxin lipopolysaccharide (LPS) results in a release of ATP and subsequent production of IL-1β and IL-10 (27,29,30). LPS-stimulated ATP release also promotes release of IL-1α from endothelial cells and IL-6 release from fibroblasts (39,59). Microbial components and uric acid (a "danger signal" released from dying cells) have both been shown to stimulate IL-1β and IL-18 secretion from monocytes (37). In what may represent a "last ditch" response to infection, autocrine ATP signaling in response to pathogens can also stimulate apoptosis through activation of the P2X7 receptor (27,59).

In addition to the host/pathogen interactions listed above, bacterially derived N-formyl peptide fMLP stimulates release of ATP from neutrophils (52). This stimulation, and the subsequent cellular response, is the focus of this thesis and is described in detail in the following data chapters.

Table 1: The eight P2Y receptor isotypes

Receptor	Primary Endogenous Agonists	Associated G protein
P2Y1	ADP	G_q
P2Y2	ATP, UTP	$G_q/G_{i/o}$
P2Y4	UTP	$G_q/G_{i/o}$
P2Y6	UDP	G_q
P2Y11	ATP	G_s/G_q
P2Y12	ADP	$G_{i/o}$
P2Y13	ADP	$G_s/G_{i/o}$
P2Y14	UDP-glucose	$G_{i/o}$

Table 2: Autocrine/Paracrine activity of endogenously released ATP. This table is a compilation of known autocrine/paracrine ATP signaling systems, sorted by cell type. For each entry, the ATP release stimulant, target receptor, and physiological effect are given (pp 23-27).

Table 2: Autocrine/Paracrine activity of endogenously released ATP

Cell type	Stimulation	P2 Target	Physiological Effect
CNS/Neuroendocrine			
Astrocytes	Mechanical	P2Y/P2Y2	↑PLC activity (22), ↑$[Ca^{2+}]_I$ (22,23)
	Hypotonic stress	P2Y/P2Y1	Activation/modulation of volume-regulated channels (24,25)
Chromaffin cells	Ba2+	P2	Inhibition of non-L type Ca^{2+} channels (26)
Microglia	LPS	P2X7	↑IL-1β release, ↑apoptosis (27,28)
		P2Y1,11	↑IL-10 release (29,30)
	$A\beta_{1-42}$	P2X7	↑ROS generation (31)
Neuroendocrine cells	Basal	P2Y12	↓adenylyl cyclase activity (32)
Neural Progenitor	Basal	P2Y(1)	↑$[Ca^{2+}]_I$ (33,34)
Anterior Pituitary	A23187	P2Y2	Release of lutenizing hormone (35)
	EDTA/GnRH	P2X2/5	↑$[Ca^{2+}]_I$ (36,37)
	Thyrotropin releasing hormone	P2	↑prolactin release (38)

Table 2: Autocrine/Paracrine activity of endogenously released ATP, cont'd

Cell type	Stimulation	P2 Target	Physiological Effect
Heart/Circulatory			
Endothelial cells	LPS	P2X7	↑IL-1α release (39)
	Hypotonic stress	P2,P2X4/5	↑$[Ca^{2+}]_I$ (40,41,42,43), ↑NO production (40)
	Hypoxia	P2	↑Growth factor induced DNA synthesis (44)
Glomerular Vasculature	β-blockers	P2Y	↑NO release (45)
Vascular Smooth Muscle	Stretch/Mechanical stress	P2	↑JNK/SAPK activity (46)
Blood Cells			
Erythrocytes	*P. falciparum* infection	P2Y1	↑Osmolyte permeability (47)
Lymphoid Cells	Basal	P2X7	↑Proliferation (48)
Macrophages	*M. tuberculosis* infection	P2X7	Apoptosis (49)
Megakaryocytes	Spontaneous	P2Y1	↑repetitive inward Ca^{2+} currents (50)
Monocytes	Microbial components/uric acid	P2X7	↑1L-1β, IL-18 secretion (51)
Neutrophils	fMLP	P2Y2	Cell polarization (52)

Table 2: Autocrine/Paracrine activity of endogenously released ATP, cont'd

Cell type	Stimulation	P2 Target	Physiological Effect
Platelets	Thrombin/Thromboxane	P2X1	↑$[Ca^{2+}]_I$ (53)
Connective Tissue			
Osteoblasts	Mechanical/Hypotonic stress	P2Y1/P2Y2	↑$[Ca^{2+}]_I$ (54,55,56,57), Egr1 synthesis (57)
Fibroblasts	Mechanical stimulation	P2Y2	↑$[Ca^{2+}]_I$ (58)
	LPS, PMA	P2X7	↑ Fibronectin, IL-6 release, apoptosis (59)
Multipotent Stromal Cells	Oscillatory fluid flow	P2/P2Y1	↑$[Ca^{2+}]_I$, Calcineurin activation, NFAT translocation, proliferation (60,61)
Tendon	Medium change/UTP	P2Y6	↓IL-1β, COX2, MMP-3 (62)
Eye			
Retinal Glial Cells	Hypotonic stress	P2Y1	↑K^+, Cl^- channel conductance (63)
GI Tract			
Colon Cancer Cells	Gram-negative flagella	P2Y	↑$[Ca^{2+}]_I$, ↑Erk1/2 phos., ↑mucin transcription, PLC activation (64)
	Hypotonic stress	P2X7	↑caspase 3/8 and annexin V activation, cytc release, cell death (65)
	Flagellin	P2	↑$[Ca^{2+}]_I$,Erk1/2 phos. (66)

Table 2: Autocrine/Paracrine activity of endogenously released ATP, cont'd

Cell type	Stimulation	P2 Target	Physiological Effect
Distal Colon	Mechanical/Hypotonic stress	P2Y	↓Short circuit current (67)
Kidney			
HEK 293	Basal	P2X7	↑proliferation in absence of serum (68)
Nephron	Mechanical/Hypotonic stress	P2	↑$[Ca^{2+}]_I$ (69)
Renal Epithelial	Stretch	P2	↑epithelial sodium channel activation (70)
	Aldosterone	P2	↑$E_{Na}C$ activity, contraction (71)
	Hypotonic stress	P2	↑$[Ca^{2+}]_I$ (72)
	Basal	P2Y	↓Arach. acid release, cAMP production (21)
Muscle			
Dystrophic Myotubules	Basal/Stretch	P2	↑Na^+/H^+ exchanger activity (73)
Pancreas/Liver/Bile Duct			
Pancreatic β-cells	Glucose	P2Y	↑$[Ca^{2+}]_I$ (74)
Hepatocytes	Hypotonic stress	P2	↑Cl^- permeability/regulatory volume decrease (RVD) (75,76,77,78)
	Mechanical	P2	↑$[Ca^{2+}]_I$ (79)
Biliary Epithelial	Hypotonic stress	P2	↑Cl^- permeability (80)
Cholangiocytes	Forskolin	P2	↑$[Ca^{2+}]_I$, HCO_3^- secretion (81)

Table 2: Autocrine/Paracrine activity of endogenously release ATP, cont'd

Cell type	Stimulation	P2 Target	Physiological Effect
Reproductive			
Cervical Epithelial Cells	Media serum removal	P2X7	↑Caspase 3/9, apoptosis (82)
Prostate Cancer	Mechanical	P2	↑$[Ca^{2+}]_I$ (83)
	DC electrical field pulse	P2	↑$[Ca^{2+}]_I$, tumor growth, c-Fos Induction (84)
Respiratory			
Airway Epithelial	PKA/ATP	P2Y2	Cl^- channel stimulation (85)
	Medium displacement	P2Y2	↑Inositol Phosphate synthesis (86)
	Hypotonic stress	P2	Regulatory volume decrease (87,88)
	1-EBIO/chlorzoxazone	P2Y1	Cytosolic Ca^{2+} mobilization (89)
	Hypotonic stress	P2Y6	↑$[Ca^{2+}]_I$ (90)
Skin			
Keratinocytes	Media change	P2Y	↑IL-6, ↑$[Ca^{2+}]_I$ (91)
Thyroid			
Thyrocytes	Basal	P2Y2	↑IL-6 secretion, ↑$[Ca^{2+}]_I$ (92)
	Basal	P2Y1/2	↑Erk1/2 phos., ↑AP1 activation ↑Cyclin D1 expression, ↑Hsp90 (93)

Chapter 4

A novel method using fluorescence microscopy for real-time assessment of ATP release from individual cells.

Citation: Corriden, Ross; Insel, Paul A.; Junger, Wolfgang G.. "A novel method using fluorescence microscopy for real-time assessment of ATP release from individual cells", Am J Physiol Cell Physiol. 2007 Oct; 293(4):C1420-5.

Abstract

Many cell types release ATP in response to mechanical or biochemical stimulation. The mechanisms responsible for this release, however, are not well understood and may differ among different cell types. In addition, there are numerous difficulties associated with studying the dynamics of ATP release immediately outside the cell membrane. Here we report a new method that allows the visualization and quantification of ATP release by fluorescence microscopy. Our method utilizes a two-enzyme system that generates NADPH when ATP is present. NADPH is a fluorescent molecule that can be visualized by fluorescence microscopy using an excitation wavelength of 340 nm and an emission wavelength of 450 nm. The method is capable of detecting ATP concentrations <1 μM and has a dynamic range of up to 100 μM. Using this method, we visualized and quantified ATP release from human polymorphonuclear leukocytes and Jurkat T cells. We show that upon cell stimulation the concentrations of

ATP can reach levels of up to 80 μM immediately outside of the cell membrane. This new method should prove useful for the study of the mechanisms of release and the functional role of ATP in various cell systems, including from individual cells.

Introduction

Release of cellular ATP into the extracellular space is physiologically significant and has been shown to regulate functional responses of excitatory and non-excitatory cells (Burnstock, 2007; Bodin & Burnstock, 2001; Fredholm, 1997; North & Verkhratsky, 2006; Schwiebert & Zsembery, 2003). Released ATP modulates cell function by activating ionotropic P2X and G-protein coupled P2Y receptors (Burnstock, 2006). Through the activation of these receptors, ATP release is linked to numerous physiological responses, including the "basal" activation of signal transduction pathways and the reaction of cells to mechanical and osmotic stress and membrane deformation during the course of cell migration (Chen & Corriden et al., 2006; Chen et al., 2004; Dubyak, 2000; Lee et al., 2005; Loomis et al., 2003; Ostrom, et al., 2000, Ostrom et al., 2001 Yegutkin et al., 2000).

While the role of ATP as an autocrine and paracrine regulatory signaling molecule has been extensively studied, the precise mechanisms of ATP release from different cells have been difficult to define and likely differ among cell types (Bell et al., 2006; Dutta, et al., 2004; Eltzschig et al., 2006; Ito et al., 2004; Schwiebert, 2003, Stout et al., 2002). A major limitation in the study of the mechanisms of ATP release is the lack of methods that allow the visualization of release from individual cells in real-time. This shortcoming has made it difficult to determine whether release of ATP occurs at a

specific cellular location and to quantify ATP concentrations in regions close to the cell membrane where they would be highest and where nucleotides would interact with P2 receptors. Incubation of tissues with quinacrine, a fluorescent dye that selectively labels high concentrations of intracellular ATP was an early and effective, though invasive, method for visualization of granular ATP release from excitatory cells (Olson et al., 1976; Alund & Olson, 1979). Currently the most widely used methods to study ATP release are based either on the luciferin/luciferase bioluminescence assay or on high performance liquid chromatography (HPLC). Both methods allow the quantification of ATP concentrations in the bulk media, but as generally employed, cannot provide direct information regarding concentrations in membrane microenvironments that are relevant for the cellular responses to ATP. Several elegant methods have been proposed to overcome this limitation including the use of ATP biosensors (Beigi et al, 1999; Hayashi et al., 2004; Hazama et al., 1998; Llaudet et al., 2005; Nakamura et al., 2006; Pellegatti et al., 2005) and measurement of the changes in fluorescent properties of luciferin after its conversion by luciferase (Sorensen & Novak, 2001). While powerful, these techniques are sometimes technically challenging, often requiring generation and/or positioning of reporters in a manner that does not allow for visualization of rapid dynamics of ATP release from individual cells.

Here we present a method that utilizes fluorescence microscopy to visualize ATP release from individual cells and to estimate the concentrations of ATP at different regions in the extracellular space. The assay is based on a tandem enzyme reaction driven by hexokinase and glucose-6-phosphate dehydrogenase, which, in the presence of ATP and glucose, converts NADP to NADPH at an equimolar ratio. NADPH is a highly

fluorescent compound that can be easily imaged using fluorescence microscopy (Piston & Knobel, 1999). This conceptually simple assay has the potential to be easily adapted for use by laboratories interested in the study of a wide variety of cellular systems in which ATP release and response may be involved.

Materials and Methods

Materials: Unless otherwise indicated, all chemicals were obtained from Sigma-Aldrich Chemical Co. (St. Louis, MO). HBSS was from Irvine Scientific; Santa Ana, CA. Phytohemagglutinin was from Roche Applied Science; Indianapolis, IN.

Microscope system: All microscope studies were performed using an inverted Leica DMIRB microscope (Wetzlar, Germany) equipped with a PSMI-2 stage incubator controlled by a TC-202A temperature controller (Harvard Apparatus; Holliston, MA) and a Hamamatsu Orca II camera (Hamamatsu; Hamamatsu City, Japan). Images were acquired using Openlab software (Improvision; Coventry, England). Based on the fluorescence properties of NADPH, we used a filter set consisting of a 340 nm band pass exciter with a band width of 30 nm (Omega Optical; Brattleboro, VT), a 450 nm bandpass emitter with a band width of 40 nm (Chroma Technology; Rockingham, VT), and a 400 nm dichroic mirror (Chroma Technology). UV illumination was generated using a 100-W short arc mercury lamp (Ushio, Tokyo, Japan). The microscope was isolated from vibrations using a TMC Micro-g 63-542 vibration isolation table (Technical Manufacturing Corporation; Peabody, MA). To generate an ATP gradient and to mechanically perturb cells, we used an InjectMan NI 2 micromanipulator in combination

with a FemtoJet microinjection system from Eppendorf (Eppendorf; Hamburg, Germany).

Cell culture and PMN isolation: The human Jurkat T cell line (ATCC; Manassas, VA) was cultured in RPMI supplemented with 10% heat inactivated FCS (Omega Scientific; Tarzana, CA). Human polymorphonuclear neutrophils (PMN) were isolated from the peripheral blood of healthy adult volunteers as described previously (Junger et al., 1998).

Optical properties of NADPH: As shown in Fig. 1A, increasing concentrations of ATP elicit the conversion of corresponding concentrations of NADP to NADPH. NADPH has a maximum absorbance at 340 nm (Piston & Knobel, 1999). An emission spectrum generated using a SFM25 Kontron spectrofluorometer (Kontron Instruments; Basel, Switzerland) set to an excitation wavelength of 340 nm showed a maximum emission peak at a wavelength of 450 nm (Fig. 1B). Based on these data we chose a filter set for our microscope system consisting of a 340±15 nm band pass exciter, a 450±20 nm band pass emitter, and a 400 nm dichroic mirror to detect the fluorescent signal of NADPH.

Detection of exogenous ATP: All experiments were performed using an assay solution containing 2 U/ml hexokinase (Sigma; catalog number H-6380), 2 U/ml glucose-6-phosphate dehydrogenase (Sigma; catalog number G-5885), 2 mM NADP (Sigma; catalog number N-1511), and 10 mM D-glucose (Sigma; catalog number G-400) diluted

in HBSS. Depending on the experimental design, ATP was either added to this solution in bulk or it was slowly released into the solution at constant rate from a micropipette tip. We used a Leica PL Fluotar oil immersion objective with a magnification of 100x and a nominal aperture of 1.30 and recorded images with the Orca II camera using a 700 ms exposure time. Openlab software was used to extract fluorescence intensity values (expressed as grey values) from recorded images. Grey values from selected regions of interest (ROIs) were averaged and converted to ATP concentrations using standard curves generated with ATP standard solutions.

Detection of ATP using the luciferase assay: A luciferase/luciferin method standard curve was generated using the Roche Applied Science Adenosine 5'-triphosphate (ATP) Bioluminescence Assay Kit (Roche Diagnostics Corporation; Indianapolis, IN). Equal volumes (100 µl) of ATP solution and the luciferase/luciferin substrate mixture provided with the kit were placed in a Turner Designs 20/20 luminometer (Turner Designs; Sunnyvale, CA), and the luminescence was measured by integration over a 3-s time interval. These measurements were repeated three times and expressed as an average.

Stimulation of ATP release from cells: In order to remove existing extracellular ATP, Jurkat cells or PMN were gently washed 3 times with fresh HBSS and allowed to settle at room temperature. Cells were then gently resuspended in 50 µl of HBSS supplemented with 10 mM D-glucose, placed onto a cover slip in a stage incubator with the temperature set to 37ºC. To minimize release of ATP due to mechanical stress, the

cells were kept on a vibration isolation table for the entire duration of the experiment. Prior to assaying ATP release, 50 µl of a 2-fold concentrated assay solution containing enzymes and substrate was added to the cells. For experiments where ATP was released through cell lysis or osmotic stress, 10 µl of a 1% Triton X-100 solution in HBSS or 10 µl of 1,000 mM NaCl solution in HBSS, respectively, was added to the cells. For experiments with activated Jurkat cells, 1 µl of a suspension of 1 x 10^7 Macsibeads/ml coated with anti-CD3 and anti-CD28 antibodies as specified for the Macsibeads kit (Miltenyi Biotech; Bergisch Gladbach, Germany) were incubated with the cells. In experiments using PMN, cells were stimulated with a solution of 100 nM formyl-methionyl-leucyl-phenylalanine peptide (fMLP; Sigma; St. Louis, MO) that was released from a micropipette tip. To account for cellular autofluorescence in ROIs above the cell body, gray value readings in these regions were obtained and then subtracted from subsequent readings obtained after cell stimulation. For each type of stimulation, control experiments were performed without NADP in the substrate mixture to ascertain that cell stimulation did not alter autofluorescence readings.

Results and Discussion

Optimizing the fluorescence ATP assay system

The hexokinase/glucose 6-phosphate dehydrogenase (G6PD) reaction has previously been used to quantify glucose concentrations (Neeley, 1972). The two step reaction, summarized in Figure 1A, hydrolyzes ATP resulting in the formation of equimolar concentrations of NADPH, a strongly fluorescent product with an absorption maximum at 340 nm (Piston & Knobel, 1999). We evaluated the emission spectrum

using a SFM25 Kontron spectrofluorometer (Kontron Instruments; Basel, Switzerland) set to an excitation wavelength of 340 nm (Fig. 1B). Based on these data we chose an appropriate filter set (described in the Methods section) for the microscope setup used in our application.

We then tested various enzyme and substrate concentrations in a cell free system to determine those that would be optimal for our assay so as to maximize the speed of the sequential reactions that lead to the formation of NADPH. This is particularly important in cell systems where the half-life of extracellular ATP is reduced by ecto-enzymes that hydrolyze the nucleotide (Zimmermann, 2000). In order to maximize reaction speed, we optimized the concentrations of the enzymes, hexokinase and G6PD, and of the substrates NADP and glucose. The effect of the substrate/enzyme concentrations on the rate of NADPH generation was tested by adding increasing concentrations of the reaction components to HBSS and monitoring the speed of NADPH formation in response to the addition of 1 mM ATP using fluorescence microscopy. In order to avoid substrate limitation, the concentration of NADP in the assay solution had to exceed maximum concentrations of ATP expected in the extracellular space, which was estimated to be about 50 μM (Hayashi et al., 2004). We found that 2 mM NADP yielded optimal results and the highest reaction speed. However, NADP concentrations >2 mM reduced the reaction speed, possibly due to substrate inhibition (Fig. 2A), as previously described for some isoforms of G6PD (Tsai & Chen, 1998). Increasing the concentrations of hexokinase (Fig. 2B) or G6PD (Fig. 2C) increased the conversion of 2 mM NADP to NADPH. Based on these experiments, we determined that 2 U/ml of each enzyme was

optimal to maximize reaction speed. Higher enzyme concentrations did not significantly increase reaction velocity.

As shown in Fig. 1, the tandem reaction requires glucose as a co-substrate. We tested if increasing glucose concentration would increase the reaction speed in our assay system. Predictably, the addition of 10 or 20 mM glucose to the 5.5 mM glucose contained in HBSS increased the initial rate of the reaction from 10 to 60 fluorescence units per second (grey value); however only minimal increases in the reaction rate were seen when >10 mM glucose was added (Fig. 2D). This may be a result of substrate inhibition (Purich et al., 1973). Based on the data from experiments shown in Fig. 2, we determined that the following assay mixture results in maximal reaction speed:

2 U/ml hexokinase

2 U/ml G6PD

2 mM NADP

10 mM D-glucose

All components were diluted in HBSS.

Using these assay components in the microscope setup described above, we found that an exposure time of 700 ms was necessary to capture fluorescent signals of low concentrations of NADPH. Increasing the exposure time of the camera to 1,000 ms did not significantly improve the resolution of the assay because of increased background noise. Therefore, we chose to set the camera exposure time to 700 ms for all experiments.

Verification of the fluorescence microscope assay system

To test the ability of the assay system described above to detect ATP concentration gradients, we used a solution of 100 μM ATP in HBSS in a micropipette mounted on a microinjector system and slowly released ATP into a solution containing the enzyme and substrate mixture. We obtained a fluorescence signal that emanated from the micropipette tip and increased in intensity as a function of time as a consequence of ATP accumulation around the pipette tip (Fig. 3A). Repeating this experiment using lower concentrations of ATP revealed a similarly rapid conversion of NADP to NADPH at the site of ATP release, though yielding lower fluorescence intensities (data not shown).

We used ATP standard solutions to estimate ATP concentrations using this assay. Solutions of increasing ATP concentrations were added to the assay solution and reactions were allowed to go to completion: Samples of each solution were placed on cover slips, and using the microscope settings described above, fluorescence images were obtained to determine the NADPH fluorescence signal corresponding to each ATP concentration. Because the concentration of ATP, and therefore NADPH, was uniform for each sample, we were able to extract the average gray value from each image and correlate these values to respective ATP concentrations. These signals increased in a nearly linear fashion at ATP concentrations between 0 and 400 mM (Fig. 3B). At higher ATP concentrations, the fluorescence signal reached a plateau.

We compared the sensitivity and range of our method with that of the luciferin/luciferase assay that is commonly used to measure ATP concentrations in bulk

solutions. The luciferin/luciferase assay was more sensitive and had a broader dynamic range extending from the low nM to the mM range (Fig. 3C). Several groups have previously noted that extracellular ATP can reach concentrations as high as 100 μM (Beigi et al., 1999; Schweibert & Zsembery, 2003). Thus our method can detect the dynamics of release of such ATP concentrations, despite its more limited dynamic range and sensitivity compared to luciferin/luciferase.

Visualization of ATP release from living cells

After establishing that our fluorescence assay system was potentially suitable to visualize and quantify physiologically relevant ATP concentrations, we tested directly if this system would allow the visualization and quantification of ATP release from living cells. As a first step for validating our method, we sought to visualize ATP release during lysis of Jurkat T cells. The cells were placed onto an inverted microscope, bathed in the assay mixture and lysed with Triton X-100 to release their cytosolic ATP (Fig. 4 A&B). Cell lysis rapidly increased NADPH fluorescence, corresponding to 10 μM ATP (Fig. 4B). This fluorescence signal rapidly dissipated, probably as a consequence of dilution or hydrolysis of ATP by ecto-nucleotidases and related enzymes. In the absence of hexokinase, we observed no increase in the fluorescence signal. However, we noted autofluorescence of untreated cells in experiments shown in both Figs. 4A and B, suggesting that our optical assay system can detect the fluorescence signal generated by endogenous NADH or NADPH within the cells. Upon cell lysis, this autofluorescence signal rapidly disappeared and became undetectable after 30 s (Fig. 4A).

Hyperosmotic conditions can rapidly release ATP from Jurkat T cells (Loomis et al., 2003). We tested if we could visualize this ATP release with our assay system. We added a small aliquot of 1 M NaCl to Jurkat T cells bathed in assay solution in order to increase the osmolarity of the culture medium by 20 mM. After addition of NaCl, ATP was rapidly (<10 sec) released (Fig. 4C). Quantification of the signal in a region of interest (ROI) outside of the cell revealed a steady release of ATP, increasing extracellular ATP concentration by 15 μM within 60 s after exposure of the Jurkat cells to the hyperosmotic conditions (Fig. 4C).

A primary goal for developing the fluorescence assay described here was to allow the visualization of ATP release during cellular activation. To this end, we assessed ATP release in response to stimulation of two different cell types: Jurkat cells and human polymorphonuclear neutrophils (PMN). Jurkat cells were stimulated with beads coated with antibodies to CD3 and CD28, which stimulate the receptors required for T cell activation. PMN were stimulated with the bacterial cell wall-derived chemoattractant formyl peptide (fMLP). Both treatments have been previously shown to induce robust ATP release (Loomis et al., 2003; Yip et al., 2007; Chen et al., 2004, Chen et al, 2006). Immediately after stimulation of Jurkat cells, we found that ATP was released from the entire area of the cell membrane and liberally emanated from the cells some distance into the extracellular space (Fig. 5A; compare signal at ROI 1 vs. ROI 2). The NADPH signal was particularly strong at localized membrane regions, suggesting the existence of distinct and spatially segregated ATP release sites. A region selected immediately outside the cell membrane (ROI 1) revealed that the ATP concentrations in the extracellular space close to the cell membrane reached ~80 μM within 2 min of initiation of cell

stimulation. Fig. 5B shows the response of Jurkat cells to stimulation with a second type of stimulus, the lectin phytohemagglutinin (10 μg/ml). ATP release occurred at a nearly constant rate with ATP emanating far into the extracellular space, where ATP concentrations of ~20 μM were observed within 2 min of cell stimulation.

In contrast to T cells, stimulation of PMN with 10 nM fMLP caused polarization of cells and concomitant polarized ATP release. In the experiment shown in Fig. 5C, we estimated the concentrations of ATP in three separate ROIs. ROI 1 was chosen within the cell body at an area with dynamic changes in ATP concentrations. ROI 2 was selected at another site within the cell body, and ROI 3 was chosen close to the uropod (i. e., the trailing edge) of the same cell. At these different sites, we observed different dynamics of ATP release with concentrations of ATP increasing to 25 μM, a value that is consistent with data reported previously by others (Hazama et al., 1998). The release of ATP at the cell surface (ROI 1) seemed to occur in fluctuating bursts, suggesting that release occurs via degranulation. In contrast, ATP release at ROI 2 showed less fluctuation. ATP close to the uropod (ROI 3) remained low and did not fluctuate, implying that fMLP stimulation did not promote release of ATP from that region of the cell. Assessment of the concentration of ATP at the leading edge of PMN in the process of cell migration, as shown in Fig. 5D, revealed that ATP concentrations at the leading edge (ROI 1) increased concomitantly with pseudopod protrusion, while little ATP was released at the uropod (ROI 2) and in the center of the cell body (ROI 3).

ATP release from cells occurs in a 3-dimensional space. The determination of ATP concentrations in a 3-dimensional space would require confocal microscopy. The 2-dimensional microscopy method shown here suffers from the limitation that it cannot

resolve ATP concentration differences along the z-plane. These problems could be overcome with more sophisticated equipment such as spinning disc confocal or two-photon microscopy systems.

Conclusions

The assay system described herein allows the detection of ATP release from living cells. Using this assay, we show that Jurkat T cells and isolated human PMN differ profoundly with regard to the concentration and speed of ATP that they release, as well as in the subcellular locale from which ATP release occurs. This new assay should prove useful for the visualization and quantification of ATP release, including from single cells, and may provide a convenient means to study spatiotemporal aspects of ATP release from numerous cell types and tissue preparations.

Acknowledgements:

This study was supported in part by National Institute of General Medical Sciences Grants R01 GM-51477, GM-60475 (W.G.J.), and GM 66232 (P.A.I.), and CDMRP Grant PR043034 (W.G.J.).

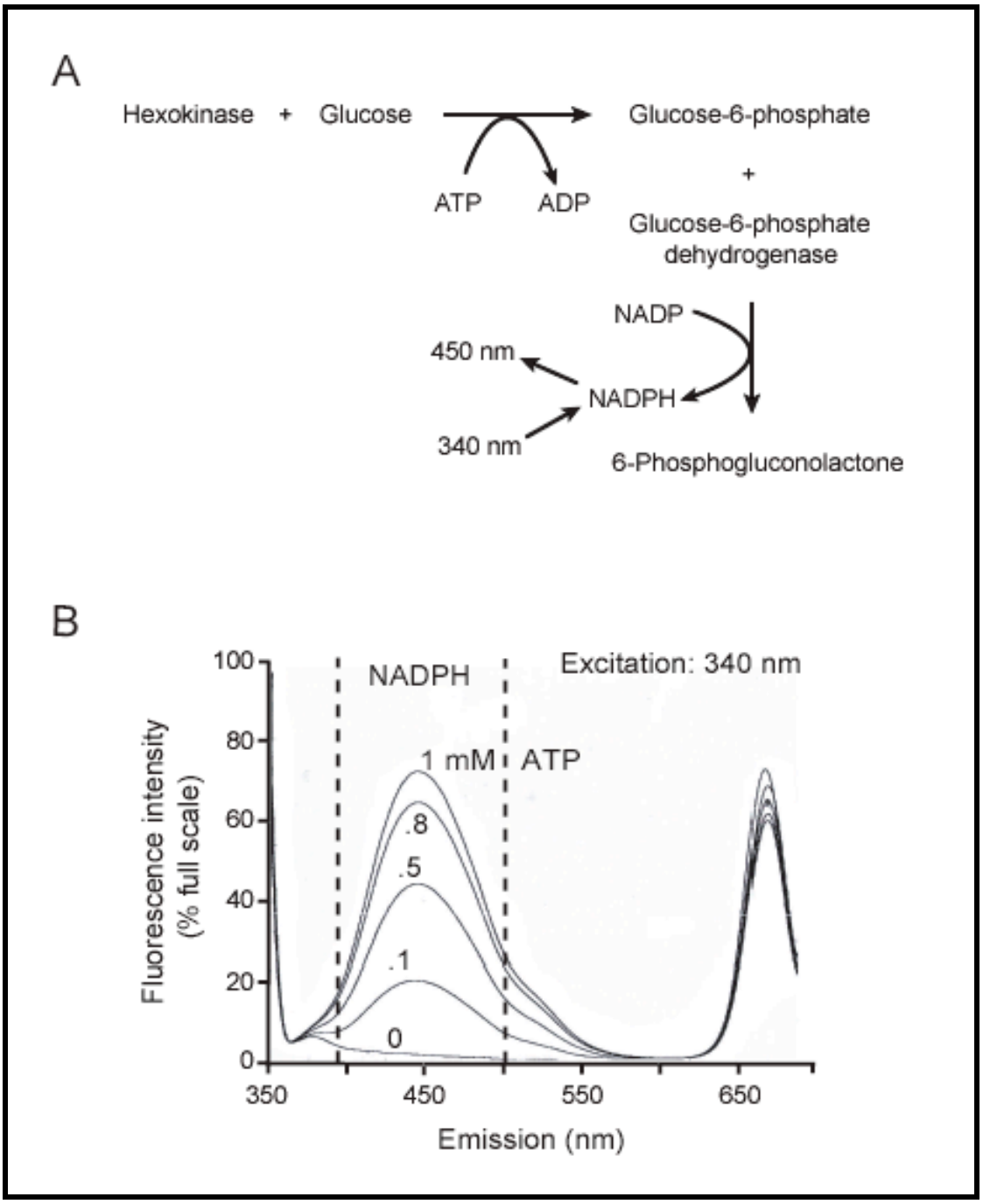

Figure 1: Assay system used to visualize ATP release. A) Summary of the tandem enzyme reaction resulting in formation of the fluorescent product NADPH in the presence of ATP and glucose. B) Emission spectra of assay mixtures after the addition of increasing concentrations of ATP. Emission data were obtained with a SFM25 Kontron spectrofluorometer adjusted to an excitation wavelength of 340 nm. The emission peak at 450 nm corresponds to NADPH.

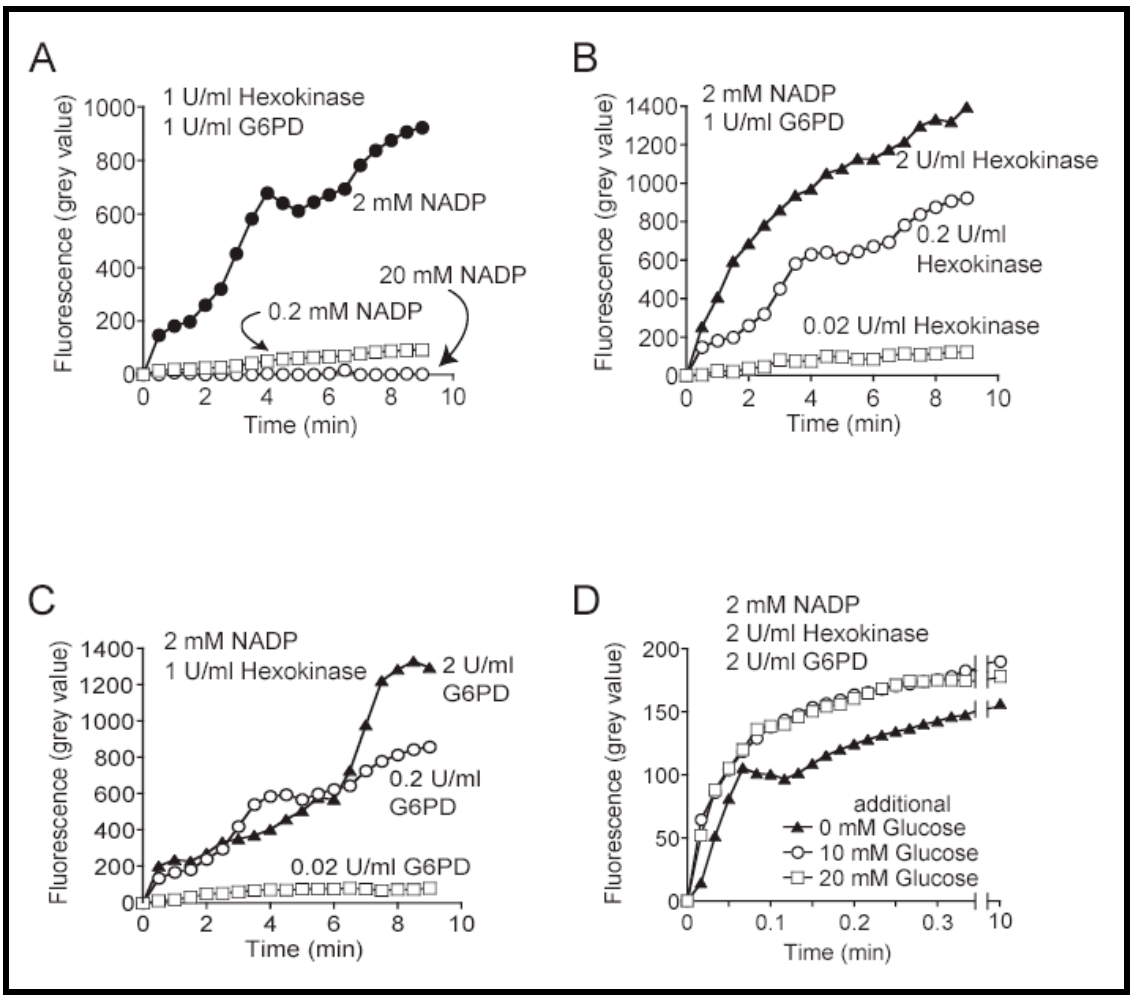

Figure 2: Optimization of ATP assay. A). Effect of increasing concentrations of the substrate NADP on the kinetics of the tandem enzyme assay in a cell free system. Increasing concentrations of NADP were added to HBSS containing 1 U/ml hexokinase, 1 U/ml glucose-6-phosphate dehydrogenase (G6PD), and 1 mM ATP and fluorescence intensity (grey values) was measured over 10 min. B) Increasing concentrations of hexokinase were added to HBSS containing 2 mM NADP, 1 U/ml G6PD, and 1 mM ATP. Changes in fluorescence intensity were measured over a period of 10 min. C) Increasing concentrations of G6PD were added to HBSS containing 2 mM NADP, 1 U/ml hexokinase, and 1 mM ATP and fluorescence intensity was measured over 10 min. D) Increasing concentrations of D-glucose were added to HBSS containing 2 U/ml hexokinase, 2 U/ml G6PD, 2 mM NADP, and 100 µM ATP. Changes in fluorescence intensity were measured over 10 min.

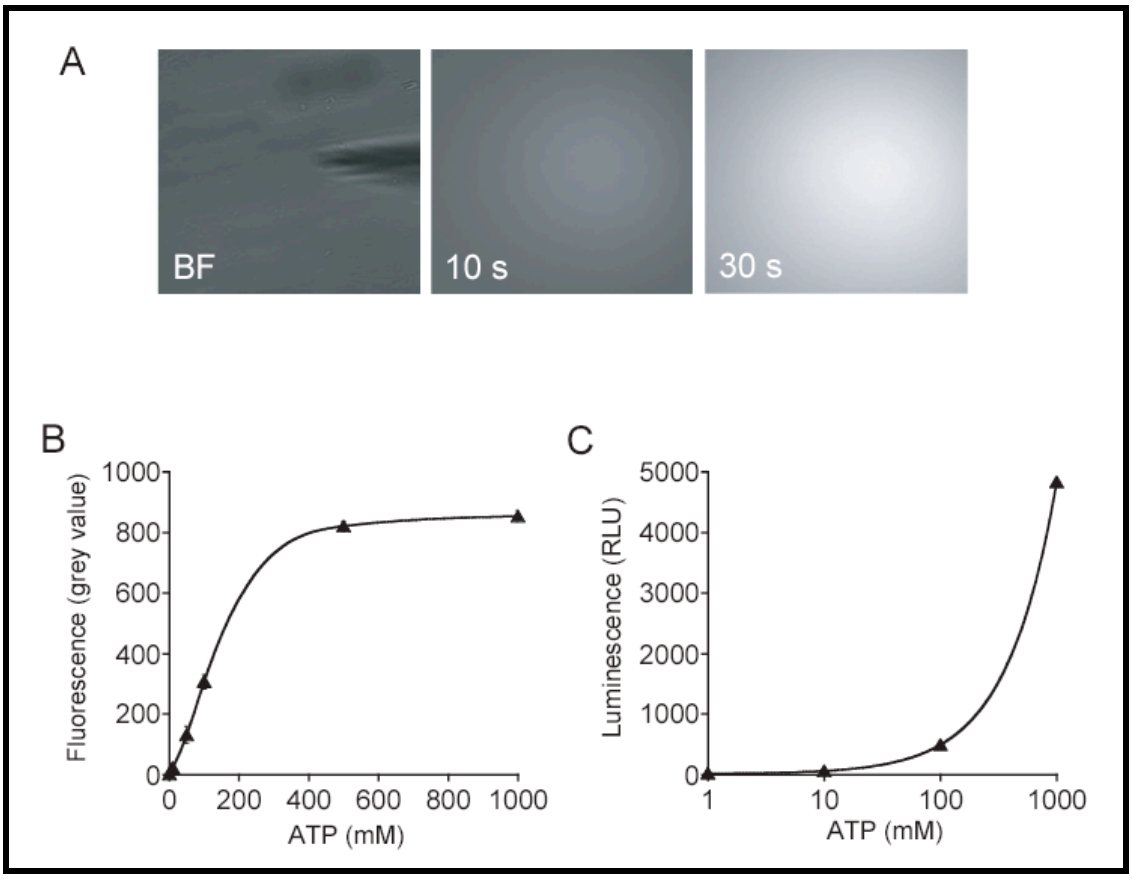

Figure 3: Fig 3) Quantification of ATP assay. A) ATP (100 _M) was released from a pipette tip into an assay mixture consisting of 2 U/ml hexokinase, 2 U/ml glucose 6-phosphate dehydrogenase, and 2 mM NADP, in HBSS with 4.5 mM additional glucose and NADPH formation was visualized using fluorescence microscopy. B) ATP response of fluorescence assay: increasing concentrations of ATP were added to the assay mixture described above and fluorescence intensity (grey) values were recorded by fluorescence microscopy, averaged, and plotted against ATP concentration. C) ATP response of luciferin/luciferase luminescence assay. Increasing concentrations of ATP were added to the assay described and relative luminescence unit (RLU) were determined as described in Methods.

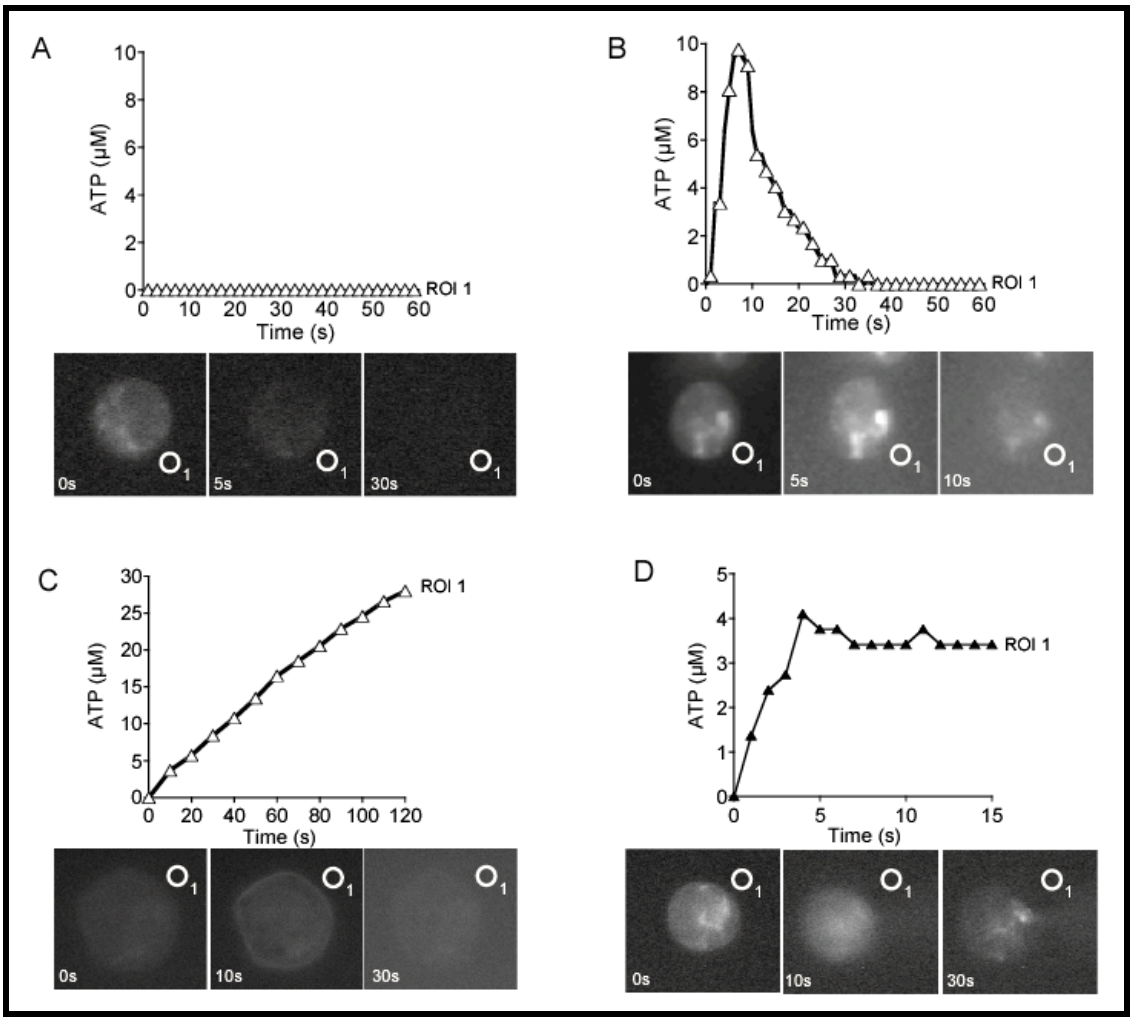

Figure 4: Fig 4) Application of NADPH based fluorescence microscope assay to visualize ATP release from living cells. The frames on the bottom of each panel show image sequences with regions of interest (ROI) marked with circles at which average fluorescence intensities (grey values) were determined. The graphs on top of each panel depict corresponding ATP concentrations determined with ATP standard curves as shown in Fig. 3B. A) Jurkat cell lysed with 0.1% Triton X-100 in the absence of assay solution. B) Jurkat cell lysed with 0.1% Triton X-100 in the presence of assay solution. C) Jurkat cell treated with 20 mM hypertonic solution (HS). D) Release of ATP from a Jurkat cell after mechanical stimulation with a micropipette tip.

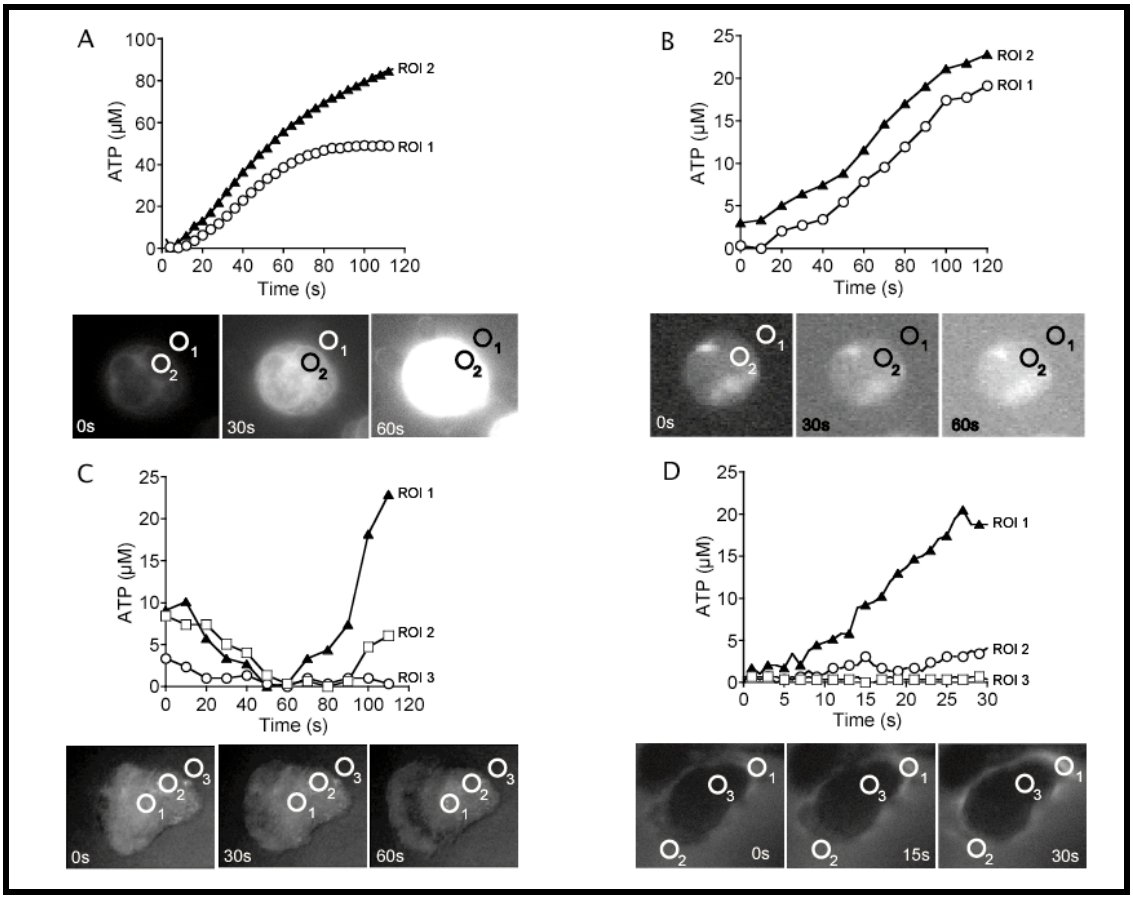

Figure 5: Detection of ATP release of different immune cell types in response to physiological cell stimulation. A) Jurkat cell stimulated with anti-CD3/CD28 antibodies bound to microbeads. B) Jurkat cell stimulated with PHA. C) Human peripheral blood neutrophil stimulated with 10 nM fMLP. D) Release of ATP from a migrating human neutrophil stimulated with 10 nM fMLP.

Acknowledgements for thesis:

Chapter 4, in full, is a reprint of the material as it appears in the American Journal of Physiology – Cell Physiology, October 2007, Corriden, Ross; Insel, Paul A.; Junger, Wolfgang G.; 293(4):C1420-5. The dissertation author was the primary investigator and author of this paper.

Chapter 5

ATP release guides neutrophil chemotaxis via P2Y2 and A3 receptors

Citation: Corriden, Ross*; Chen, Yu*; Inoue, Yoshiaki; Yip, Linda; Hashiguchi, Naoyuki; Zinkernagel, Annelies; Nizet, Victor; Insel, Paul A.; Junger, Wolfgang G.. "ATP release guides neutrophil chemotaxis via P2Y2 and A3 receptors", *Science*. 2006 Dec 15;**314**(5816):1792-5. (*both authors contributed equally to this work)

Abstract

Cells must amplify external signals to orient and migrate in chemotactic gradient fields. We find that human neutrophils release adenosine triphosphate (ATP) from the leading edge of the cell surface to amplify chemotactic signals and direct cell orientation by feedback through P2Y2 nucleotide receptors. Neutrophils rapidly hydrolyze released ATP to adenosine that then acts via A3-type adenosine receptors, which are recruited to the leading edge, to promote cell migration. Thus, ATP release and autocrine feedback through P2Y2 and A3 receptors provide signal amplification, controlling gradient sensing and migration of neutrophils.

Introduction/Results/Discussion

Neutrophils are primary phagocytic cells with important roles in host defense and tissue repair. However, activated neutrophils damage host tissues and contribute to

chronic inflammatory diseases, including rheumatoid arthritis, inflammatory bowel disease, and asthma (1). A key feature of neutrophils is their ability to detect and migrate to compromised tissues by following a concentration gradient of chemotactic substances released from microbial pathogens or injured cells.

Neutrophils can respond to chemoattractant gradients that differ in concentration by as little as 1% across the length of the cell body (2). Chemotaxis must involve signal amplification because a strongly polarized distribution of intracellular signal-transduction components is observed even in shallow gradients. The mechanisms of signal amplification are unclear (3, 4). We identified the polarized release of adenosine triphosphate (ATP), the activation of P2Y2 receptors, and the translocation and activation of A3 adenosine receptors as key mechanisms of signal amplification that control cell orientation and direct the migration of neutrophils.

Membrane deformation caused by mechanical or osmotic stress induces the release of cellular ATP from mammalian cells; however, detailed information on the underlying mechanisms is lacking (5, 6). Because cell migration also involves membrane deformation, we tested whether the stimulation of human neutrophils with the chemoattractant N-formyl-Met-Leu-Phe (FMLP) causes ATP release. Treatment of cells (10^7 cells in 250 μl of solution) with 100 nM FMLP rapidly tripled extracellular ATP concentrations in bulk media (Fig. 1, A and B) by inducing the release of 0.5% of their ATP pool. Concentrations of extracellular ATP and its hydrolytic products adenosine monophosphate (AMP) and adenosine peaked 5 min after FMLP stimulation; but while the concentration of ATP returned to basal levels after 15 min, AMP and adenosine concentrations remained >5–fold above baseline (Fig. 1B), which is consistent with the

presence of ecto–adenosine triphosphatases (ecto-ATPases) (7, 8). Neutrophils completely hydrolyzed exogenous ATP (5 μM) within 2 min after ATP addition, which suggests that they have potent ecto-ATPase activity (Fig. 1C).

Because membrane deformation occurs predominantly at the leading edge closest to the chemoattractant source, we hypothesized this region to be the principal site of ATP release. Fluorescent microscopy that was used to visualize ATP release [based on conversion of nicotinamide adenine dinucleotide phosphate ($NADP^+$) to its reduced form NADPH] revealed that neutrophils discharge ATP within seconds after FMLP stimulation (Fig. 1D and movies S1 to S3), with ATP release highest near the cell membrane with the greatest degree of protrusion (Fig. 1D, inset).

Extracellular ATP and adenosine modulate neutrophil functions, including chemotaxis (8, 9). We tested the effect of apyrase, which hydrolyzes ATP, on chemotaxis in a trans-well system composed of upper wells with neutrophils and lower wells with 1 nM FMLP separated by a filter with 3-μm pores. Addition of apyrase to the upper wells reduced chemotaxis by nearly 100% (Fig. 2A). Apyrase also inhibited FMLP-induced superoxide formation, implying that FMLP-promoted responses require ATP. Addition of apyrase to the lower wells reduced chemotaxis only by 40%, which suggests that ATP release is essential for the initiation of chemotaxis but not for maintaining migration once it is initiated. Microscopic analysis of neutrophil chemotaxis toward the tip of a micropipette filled with 100 nM FMLP confirmed this conclusion: Although 79% of control cells migrated toward FMLP with <60° angular deviation from a straight path, the addition of apyrase (10 U/ml) diminished the proper orientation of cells so that only 17% migrated correctly to the chemotactic source (Fig. 2B and movies S4 and S5). Other

ATP-hydrolytic enzymes (e.g., ATPase and alkaline phosphatase) had similar effects (fig. S1, A and B), confirming ATP release to be crucial for gradient sensing and cell orientation.

Using the trans-well assay, we found that the nonhydrolyzable ATP analog adenosine 5'-O-(3-thiotriphosphate) (ATP--S) increased FMLP-promoted chemotaxis and cell migration in the absence of FMLP, regardless of whether ATP--S was added to the upper or lower well (Fig. 2B), which indicates that extracellular ATP induces chemokinesis (random cell migration) but is not chemotactic. Uniformly added ATP--S (100 μM) impaired chemotaxis to a point source of FMLP, with only 31% of cells migrating along the correct path (Fig. 2C and movie S6), which implies that ATP--S treatment obscures polarized ATP released from the cells and interferes with gradient sensing and proper cell orientation

Adenosine and ATP are respective ligands of a family of four P1 adenosine (A1, A2a, A2b, and A3) and 15 P2 nucleotide receptors that include ionotropic P2X (P2X1-7) and G protein–coupled P2Y(P2Y1,2,4,6,11,14) subtypes (10, 11). We used the general P2-receptor antagonist suramin to test the role of P2 receptors in chemotaxis. Suramin reduced chemotaxis by 80% (Fig. 2D), whereas the P2X-selective antagonists 1-[N,O-bis(5-isoquinolinesulphonyl)-N-methyl-L-tyrosyl]-4-phenylpiperazine (KN-62) and oxidized ATP did not (fig. S1C), implying that P2Y receptors are involved in neutrophil chemotaxis.

Real-time reverse transcription polymerase chain reaction (RT-PCR) analysis suggests that neutrophils and human promyelocytic HL60 cells express predominantly A2a-, P2Y2-, and A3-receptor–derived mRNA (Fig. 3, A and B). Immunostaining

showed that A3 receptors, but not A2a or P2Y2 receptors, are concentrated at the leading edge of polarized cells (fig. S2, A and B), which suggests that A3 receptors may be involved in chemotaxis. In the trans-well assay, adenosine (1 nM to 1 μM) enhanced chemotaxis, particularly when added in the lower wells along with FMLP (Fig. 4A). Higher concentrations of exogenous adenosine slightly diminished chemotaxis (Fig. 4A and fig. S3A), likely by either activating A2a receptors, which are widely recognized for their inhibitory effects on neutrophils (8–12) or obscuring endogenous adenosine generated at the leading edge of migrating cells. Removal of extracellular adenosine with adenosine deaminase (ADA), which converts adenosine to inosine, or inhibition of A3 receptors with 3-ethyl-5-benzyl-2-methyl-4-phenylethynyl-6-phenyl-1,4-(±)-dihydropyridine-3,5-dicarboxylate (MRS 1191) inhibited chemotaxis toward FMLP (Fig. 4, B and E), platelet-activating factor, 3% autologous zymosan-activated serum, interleukin-8, and live bacteria (fig. S3, B to D). Inosine generated by ADA did not affect chemotaxis (fig. S3E).

The finding that the agonists and the antagonist of A3 receptors (but not of other P1-receptor subtypes) affected neutrophil chemotaxis further suggested a special role for A3 receptors in chemotaxis (Fig. 4, C and D). To determine whether A3 receptors control gradient sensing or migration speed, we examined the effect of MRS 1191 on neutrophil chemotaxis under the microscope. MRS 1191 (10 μM) reduced the migration speed of cells toward FMLP from 2.4 ± 1.0 to 0.5 ± 0.7 μm/min (Fig. 4E and movies S7 and S8), whereas gradient sensing seemed largely unaffected. Thus, A3 receptors appear to be the key adenosine receptors that regulate neutrophil chemotaxis by controlling cell migration.

Flow cytometric analysis revealed that FMLP stimulation rapidly increases

surface expression of A3 receptors in human neutrophils (Fig. 5A). This finding was confirmed with HL60 cells stably transfected with an A3 receptor–enhanced green fluorescent protein (EGFP) construct and differentiated with dimethyl sulfoxide to induce a neutrophil-like phenotype capable of chemotaxis (13, 14). A3 receptors in resting cells were predominantly localized in cytosolic granules (Fig. 5B). Upon exposure to an FMLP gradient, A3 receptors, but not P2Y2 receptors, rapidly translocated to the cell surface near the leading edge, accumulated on filopodia-like protrusions, and colocalized with F-actin (Fig. 5C and movies S9 and S10), a marker for the leading edge of polarized cells (15).

We further studied the chemotaxis of neutrophils from bone marrow of A3- and P2Y2-receptor knockout (KO) mice ($A3^{-/-}$ and $P2Y2^{-/-}$) using the murine chemotactic peptide Trp-Lys-Tyr-Met-Val-Met-NH_2 (W-peptide) (16). Chemotaxis of neutrophils from both KO mouse strains was less than that of wild-type mice (Fig. 6, A and B). Neutrophils lacking A3 receptors showed correct directionality but diminished speed, whereas cells without P2Y2 receptors showed a loss in gradient sensing. We confirmed the importance of both receptors for neutrophil chemotaxis in vivo by assessing cell recruitment to the peritoneal cavity of KO mice intraperitoneally injected with 1 nM W-peptide or 10^8 Staphylococcus aureus bacteria (Fig. 6C).

Our results lead to a model in which polarized ATP release, in response to chemotactic receptor stimulation, facilitates gradient sensing by activating multiple adjacent P2Y2 receptors that control cell orientation in a chemotactic gradient. Adenosine formation and A3-receptor accumulation at the leading edge likely constitute a second stage of autocrine signal amplification that facilitates chemotaxis by controlling migration

speed (Fig. 6D). Other receptors, such as A2a receptors, may contribute to chemotaxis by facilitating membrane retraction at the receding end. This system may help neutrophils locate bacteria and damaged tissues, which also generate extracellular ATP (17). In view of their importance for cell migration, P2Y2 and A3 receptors are potential therapeutic targets for the treatment of inflammatory diseases (18, 19).

Chemotaxis in *Dictyostelium discoideum* is controlled by extracellular signaling systems that use cyclic AMP (cAMP) production and the activation of cAMP receptors (20–22). The results shown here define an analogous mammalian navigation system based on polarized ATP release and purinergic receptor activation in neutrophils.

Materials and Methods

Materials

Adenosine receptor analogs, nucleotides, ATP£^S, fMLP, the A1 receptor agonist CPA (N6-cyclopentyladenosine), A2a & A2b receptor agonist CGS-21680 (2-p-[2-carboxyethyl] phenethylamino-5'-N-ethylcarboxamidoadenosine hydrobromide-hemicarbonate salt), A3 receptor agonist IB-MECA (N6-[3-Iodobenzyl]adenosine-5' Nmethyluronamide) and DMSO were obtained from Sigma-Aldrich Co. (St. Louis, MO). W-peptide (WKYMVM) was obtained from Phoenix Pharmaceuticals (Belmont, CA). Platelet activating factor-16 (PAF) and Interleukin 8 (IL-8) were from EMD Calbiochem (San Diego, CA). Microscope studies were performed using a Leica DMIRB microscope (Bensheim, Germany) connected to a Hamamatsu ORCA camera (Hamamatsu, Japan) and images were obtained using Openlab software (Improvision, Lexington, MA).

Cell culture and neutrophil isolation

Human neutrophils were isolated from peripheral blood of healthy adult volunteers as described previously (23). Homozygous A3-/- mice were provided by Merck Research Laboratories (West Point, PA), P2Y2-/- mice were obtained from Dr. Beverly H. Koller (University of North Carolina, Chapel Hill, North Carolina), and C57BL/6J mice (Jackson Laboratory, Bar Harbor, Maine) served as wild-type controls. Bone marrow cells of 6-10 week old mice were obtained as described previously (24). Murine neutrophils were isolated by Percoll gradient separation (55/68% interface) and washed twice with HBSS before overnight incubation in RPMI (Irvine Scientific, Santa Ana, CA) supplemented with 10% fetal calf serum (FCS). HL60 cells were cultured in Iscove's medium (ATCC, Manassas, VA) supplemented with 20% FCS. Differentiation of HL60 cells was accomplished by incubating cells with 1.3% DMSO seven days prior to experimentation.

HPLC analysis of extracellular nucleotides

Nucleotides released from neutrophils (10^7 cells in 250 µl) were analyzed by HPLC analysis as described previously (9), except that the HPLC gradient was slightly modified: 0-10 min, 5-100% elution buffer B; 10-13 min, 100% buffer B; 13-13.5 min, 100-5% buffer B; 13.5-15 min, 5% buffer B. Nucleotides were identified by their retention times and concentrations estimated using known standards.

Assay for visualization of ATP release

Neutrophils were incubated at 37°C in HBSS containing a mixture of 8 U/ml each

of hexokinase and glucose 6-phosphate dehydrogenase and 5 mM NADP. In the presence of ATP, these enzymes catalyze the formation of NADPH, a fluorescent molecule that was visualized using fluorescence microscopy with an excitation wavelength of 340 nm and an emission at 460 nm. The fluorescence intensity of regions outside the cells was measured using Openlab software and ATP concentrations were estimated using ATP standard solutions of known concentrations.

Oxidative burst assays

Oxidative burst was measured by assessing superoxide formation using the cytochrome C reduction assay previously described (9, 23).

Transwell chemotaxis assays

Transwell assays were performed with 96-well MultiScreen MIC Plate containing a filter plate with a pore size of 3.0 μm (Millipore, Bedford, MA). As chemoattractant we used 1 nM fMLP, 100 nM PAF, 3% autologous zymosan-activated serum (C5a), 2 ng/ml IL-8 (for human neutrophils), or 100 nM W-peptide (for murine neutrophils) in each well (150 μl) of the lower receiver plate. A suspension of 100 μl human or murine neutrophils (1×10^7/ml) was added into each well of the upper filter plate. After 50 min incubation at 37°C, the upper filter plate was removed. For human neutrophil assays, the cells in the lower wells were collected and sedimented by centrifugation at 16,000 x g for 10 s at room temperature. Elastase activity of the lysed cell suspension in the lower well was used as an indicator of the number of migrated cells as previously described (18). Briefly, after removal of the remaining supernatants, we mixed cells with 160 μl of a buffer

consisting of 50 mM Tris/HCl and 100 mM NaCl, pH 7.4 containing 0.05% (v/v) Triton X-100. Enzymatic reactions were started by the addition of the elastase-specific chromogenic substrate N-methoxysuccinyl-Ala-Ala-Pro-Val-p-nitroanilide (Sigma) at a final concentration of 1 mM. After 30 min at room temperature, the change in optical density was measured at a wavelength of 405 nm. For murine cells, neutrophils migrated into the lower wells were counted by microscopy. As a control, each set of experiments included wells containing HBSS with 10% FCS without chemoattractant in the lower well. Each condition was tested in triplicate.

Chemotaxis assays by microscopy

Human neutrophils, HL60 cells, or murine bone marrow neutrophils ($2.5x10^6$/ml) were plated on 25 mm glass coverslips (Fisher Scientific, Pittsburgh, PA) coated with 50 µg/ml fibronectin and placed into a temperature-controlled stage incubator (Harvard Apparatus, Holliston, MA) at 37°C. Cells were pre-treated with reagents as described and exposed to a chemoattractant gradient field generated by slowly releasing 100 nM fMLP (for human neutrophils) or 100 nM W-peptide (for mouse bone marrow neutrophils) from a micropipette tip placed in proximity of the cells. Cell migration was tracked by obtaining 20 serial images at 25-s intervals. From these images, the migration paths of individual cells were plotted and the total distance traveled toward the point source of fMLP was measured for each cell. From these data we obtained migration speed and path deviation for each cell.

Cell labeling for fluorescence microscopy

Antibody staining of receptors was performed by plating neutrophils or differentiated HL60 cells ($2.5x10^6$/ml) on glass coverslips and the cells were stimulated with 100 nM fMLP for 10 min at 37°C. The cells were fixed with 3.7% paraformaldehyde in phosphate-buffered saline (PBS; Irvine Scientific) for 10 min at room temperature, permeabilized with 0.1% Triton X-100 for 5 min, and labeled with antibody as described previously (9). For actin staining, differentiated HL60 cells were plated on glass coverslips, stimulated with 100 nM fMLP for 10 min, fixed by treatment with 3.7% paraformaldehyde for 10 min, washed with PBS, and permeabilized by the addition of a 0.1% solution Triton X-100 of for 10 min at room temperature. Coverslips were blocked for 1 h using a blocking solution containing 4% BSA in PBS, and then stained with rhodamine phalloidin according to the supplier's instructions (Invitrogen, Carlsbad, CA).

Real-Time PCR

The relative level of expression of mRNA of all known mammalian P1 and P2 receptors in human neutrophils and HL60 cells were determined with Real-Time RT-PCR using neutrophils isolated from 3 individual human donors. Primers were designed based on human P1 and P2 receptor sequences obtained from Genbank using the Primer 3 program (http://frodo.wi.mit.edu/cgibin/primer3/primer3_www.cgi) and published data (25). Total RNA was extracted from $4x10^8$ neutrophils using Trizol (Invitrogen), treated with 1 U/µg total RNA DNase I (Invitrogen), and first strand cDNA was synthesized using Superscript II RNase H- reverse transcriptase (Invitrogen), according to the

manufacturer's instructions. A negative control sample, lacking reverse transcriptase, was prepared simultaneously. The amplification efficiency of each primer set was determined to ensure equal efficiency. Templates were generated by PCR using Platinum PCR Supermix (Invitrogen), containing 100 nM sense and anti-sense primers and 1 μl cDNA. PCR products were serially diluted 10^5 to 10^{11} fold and used as the template for Real-Time PCR with the Qiagen QuantiTect SYBR Green PCR kit. Reactions were amplified and subjected to melting curve analysis using DNA Engine Opticon 2 Real-Time PCR detection system (BioRad, Hercules, CA) and the following cycling parameters: 1 cycle at 95°C (10 min) and 45 cycles at 94°C (30 s), 60°C (30 s), 72°C (30 s). A standard curve was generated by plotting the threshold cycle (Ct) against the Log (initial starting quantity). The efficiency of each primer set was calculated using the slope of this curve and the following equation: Efficiency = 10(-1/slope)-1. P1 and P2 receptor gene expression levels were measured in samples using Real-Time PCR as described above (n = 3) and the comparative Ct method for relative quantification of gene expression, which was normalized against β-actin mRNA levels.

Determination of cell surface expression of A3 receptors by flow cytometry

Neutrophils (1 x 10^6) were stimulated with 100 nM fMLP at 37°C for different times.Samples were then placed on ice and stained with a rabbit anti-human A3 adenosinereceptor antibody (Alpha Diagnostic, San Antonio, TX; 10 ng/ml) followed by a goatanti-rabbit IgG-FITC antibody (Sigma; at 1:100 dilution). The cells were washed withHBSS, fixed with sheath fluid containing 0.5% paraformaldehyde, and analyzed by flowcytometry using a BD FACSCalibur System (BD Biosciences, Rockville, MD)

equippedwith a 488 nm air-cooled argon-ion laser and interfaced to a computer equipped with Cellquest Pro software (BD Biosciences). Neutrophils were gated to exclude from analysis other cell types, debris, and aggregates. A total of 10^4 neutrophils per sample were analyzed.

Live cell imaging of P1 and P2 receptor localization

Using the mammalian expression vector pEGFP-N1 (Clontech Laboratories, Mountain View, CA), we generated plasmids encoding EGFP-fusion proteins of the human A3 and P2Y2 receptors using genes obtained from UMR cDNA Resource Center (Rolla, MO). The constructs were transfected into HL60 cells by electroporation (5 μg/ml plasmid) using a pre-set protocol on the GenePulser II electroporation system (BioRad, Hercules, CA). After 48 h in complete Iscove's medium supplemented with 20% FCS, stably transfected clones were selected by the addition of 2% G418 (Invitrogen) and incubated under the same conditions for 4 weeks. Fluorescent imaging was carried out using the microscope assays described above.

Endothelial Transcytosis Assay

Human brain microvascular endothelial cells (hBMEC) immortalized by transfection with SV40 large T antigen were obtained from Kwang Sik Kim (Johns Hopkins University, Baltimore, Maryland, USA); these cells show the morphological and functional characteristics of primary brain endothelium. hBMEC were propagated in\ RPMI 1640 medium (Life Technologies and Co, Bedford, Massachusetts, USA) supplemented with nonessential amino acids +10% FBS + 10% Nu-SerumTM IV (BD

Biosciences, San Jose, CA) at 37°C in 5% CO2. Polar hBMEC monolayers were established on collagen-coated TranswellTM plates 6.5 mm in diameter and with 3 μm pores (BioCoat, BD Biosciences, San Jose, CA). Human neutrophils (106 cells in 100 μl HBSS) were added to the upper well of the transwell chamber and treated with either 10 U/ml ADA or 10 μM MRS 1191. As a chemotactic stimulus, either 2 ng/ml IL-8 or 6 x 10^5 CFU of Staphylococcus epidermidis (ATCC 12228) in 600 μl HBSS were added to the bottom of the transwell chamber. The plates were incubated for 160 min at 37°C in 5% CO2 and numbers of neutrophils that crossed the monolayers were enumerated using microscopy. Integrity of the hBMEC monolayers was confirmed by impermeability to 4% Evans blue-labeled bovine serum albumin (BSA). Each assay condition was performed in triplicate and repeated three times with similar results.

Assessment of neutrophils migration in mouse peritonitis models

Male WT, P2Y2-/-, and A3-/- mice (8-12 weeks old; 6 animals per group) were used. To determine the role of P2Y2 and A3 receptors in neutrophils migration in vivo, either 1 ml of W-peptide (1 nM), Staphylococcus aureus (108/ml), or vehicle (saline) was injected intraperitoneally. After 2 h (in the W-peptide groups) or 4 h (in the S. aureus groups), animals were euthanized. The peritoneal cavities were lavaged with 3 ml ice cold HBSS containing 1% mouse serum, and neutrophil numbers were counted.

Figure 1: Release of ATP by FMLP-stimulated neutrophils and formation of adenosine. (A) ATP released in response to FMLP was determined with high-performance liquid chromatography (HPLC) analysis of extracellular ATP and its breakdown products. A pair of chromatograms shows ATP and its hydrolytic products in the extracellullar environment of neutrophils before (lower trace) or after (upper trace) stimulation with 100 nM FMLP. ADP, adenosine diphosphate. (B) Extracellular concentrations of ATP, AMP, and adenosine measured with HPLC analysis at different time points after stimulation of neutrophils with 100 nM FMLP. (C) Extracellular ATP, AMP, and adenosine at different times after addition of exogenous ATP to isolated neutrophils. Error bars indicate SD of triplicate determinations. (D) Release of ATP from living cells stimulated in a gradient field of FMLP generated with a micropipette (asterisks) was visualized with the use of a two-enzyme assay system that catalyzes the conversion of $NADP^+$ to NADPH in the presence of ATP. The generation of NADPH was monitored in real time by means of fluorescence microscopy (excitation wavelength, 340 nm; emission wavelength, 460 nm). Images were captured at 12 frames per minute. (Inset) Extracellular ATP concentrations based on calibration of gray values with a known ATP standard.

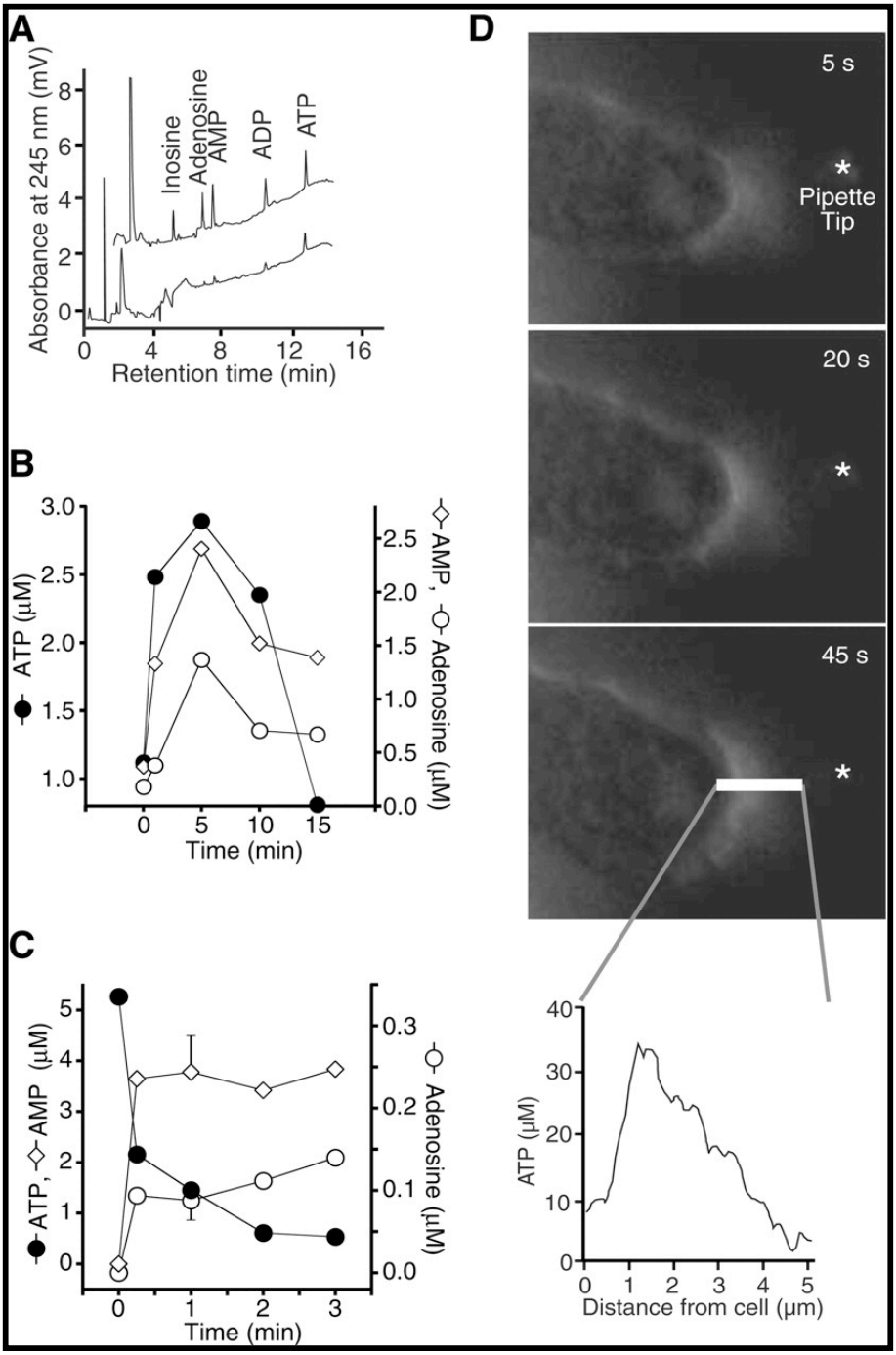

Figure 1: Release of ATP by FMLP-stimulated neutrophils and formation of adenosine

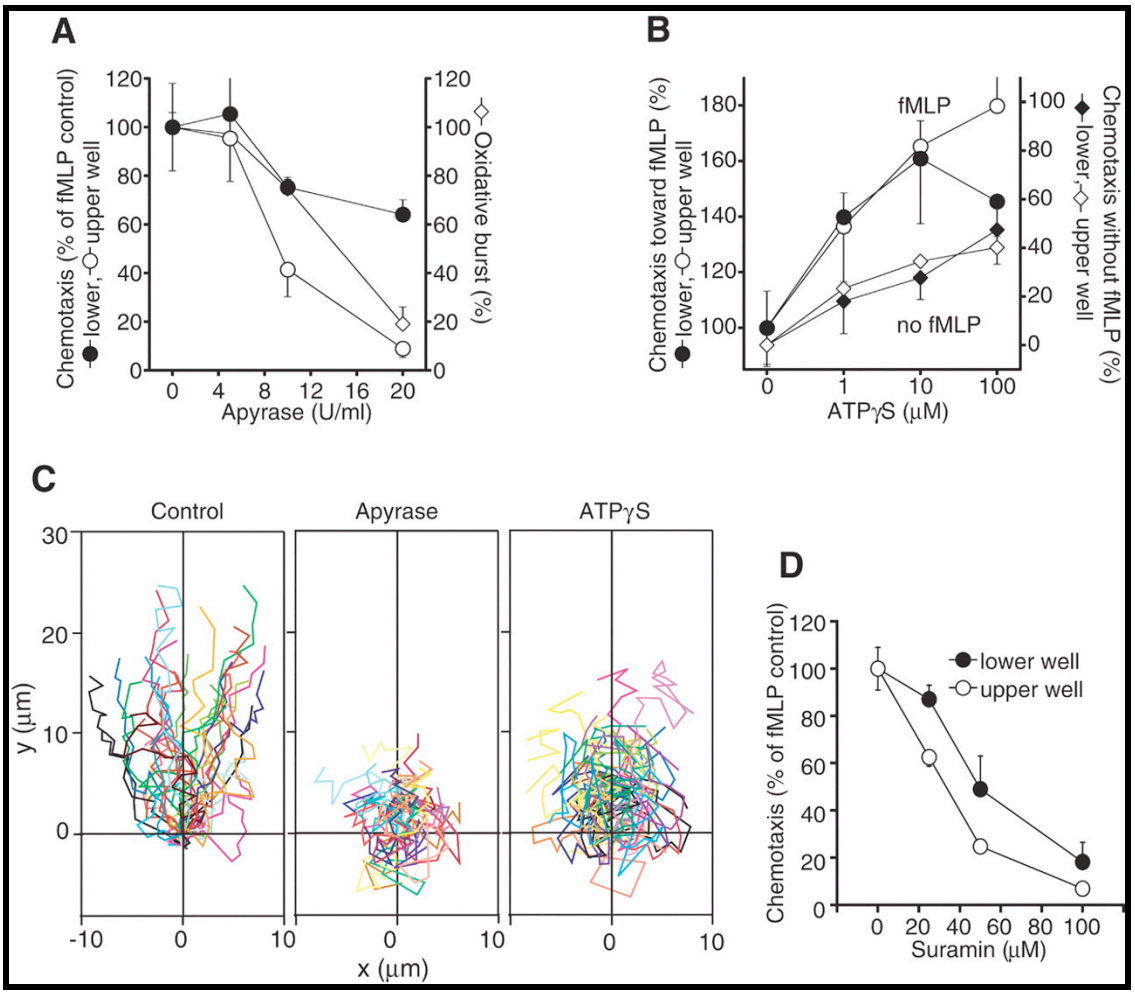

Figure 2: Effect of exogenous ATP on neutrophil chemotaxis. Trans-well assays with neutrophils in upper wells separated from lower wells containing 1 nM FMLP by a filter with 3-μm pore size were used to assess chemotaxis. (A) Effect of apyrase added to the lower or upper well on neutrophil chemotaxis and on FMLP-induced oxidative burst. Cell responses are expressed as a percent of the response to FMLP in the absence of apyrase. (B) Treatment with ATP--S in the presence (circles) or absence (diamonds) of FMLP. (C) Cell migration studied under the microscope was analyzed by tracing the paths of cells migrating toward a micropipette tip containing 100 nM FMLP in the absence (left) or presence (middle) of 10 U/ml of apyrase or 100 μM ATP--S (right). The y axis of the traces represents the direction toward the chemoattractant source, and the x axis shows the deviation from the straight path. Cell traces were arranged to show their origins at x = y =0.(D) Effect of the P2-receptor antagonist suramin on FMLP-induced cell migration. Error bars in (A), (B), and (D) indicate SD of triplicate determinations.

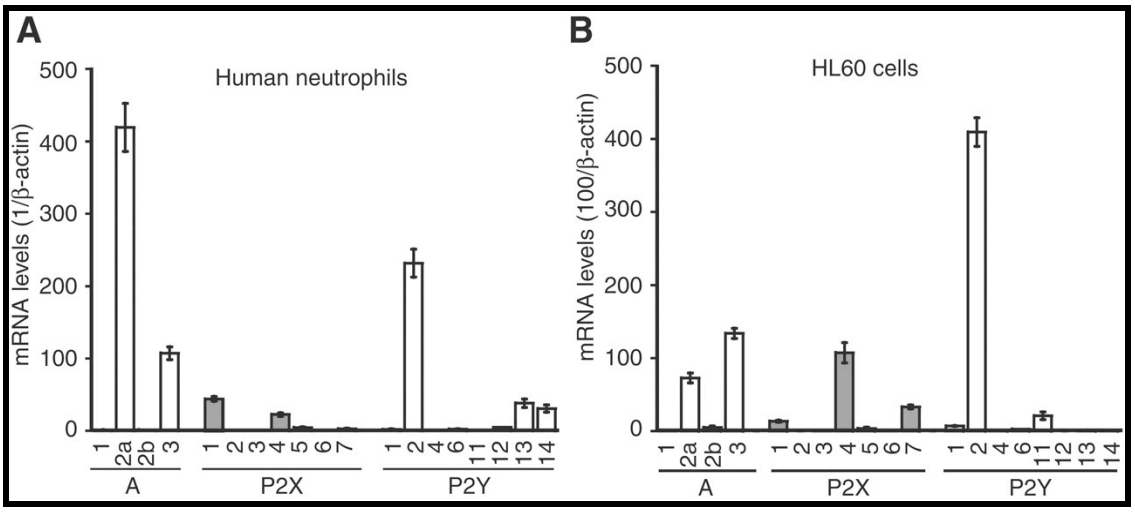

Figure 3: P1- and P2-receptor expression in neutrophils (A) **and HL60 cells** (B)**.** P1- and P2-receptor mRNA expression in human neutrophils and HL60 cells was estimated with real-time RT-PCR analysis and expressed in relation to ß-actin. Error bars in (A) and (B) indicate SD of triplicate determinations**.**

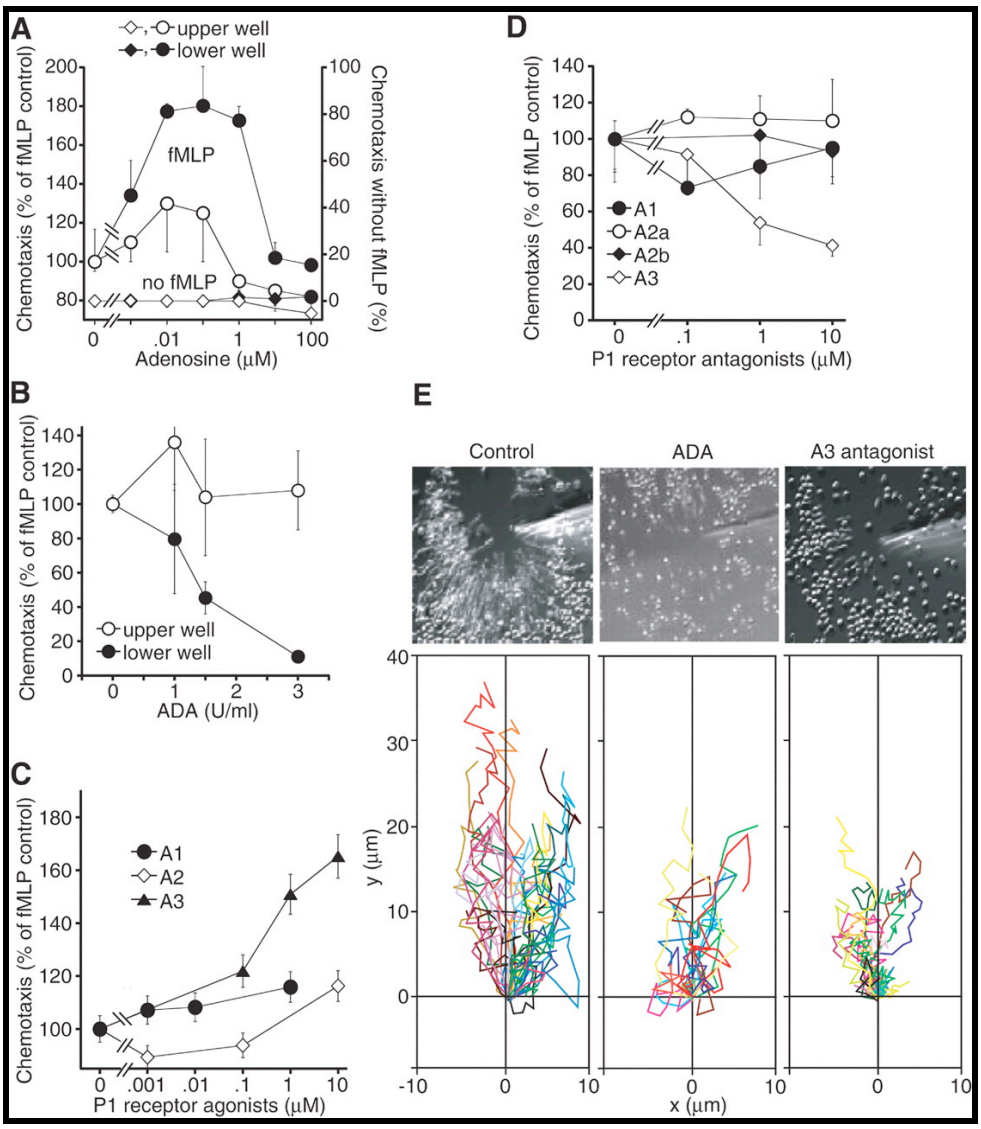

Figure 4: Role of adenosine and P1 receptors in neutrophil migration. (A) The effect of exogenous adenosine added to the lower or upper wells on neutrophil chemotaxis was assessed with the trans-well assay in the presence (circles) or absence (diamonds) of FMLP. (B) Effect of ADA on FMLP-induced chemotaxis. (C) Effects of the A3-receptor–selective agonist N(6)-(3-iodobenzyl) adenosine-5'-N-methylcarboxamide (IB-MECA) and of the A2- and A1-receptor–selective agonists 2-p-[2-carboxyethyl] phenethylamino-5'-N-ethylcarboxamidoadenosine hydrochloride (CGS 21680) and N6-cyclopentyladenosine (CPA), respectively, on chemotaxis toward FMLP. (D) Effects of A3-receptor–selective antagonist MRS 1191 and antagonists of other P1 receptors on chemotaxis toward FMLP. (E) Composite images and cell migration traces of cells migrating toward a micropipette tip containing 100 nM FMLP in the absence or presence of 10 U/ml of ADA or 10 μM MRS 1191. Error bars in (A) to (D) indicate SD of triplicate determinations.

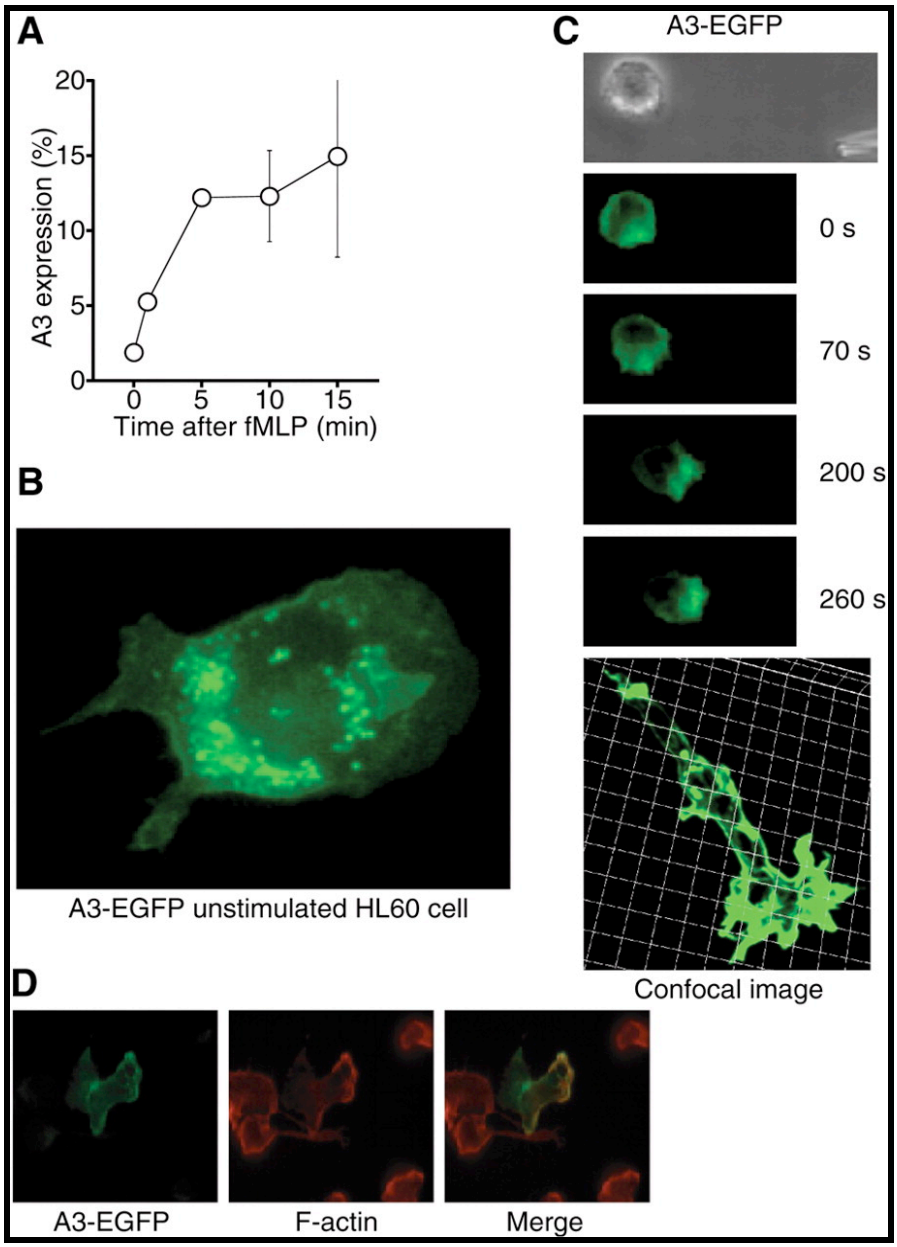

Figure 5: Localization of A3 receptors to the leading edge of migrating cells. (A) The cell surface expression of A3 receptors of human neutrophils at different time points after stimulation of cells with 100 nM FMLP was assessed with flow cytometry and a primary antibody recognizing an extracellular domain of the receptor. Error bars indicate SD of triplicate determinations. (B) Fluorescent image of an unstimulated HL60 cell expressing an A3-EGFP fusion protein. (C) HL60 cell expressing an A3-EGFP fusion protein migrating toward a micropipette tip containing 100 nM FMLP (bright field image on top). The confocal image at the bottom shows an HL60 cell migrating from the top left to the bottom right corner. (D) Colocalization of A3-EGFP fusion protein and actin in cells globally stimulated with 100 nM FMLP.

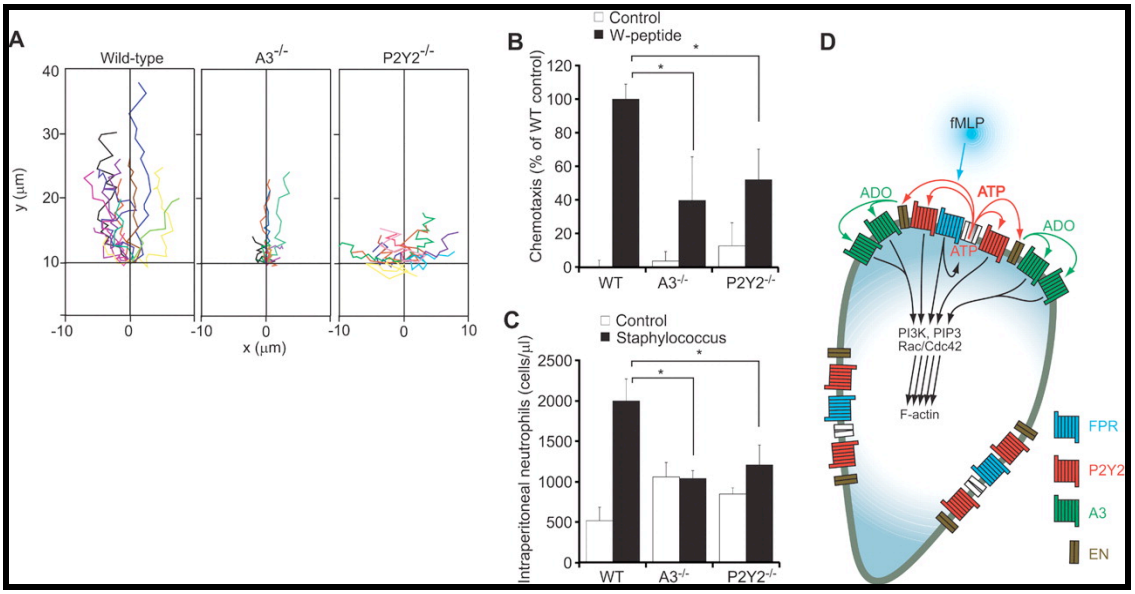

Figure 6: P2Y2 and A3 receptors control neutrophil chemotaxis in vitro and in vivo. (A) Migration paths of neutrophils [isolated from the bone marrow of wild-type (WT) mice and mice deficient of A3 and P2Y2 receptors] migrating toward the FMLP-receptor ligand W-peptide (100 nM). (B) Trans-well chemotaxis assays of neutrophils from $A3^{-/-}$, $P2Y2^{-/-}$, and WT mice toward W-peptide (100 nM). *, $P < 0.0001$ [analysis of variance (ANOVA) and Newman-Keuls multiple-comparison test, n = 6 mice per group]. (C) In vivo cell migration was assessed in WT mice and in A3 and P2Y2 KO mice by counting neutrophils in the peritoneal cavity 4 hours after intraperitoneal injection of 10^8 living Staphylococcus bacteria (solid bars) or vehicle (open bars). *, $P < 0.0001$ (ANOVA and Newman-Keuls multiple-comparison test, n = 6 animals per group). (D) Roles of ATP release, P2Y2, and A3 receptors in neutrophil chemotaxis: Activation of the formyl-peptide receptor (FPR) stimulates localized ATP release, resulting in activation of nearby P2Y2 receptors that amplify chemotactic signals and gradient sensing by stimulating the production of phosphoinositide 3-kinase (PI3K), phosphatidylinositol 3,4,5-trisphosphate (PIP3), and recruitment of Rac, Cdc42, and F-actin to the leading edge. Translocation of A3 receptors to the leading edge, adenosine (ADO) formation by ecto-ATPases/nucleotidases (EN), and autocrine activation of A3 receptors facilitate directed migration. Error bars in (B) and (C) indicate SD.

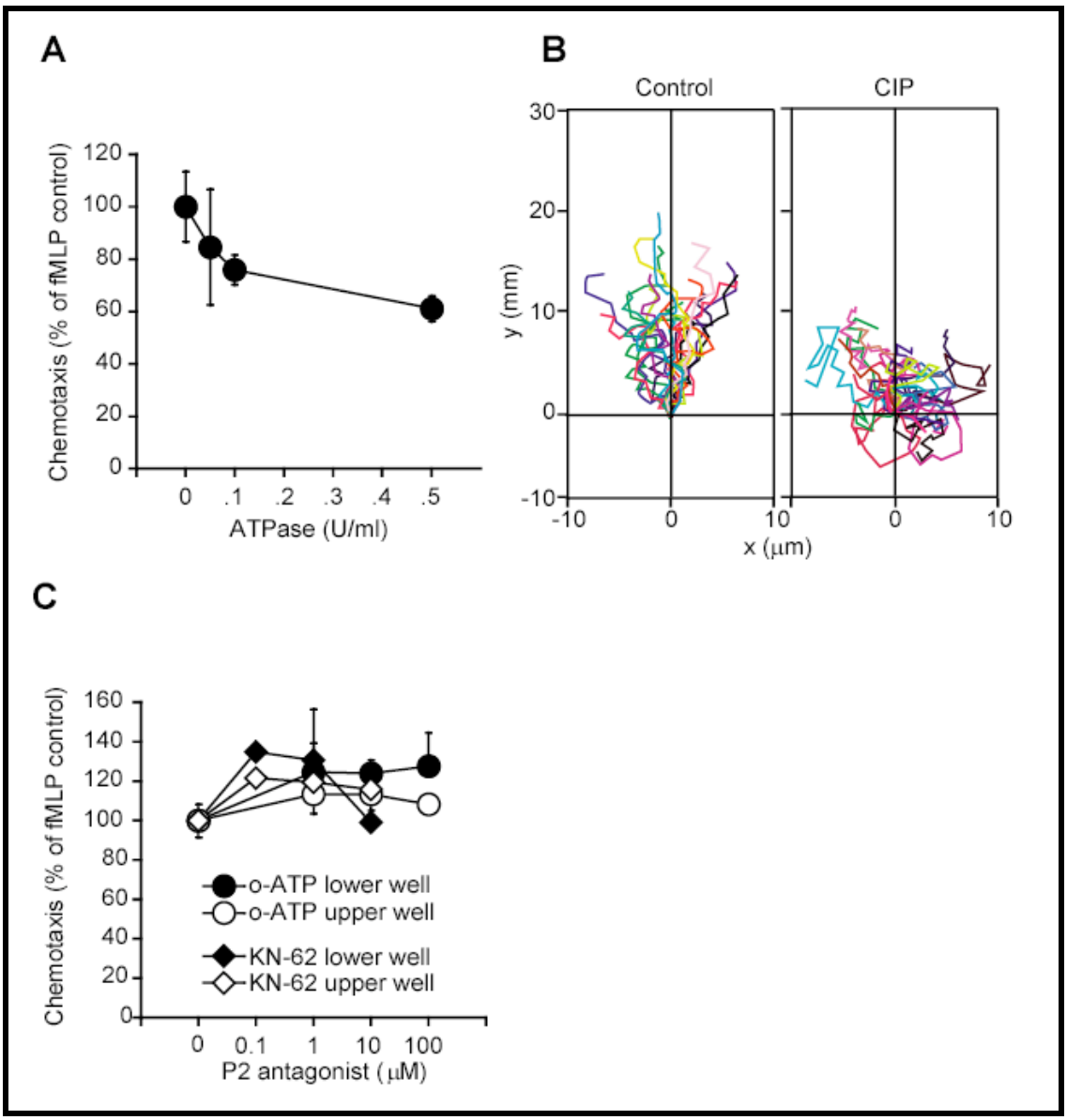

Figure 7: (Supplemental) ATPase and alkaline phosphatase hydrolyze ATP and impair neutrophil chemotaxis. (A) Effect of ATPase (porcine cerebral cortex) on the chemotaxis of human neutrophils towards fMLP assessed with the transwell assay. (B) Cell traces of human neutrophils migrating towards a micropipette tip containing 100 nM fMLP in the absence (left) or presence of 10 U/ml phosphatase (calf intestine; CIP). (C) Effect of the P2X specific P2 receptor antagonists 1-[N,O-bis(5-isoquinolinesulphonyl)-N -methyl-Ltyrosyl]-4-phenylpiperazine (KN-62) and oxidized ATP (o-ATP) on neutrophil chemotaxis using transwell assays with antagonists loaded in either the upper or lower wells.

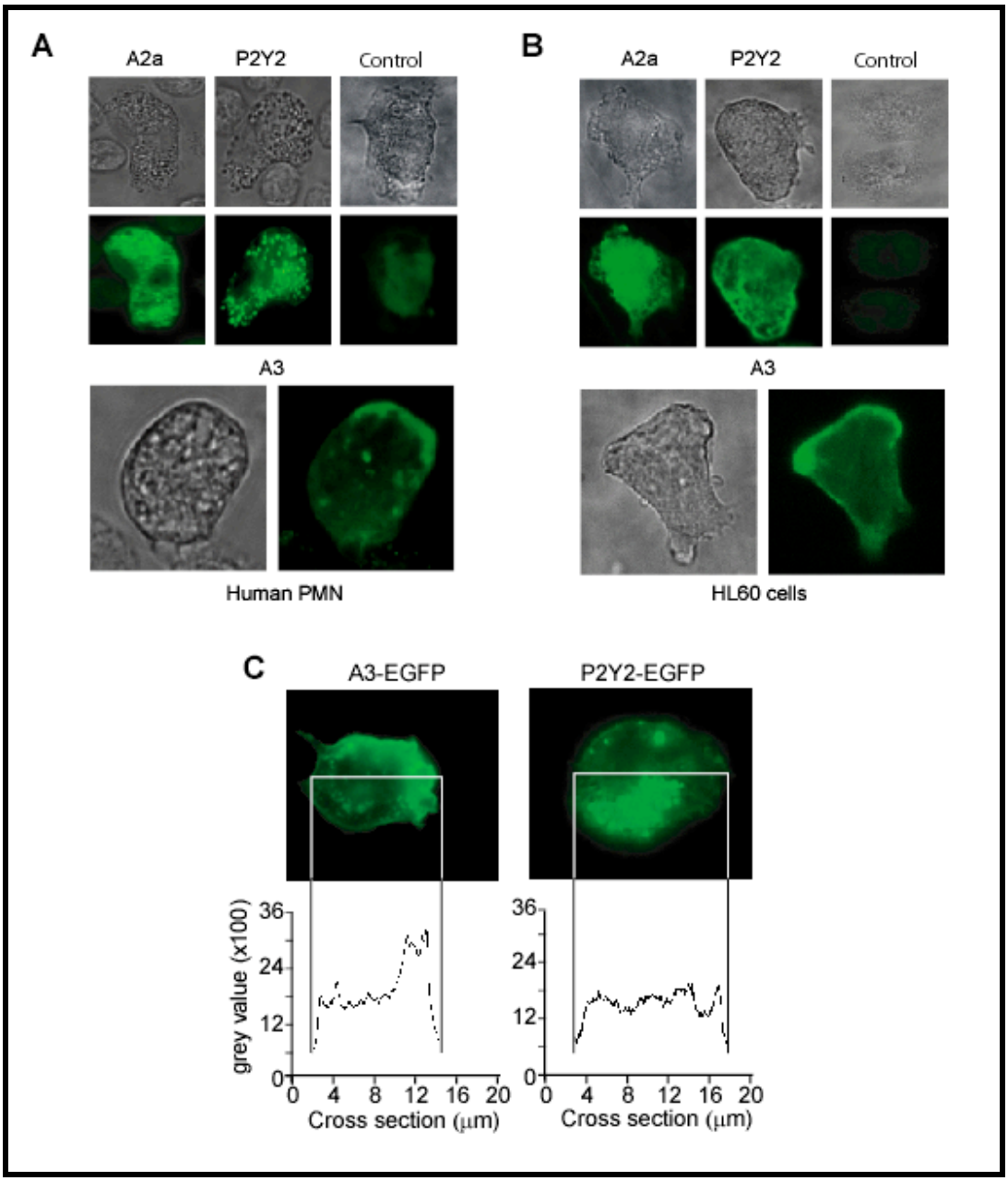

Figure 8: (Supplemental) P1 and P2 receptor localization in polarized human neutrophils and HL60 cells. (A) Immunostaining of A2a, A3, and P2Y2 receptors in neutrophils using fixed purified human neutrophils (A) or HL60 cells (B) uniformly stimulated with 100 nM fMLP prior to fixation. Images were arranged to show cells with their leading edges oriented upwards. (C) Images of HL60 cells expressing A3-EGFP (left) or P2Y2-EGFP fusion protein (right) migrating towards a micropipette tip filled with 100 nM fMLP (at right of the images). Insets show density slice of cross sections along the cell axes.

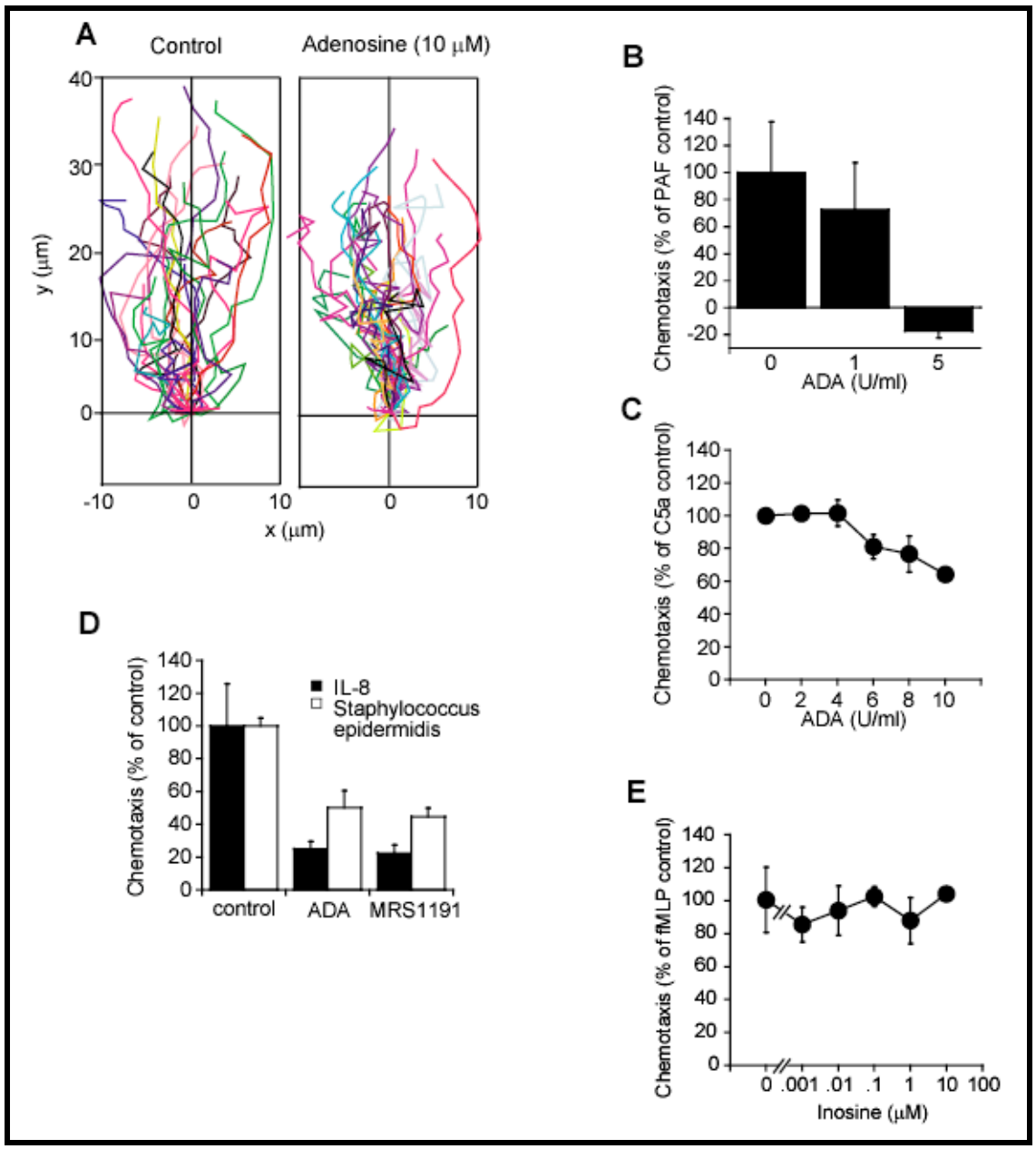

Figure 9: (Supplemental) Roles of adenosine and A3 receptors in chemotaxis. (A) Effect of 10 μM adenosine on traces of human neutrophils migrating towards fMLP analyzed with the microscope assay. (B-D) Effect of ADA or the A3 receptor antagonist MRS 1191 on chemotaxis of human neutrophils towards 100 nM platelet activating factor (PAF), C5a (3% zymosan-activated autologous serum), 2 ng/ml IL-8, or 106/ml living Staphylococcus epidermidis (ADA, 10 U/ml; MRS 1191, 10 μM) added together with drugs to the lower wells. (E) Effect of inosine added to the lower well of the transwell system on chemotaxis of human neutrophils toward 100 nM fMLP.

Acknowledgements for thesis:

Chapter 5, in full, is a reprint of the material as it appears in Science, December 2006, Corriden, Ross*; Chen, Yu*; Inoue, Yoshiaki; Yip, Linda; Hashiguchi, Naoyuki; Zinkernagel, Annelies; Nizet, Victor; Insel, Paul A.; Junger, Wolfgang G.; Dec 15;**314**(5816):1792-5. The dissertation author was one of two co-primary investigators and authors of this paper (*co-first author credit given).

Chapter 6

Ecto-nucleoside triphosphate-diphosphohydrolase (E-NTPDase1/CD39) regulates neutrophil chemotaxis by hydrolyzing released ATP to adenosine

Citation: Corriden R, Chen Y, Inoue Y, Beldi G, Robson S, Insel PA, Junger WG. ECTO-nucleoside triphosphate-diphosphohydrolase 1 (E-NTPDASE1/CD39) regulates neutrophil chemotaxis by hydrolyzing released ATP to adenosine. *J Biol Chem.* 2008 Aug 19. [Epub ahead of print]

Abstract

Polymorphonuclear neutrophils (PMN) release ATP in response to stimulation by chemoattractants, such as the peptide N-formyl-met-leu-phe (fMLP). Released ATP and the hydrolytic product adenosine regulate chemotaxis of PMN by sequentially activating P2 and P1 receptors, respectively. Here we show that that ecto-nucleoside triphosphate-diphosphohydrolase 1 (E-NTPDase1, CD39) is a critical enzyme for hydrolysis of released ATP by PMN and for cell migration in response to multiple agonists (fMLP, IL-8 and C5a). Upon stimulation of human PMN or differentiated HL-60 cells in a chemotactic gradient, E-NTPDase1 tightly associates with the leading edge of polarized human PMN and differentiated HL-60 cells during migration in a chemotactic gradient. Inhibition of E-NTPDase1 reduces the migration speed of PMN but not their ability to detect the orientation of the gradient field. Studies of PMN from E-NTPDase1 knockout

mice reveal similar impairments of chemotaxis in vitro and in vivo. Thus, E-NTPDase1 plays an important role in regulating chemotaxis of PMN by facilitating the hydrolysis of extracellular ATP.

Release of ATP from cells and subsequent activation of plasma membrane P2 (purinergic/nucleotide) receptors play important physiological roles in many cell types (1,2,3,4,5). In addition to functioning as an autocrine/paracrine molecule that regulates cell physiology, ATP can be hydrolyzed by ecto-ATPases to generate adenosine (6, 7), which regulates cell function by the activation of P1 receptors (1). P1 receptors are G-protein-coupled receptors (GPCR) while P2 receptors are of two types: P2Y receptors, which are GPCRs, and P2X receptors, which have ion channel activity (1). Release of ATP by human polymorphonuclear neutrophils (PMN) and activation of P2Y receptors by ATP and of P1 receptors by adenosine play a critical role in chemotaxis of PMN (8). ATP is released in a polarized manner at the leading edge of cells and amplifies chemotactic gradient signals by autocrine/paracrine feedback through P2Y2 receptors. Adenosine formed from released ATP stimulates cell migration towards the chemoattractant by activation of A3 adenosine receptors that accumulate at the leading edge of polarized PMN (8). The precise mechanisms by which PMN release and hydrolyze ATP, thereby regulating the responsiveness of P2Y2 receptors and generating adenosine, have not been identified.

Several families of ecto-ATPases hydrolyze extracellular nucleotides in eukaryotic cells. The largest family, the ecto-nucleoside triphosphate diphosphohydrolases (E-NTPDases), consists of eight members (E-NTPDase1-8), which hydrolyze nucleotide triphosphates and diphosphates to monophosphates (10). The ecto-

nucleotide pyrophosphatase/phosphodiesterases (E-NPPs) are the second largest family; these enzymes also hydrolyze nucleotide triphosphates to monophosphates and, in addition, they can convert cAMP to adenosine (11). Alkaline phosphatases (ALPs) are another family of ecto-ATPases, of which four isoforms have been identified (6); and finally, ecto-5í-nucleotidase (CD73), comprising one member only, catalyzes the conversion of AMP to adenosine (12).

In the current study we show that E-NTPDase1, which is also known as CD39, is expressed and catalyzes the hydrolysis of extracellular ATP by PMN and that this hydrolysis plays a critical role in chemotaxis.

EXPERIMENTAL PROCEDURES

Materials: All chemicals were obtained from Sigma (St. Louis, MO) unless otherwise noted. Monoclonal anti-tissue non-specific ALP antibody was obtained from Abcam (Cambridge, MA). Alexa Fluor 488 goat anti-mouse IgG secondary antibodies were obtained from Invitrogen (Carlsbad, CA).

PMN isolation: The BIDMC and UCSD Human Research Programs approved all experiments undertaken in this study. PMN were isolated from the peripheral blood of healthy volunteers as described previously (13). Briefly, blood was treated with 5% Dextran-500, dissolved in normal saline, and allowed to sediment at room temperature for 30 min. The cells in the supernatant were then separated by Percoll gradient centrifugation and washed as previously described (13).

HPLC analysis of extracellular nucleotides: Cell culture supernatants were collected and analyzed using HPLC as described previously (8). Nucleotides were identified and their concentrations estimated using their retention times as compared to known standards.

Malachite green assay: Solutions of malachite green (0.812 g/l deionized H2O), ammonium molybdate (0.3 M in 6N HCl), and polyvinyl alcohol (23.2 g/l H2O) were prepared as described previously (14). To produce the assay solution, 4 ml malachite green solution was mixed with 2 ml each of the ammonium molybdate and polyvinyl alcohol solutions. The supernatants of cell suspensions were collected and mixed at a ratio of 1:1 with the malachite green assay solution. After incubation at room temperature for 5 min, samples were analyzed in a plate reader at 650 nm and compared to a KH_2PO_4 standard curve to obtain the concentration of inorganic phosphate.

Immunofluorescence staining: PMN (2.5×10^6/ml) were plated on glass coverslips and stimulated with 100 nM N-formyl-methionyl-leucyl-phenylalanine (fMLP) for 10 min. The cells were permeabilized for 5 min with 0.1% Triton X-100, fixed with 3.7% paraformaldehyde in phosphate-buffered saline (PBS; Irvine Scientific) for 10 min at room temperature, and stained with antibodies using 500 ng/ml anti-tissue nonspecific ALP, 500 ng/ml anti-NTPDase1, and 4 μg/ml Alexa 488 goat anti-mouse IgG secondary antibodies, as described previously (9).

Real-time RT-PCR: Total RNA was extracted from PMN using a Trizol extraction

method (Invitrogen, Carlsbad, CA). First strand cDNA was synthesized using Superscript II RNase H-Reverse Transcriptase (Invitrogen). Real-time RT-PCR was performed using primer sets and the QuantiTect SYBR Green PCR kit from Qiagen (Hilden, Germany) and the DNA Engine Opticon 2 Real-Time PCR detection system (BioRad, Hercules, CA). The comparative method for relative quantification of gene expression (Ct method) was used and expression levels were normalized to β-actin mRNA levels.

In vitro chemotaxis assay by microscopy: PMN (2.5 x10^6/ml) were plated on 25 mm glass coverslips (Fisher Scientific, Pittsburgh, PA) coated with 50 mg/ml human fibronectin and placed into a temperature-controlled stage incubator (Harvard Apparatus, Holliston, MA) at 37°C. Cells were treated as described below and exposed to a chemotactic gradient generated by the release of 10 nM fMLP using a micropipette tip attached to a FemtoJet injector (Eppendorf, Hamburg, Germany). Cell migration was tracked by acquiring 20 sequential images in 25-s intervals.

In vitro transwell chemotaxis assay: Chemotaxis assays in a transwell system were performed using a 96 well MultiScreen MIC plate (Millipore, Billerica, MA) with a pore size of 3.0 μm. A 100 μl suspension of 1 x10^6 PMN in HBSS, with or without 100 μM ARL-67156, was added to each well of the upper filter plate. Chemoattractants, either 10 nM fMLP, 10 ng/ml IL-8, or 10% zymosan-activated serum (C5a), were added to each of the lower wells (150 μl final volume). After incubation at 37°C for 30 min, the upper plate was removed and lysed by addition of 10 μl of a buffer (500 mM Tris/Hcl and 1M NaCl, pH 7.4) containing 0.5% (v/v) Triton X-100. Reactions were started by the

addition of the chromogenic substrate N-methoxysuccinyl-Ala-Ala-Pro-Val-p-nitroanilide (final concentration, 1 mM). After 30 min at room temperature, the change in optical density was measured at a wavelength of 405 nm.

In vivo chemotaxis assay: Chemotaxis of PMN was assessed in wild-type (WT) and CD39-knockout (KO) mice as described previously (8). Briefly, one milliliter of a 1 nM solution of the mouse FPR ligand WKYMVM (W-peptide; Phoenix Pharmaceuticals, Belmont, CA) in normal saline was injected intraperitoneally. After 2 h, mice were euthanized, peritoneal cavities lavaged with 3 ml ice cold HBSS containing 1% mouse serum, and leukocyte number was counted.

RESULTS

Hydrolysis of extracellular nucleotides by PMN: Human PMN release ATP in response to stimulation with fMLP and the released ATP and its hydrolytic product adenosine regulate polarization and migration of PMN (8). To evaluate the hydrolysis of extracellular nucleotides by PMN, we added ATP, ADP, or AMP (100 μM) to PMN (5x106 in 0.25 ml HBSS) and used HPLC to assess the concentrations of each nucleotide and their hydrolytic products after different incubation periods at 37∫C. We found that PMN hydrolyzed 100 μM ATP by >80% within 10 min; AMP concentrations increased correspondingly but concentrations of ADP remained low and changed little over time (Fig. 1A). These results imply that PMN hydrolyze extracellular ATP directly to AMP, generating negligible amounts of ADP in the process. Such catalytic properties are characteristic of E-NTPDase1 (6). Consistent with a role for this enzyme in ATP

hydrolysis, we found that PMN efficiently hydrolyze extracellular ADP, reducing 100 μM ADP by ~60% within 10 min of incubation at 37°C (Fig. 1B). By contrast, PMN hydrolyzed <10% of 100 μM AMP under similar incubation conditions (Fig. 1C). Hydrolysis of AMP is thus a rate-limiting step in the generation of extracellular adenosine by PMN.

Real-time RT-PCR evaluation of ecto-nucleotidase expression: In order to determine which nucleotide-hydrolyzing enzyme(s) might mediate the hydrolysis of ATP, we used real-time RT-PCR analysis to evaluate the expression of ecto-nucleotidases in PMN and HL-60 cells, which were differentiated to a neutrophil-like phenotype (Fig. 2). Based on the enzymatic activities determined above (Fig. 1), we focused our attention on members of the E-NTPDase enzyme family, which catalyze hydrolysis of ATP and ADP but not AMP, and on enzymes that generate adenosine (6). We detected the expression of two E-NTPDases that hydrolyze ATP to AMP (E-NTPDase1 and E-NTPDase2), and tissue-nonspecific ALP, which, among other activities, hydrolyzes AMP to adenosine (6). We also found expression of two members of the E-NPP family (E-NPP1 and E-NPP2), although only one of these enzymes, E-NPP2, was expressed at significant levels. The relative expression levels of ecto-nucleotidases in differentiated HL-60 cells were similar to those in PMN with dominant mRNA expression of both E-NTPDase1 and E-NTPDase2 (Fig. 2B). HL-60 cells did not express tissue-nonspecific ALP but showed a higher relative expression of E-NPP2. E-NTPDase4 was highly expressed in both cell types (data not shown); however, this enzyme hydrolyzes UTP and UDP but not ATP (10).

Kinetics of extracellular nucleotide breakdown by PMN: Four of the eight known

E-NTPDases (E-NTPDase1, 2, 3, and 8) hydrolyze ATP (6). Each is also capable of hydrolyzing ADP but the relative efficiency of breakdown of ATP vs. ADP varies among the isoforms. Thus, the E-NTPDases can be distinguished by their enzymatic activity in hydrolyzing ATP vs. ADP. As shown above, we found that two E-NTPDases, E-NTPDase1 and 2, are expressed by human PMN. The relative efficiency of ATP vs. ADP breakdown by E-NTPDase1 is 1.0 vs. 0.5-0.9 (18, 19, 20), whereas E-NTPDase2 has a stronger preference for ATP with a relative efficiency ratio of 1:0.03 (21, 22, 23). In order to determine whether E-NTPDase1 or 2 is more important for the hydrolysis of extracellular ATP by PMN, we examined the initial rates of hydrolysis of ATP and ADP (Fig. 3) and used Lineweaver-Burke plots to derive Km and Vmax values. PMN hydrolyzed ATP more effectively (Km = 20.9 μM, Vmax = 9.48 μmol Pi/min/10^6 cells) than ADP (Km = 12.8 μM, Vmax = 1.78 μmol Pi/min/10^6 cells). The enzymatic efficiencies for breakdown of ATP and ADP, derived by dividing Vmax by Km, yielded a ratio of 1:0.31. This result implies that E-NTPDase1 likely plays a dominant role in the hydrolysis of extracellular ATP by PMN. Differentiated HL-60 cells also hydrolyzed ATP more effectively (Km = 2.46 μM, Vmax = 0.96 μmol Pi/min/10^6 cells) than ADP (Km = 1.49 μM, Vmax = 0.23 μmol Pi/min/10^6 cells). HL-60 cells, while overall not as efficient at hydrolyzing extracellular nucleotides as PMN, showed similar relative enzyme efficiencies for the breakdown of ATP and ADP (1:0.38).

PMN also hydrolyze AMP to adenosine, however at a much slower rate (Fig. 3A, inset), which made it not possible to calculate Km and Vmax. Under identical conditions, HL-60 cells did not exhibit sufficient AMP hydrolysis to generate a detectable signal.

Inhibition of E-NTPDase1 blocks ATP hydrolysis: To further test whether E-NTPDase1

preferentially mediates the hydrolysis of extracellular ATP by PMN, we used two inhibitors of this enzyme: NaN3, which inhibits E-NTPDase1 (24), and ARL67156, which inhibits E-NTPDase1 and 3 (25). Both NaN3 and ARL67156 inhibited ATP hydrolysis in a concentration-dependent manner (Fig. 4). Thus, the real-time RT-PCR results, the kinetics of enzyme activity, and the results with E-NTPDase inhibitors are all consistent with the conclusion that E-NTPDase1 plays an important role in the hydrolysis of extracellular ATP by human PMN.

Inhibitors of E-NTPDase1 inhibit PMN chemotaxis: We assessed the contribution of E-NTPDase1-mediated hydrolysis of ATP to the regulation of chemotaxis of human PMN. Purified PMN migrated towards a point source of fMLP at an average speed of 4.7±1.1 μm/min with an accuracy of gradient sensing, such that 94% of cells migrated towards the chemotactic source on paths that did not deviate >30° from a straight line (Fig. 5A). Inhibitors of ATP hydrolysis reduced the migration speed of PMN. ARL67156 reduced the average migration speed by 75% (1.2±0.6 μm/min) but most cells (83%) maintained their migration path within 30° of a straight line towards the chemotactic source, indicating that gradient sensing is not substantially altered by inhibiting ATP hydrolysis. NaN3 also inhibits NTPDase1 activity; it reduced the average migration speed by 66% (1.6±0.6 μm/min), while leaving gradient sensing largely intact (85% of cells maintained a correct migration path). The reduction in cell migration speed produced by the inhibitors leads us to conclude that a function of E-NTPDase1 is to regulate the velocity of PMN during chemotaxis.

To evaluate the ability of E-NTPDase1 activity on PMN migration to influence response to multiple classes of chemoattractants, we assessed the effect of ARL67156 on

migration towards fMLP, IL-8, and zymosan-activated serum (C5a) using a transwell assay system. Treatment with ARL67156 substantially reduced the PMN migration by all 3 classes of agonists (Fig 5B). Thus E_NTPDase1 modulates PMN chemotaxis in response to multiple types of chemoattractants.

E-NTPDase1 is localized to the leading edge of migrating PMN and HL-60 cells: Given the functional role of E-NTPDase1 in regulating PMN chemotaxis, we used immunocytochemistry to determine the localization of this enzyme in human PMN. PMN were plated onto glass coverslips and stimulated with 10 nM fMLP for 2.5 min at 37°C prior to fixation and staining with E-NTPDase1 antibodies. In 82% of polarized PMN, we observed accumulation of E-NTPDase1 at the leading edge (Fig. 6A); we found similar results in differentiated HL-60 cells (Fig. 6B). Thus E-NTPDase1 is recruited to the leading edge during cell polarization. At the leading edge, this ecto-ATPase then hydrolyzes ATP that is most prominently released at this site during cell migration (8).

E-NTPDase1 knockout mice show impaired PMN migration: To study the role of E-NTPDase1 in the migration of PMN in an in vivo setting, we assessed the influx of PMN into the abdominal cavities of E-NTPDase1- knockout mice and wild-type (WT) controls in response to formyl peptide receptor ligand W-peptide injected into the peritoneal cavity as described previously (8). Compared to an injection of saline vehicle control, injection of W-peptide increased the number of PMN that migrated in the peritoneal cavities of WT mice by 1.8-fold, while this response was significantly reduced in E-NTPDase1 knockout mice (Fig. 7A).

Impaired migration of PMN from E-NTPDase1 knockout mice was also observed in vitro using PMN isolated from the bone marrow of WT and E-NTPDase1 knockout

mice. The average migration speed of PMN from E-NTPDase1 knockout mice (0.11±0.13 μm/min) was 80% slower than that of PMN from WT controls (0.52±0.15 μm/min) but PMN from the knockout and WT mice showed no difference in their ability to polarize and migrate in the correct direction (Fig. 7B).

DISCUSSION

The results presented here extend previous findings regarding the role of polarized ATP release and the activation of P1/P2 receptors in the regulation of PMN chemotaxis (8) to include an additional important step that determines the chemotactic response: extracellular ATP hydrolysis. The current data showing the expression, functional role, and cellular localization of E-NTPDase1 (CD39) in PMN indicate that it provides a physiologically important contribution to ATP hydrolysis in those cells. E-NTPDase1 also modulates platelet function (28) and controls endothelial cell function and permeability (29). Moreover, E-NTPDase1 has been shown to be expressed in PMN (30). Together with our current findings, such data imply that E-NTPDase1 may be a general mechanism by which cells modulate the availability of extracellular ATP and adenosine for activation of purinergic receptors and perhaps other partners that modulate cellular responses.

Extracellular ATP and adenosine both play critical roles in the polarization and migration of PMN via tightly coordinated processes that involve the activation of P2Y2 and A3 receptors (8). The current data indicate that E-NTPDase1 localizes at the leading edge where most of the ATP released by PMN accumulates (Fig. 8). This suggests a dual role for E-NTPDase1: 1) initiation of adenosine formation, which contributes to directed

migration of PMN and 2) enzymatic hydrolysis and rapid decrease of ATP concentration at the leading edge. An important consequence of the latter effect would be to prevent aberrant polarization of PMN, which would occur by the activation of P2Y2 receptors that are not located at the leading edge, resulting in random migration rather than chemotaxis.

E-NTPDase1 catalyzes the first step in the production of adenosine, which activates A3 receptors, whose translocation to the leading edge of PMN promotes directional movement and defines migration speed (8). Adenosine also activates other receptors of PMN, such as A2a receptors, which are uniformly distributed and may help prevent leading edge formation at the trailing edge of migrating cells. Consistent with these ideas, we find that inhibition of E-NTPDase1 diminishes the migration speed of PMN in a gradient of fMLP. This inhibition is not unique to fMLP-promoted chemotaxis, as inhibition of E-NTPDase also decreases the migration efficiency in response to gradients of IL-8 and C5a. In addition, we find that chemotaxis of PMN in E-NTPDase1 knockout mice is impaired because of greatly reduced migration speed even though gradient sensing is maintained.

Although E-NTPDase1 plays an important role in ATP hydrolysis and PMN function, a second enzyme is required to complete the hydrolysis of ATP to adenosine. In human PMN, ALP, which is known to help regulate functions of neutrophils (31), is a likely candidate. Studies with inhibitors of ALP suggest that the enzyme contributes to the generation of extracellular adenosine and the control of PMN chemotaxis (data not shown). By contrast, differentiated HL-60 cells do not express ALP, although these cells are able to navigate chemotactic gradients. HL-60 cells express E-NPP2, also known as

autotaxin, which can facilitate hydrolysis of AMP to adenosine and thus may perform a similar function as does ALP in PMN (10).

The current data highlight the critical role of E-NTPDase1 in modulation of PMN chemotaxis by regulation of ATP hydrolysis and generation of adenosine both in vitro and in vivo. Accordingly, E-NTPDase1 represents a potential therapeutic target for the treatment of inflammatory diseases that involve the aberrant or excessive accumulation of PMN in inflamed tissues.

FOOTNOTES

*The authors thank Dr. James Feramisco and Dr. Kersi Pestonjamasp for their assistance in analysis of microscopy data. This study was supported in part by National Institutes of Health Grants R01 GM51477, GM60475 (W.G.J.), HL076540 (S.C.R.), and GM66232 (P.A.I.), CDMRP Grant PR043034 (W.G.J.), NIDDK Training Grant DK 07202 (R.C.), and a Novo Nordisk Fellowship (Y.C.).

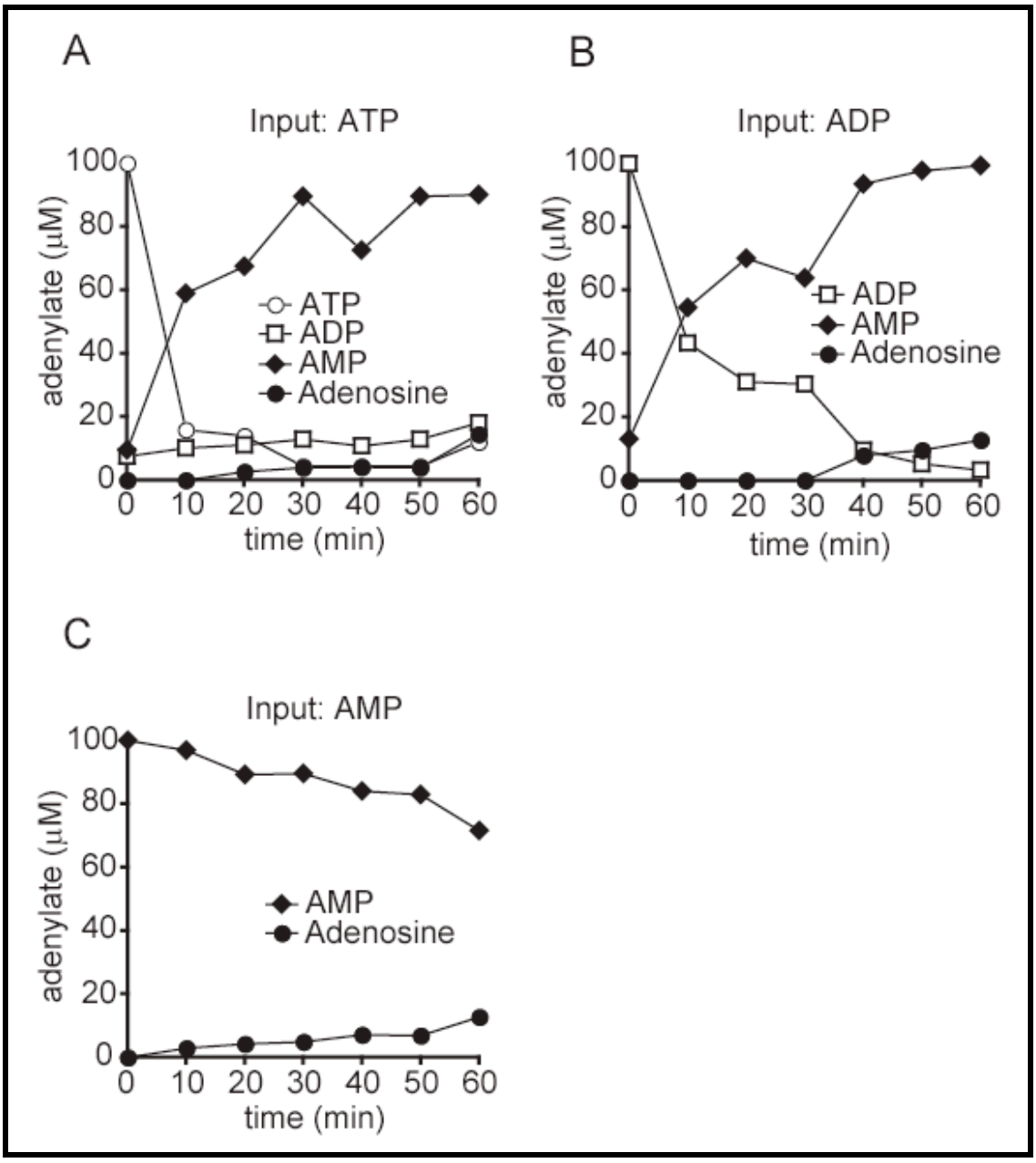

Figure 1: Hydrolysis of nucleotides by human PMN. ATP (A), ADP (B), and AMP (C) were added at final concentrations of 100 μM to a suspension of PMN in HBSS (0.25 ml; 2x107 PMN/ml). ATP and its hydrolytic products were measured by HPLC analysis after incubation at 37∫C for the indicated periods. The data shown are representative of results obtained in 3 separate experiments for each nucleotide.

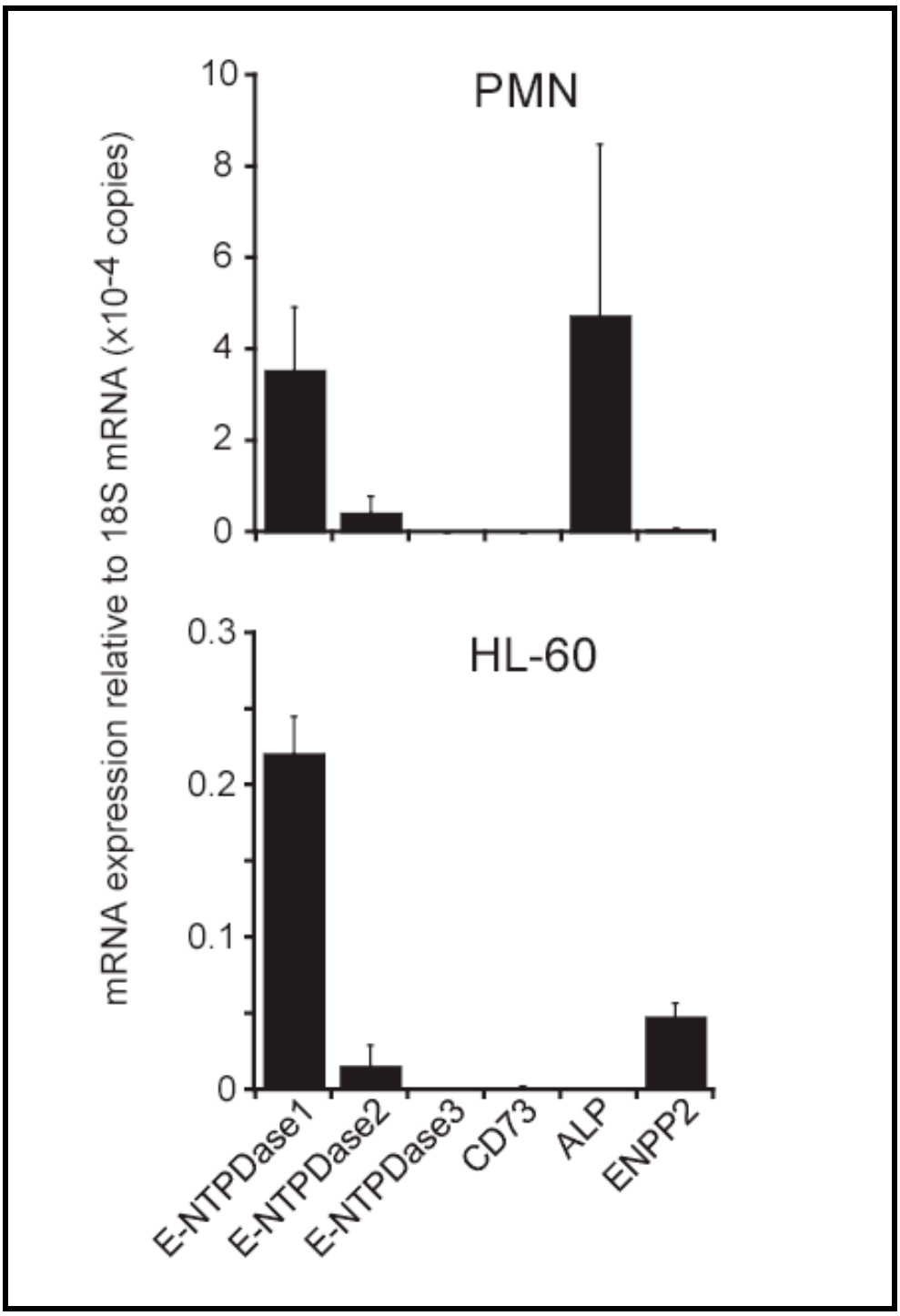

Figure 2: Quantification of mRNA levels of ecto-nucleotidases in PMN and HL60 cells. Real time PCR was used to assess mRNA expression levels (relative to 18S RNA) of ecto-nucleotidases in PMN and differentiated HL60 cells. E-NTPDase8, and ENPPs 3, 4, and 5 were not detected in either cell type. The data shown are mean ± SD for results obtained in 3 separate experiments.

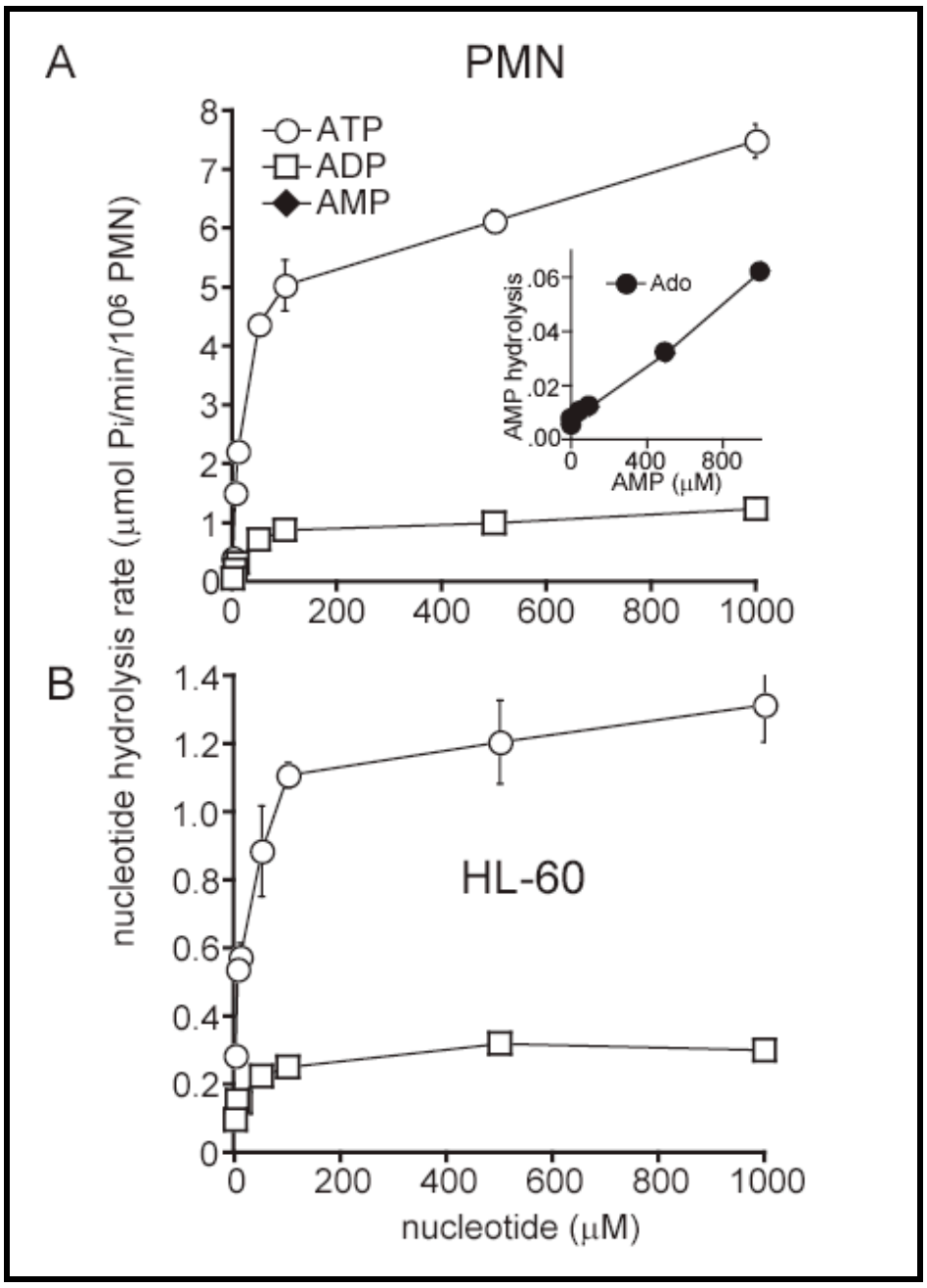

Figure 3: Kinetics of nucleotide hydrolysis by PMN and HL60 cells. Varying concentrations of ATP, ADP, and AMP were incubated with 106 PMN/ml (A) or 106 HL60 cells/ml (B) and inorganic phosphate production was assayed as indicated in Methods. The initial reaction velocity of nucleotide hydrolysis was measured for each concentration. Data in the text for Km and Vmax were derived by Lineweaver-Burke analysis. AMP hydrolysis by PMN is shown in the inset of panel A. Data for AMP hydrolysis by HL-60 cells are not shown because such hydrolysis occurred at too low a rate to be detected. The data shown represent mean ± SD for 3 separate experiments.

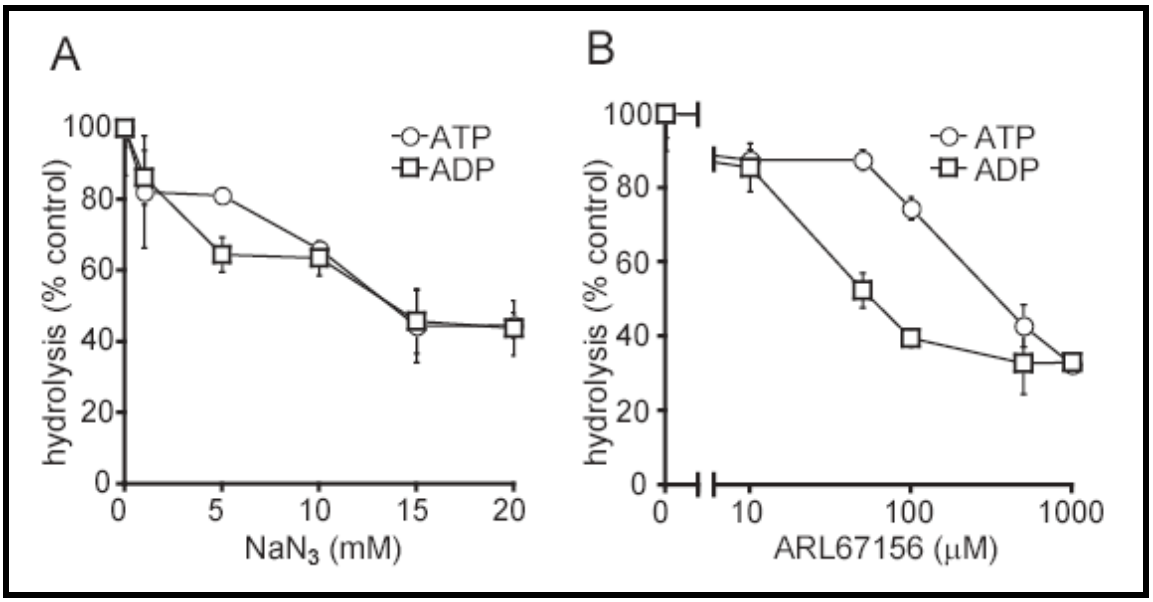

Figure 4: Inhibitors of E-NTPDase1 decrease nucleotide hydrolysis by PMN. PMN (106/ml in HBSS) were incubated at 37∫C for 15 min with increasing concentrations of NaN3, an inhibitor of E-NTPDase1 (A) or ARL67156, an inhibitor of E-NTPDases1 and 3 (B). Hydrolysis of 100 μM of the indicated nucleotides was assessed after a further 10 min using the malachite green assay. The data shown represent mean ± SD for 3 separate experiments.

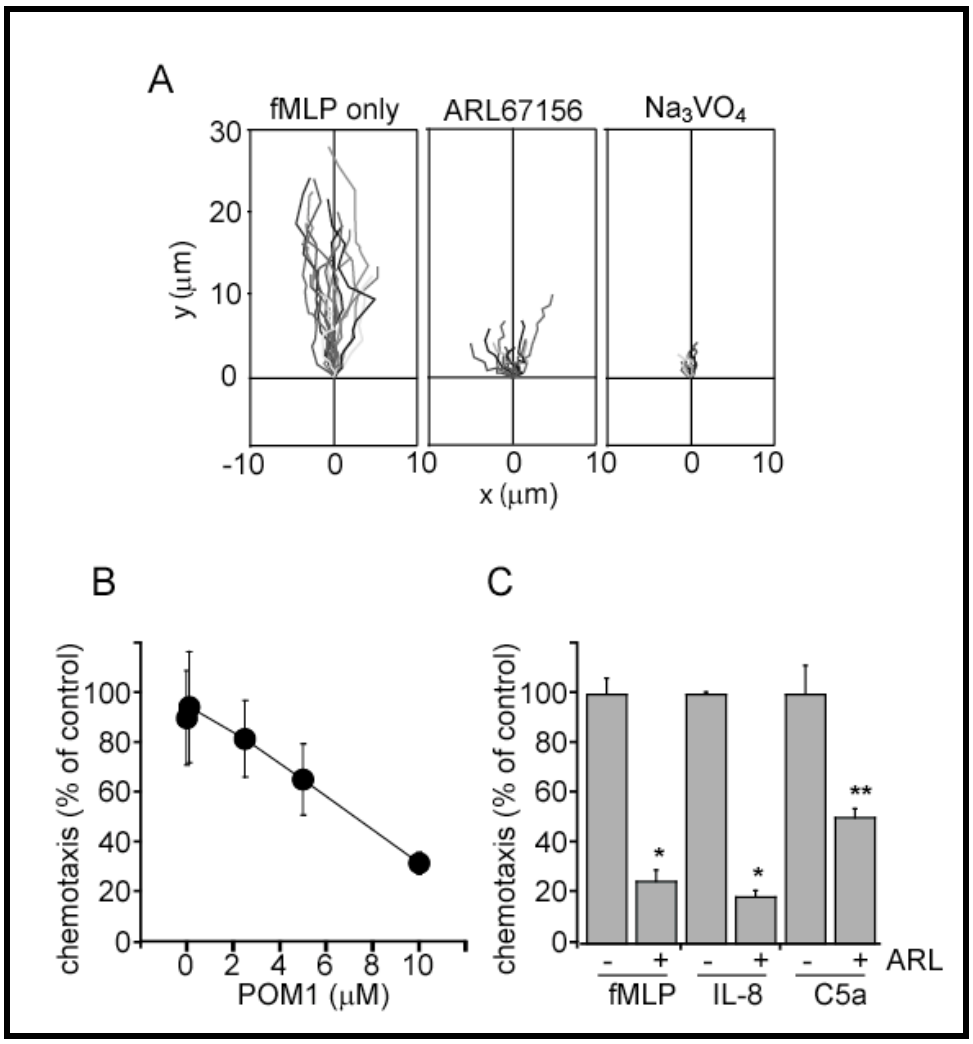

Figure 5: Inhibitors of E-NTPDase1 decrease PMN chemotaxis. (A) PMN (1 x 104) were placed on fibronectin-coated coverslips in a microincubation chamber containing 1 ml HBSS at 37∫C. Migration towards a point source of fMLP (100 nM) was monitored over 4 min using an inverted microscope, as described previously (8). Inhibitors of E-NTPDase1 (ARL67156 or NaN3) were added to the cells 10 min before generation of the chemotactic gradient. The paths of individual cells migrating in the gradient field are plotted such that the y-axis represents the straight-line paths from each cell origin to the point source of fMLP. Chemotactic patterns of control PMN (fMLP only) and PMN treated with ARL67156 (100 μM) or NaN3 (10mM) are shown. The data are representative of 3 separate experiments. (B) PMN (1 x 106), in the presense or absence of ARL67156 (100 μM) were placed in the top well of a transwell system, with the bottom wells containing fMLP (10 nM), IL-8 (10 ng/ml), or 10% zymosan activated serum (ZAS). After a 30 min incubation at 37∫C, cells in the lower well were lysed and relative migration levels were quantified by measuring elastase activity. The data shown (mean ± SEM) were obtained in 3-4 separate experiments. Statistical significance was evaluated using the students t-test (* = $p < 0.001$, ** = $p < 0.01$).

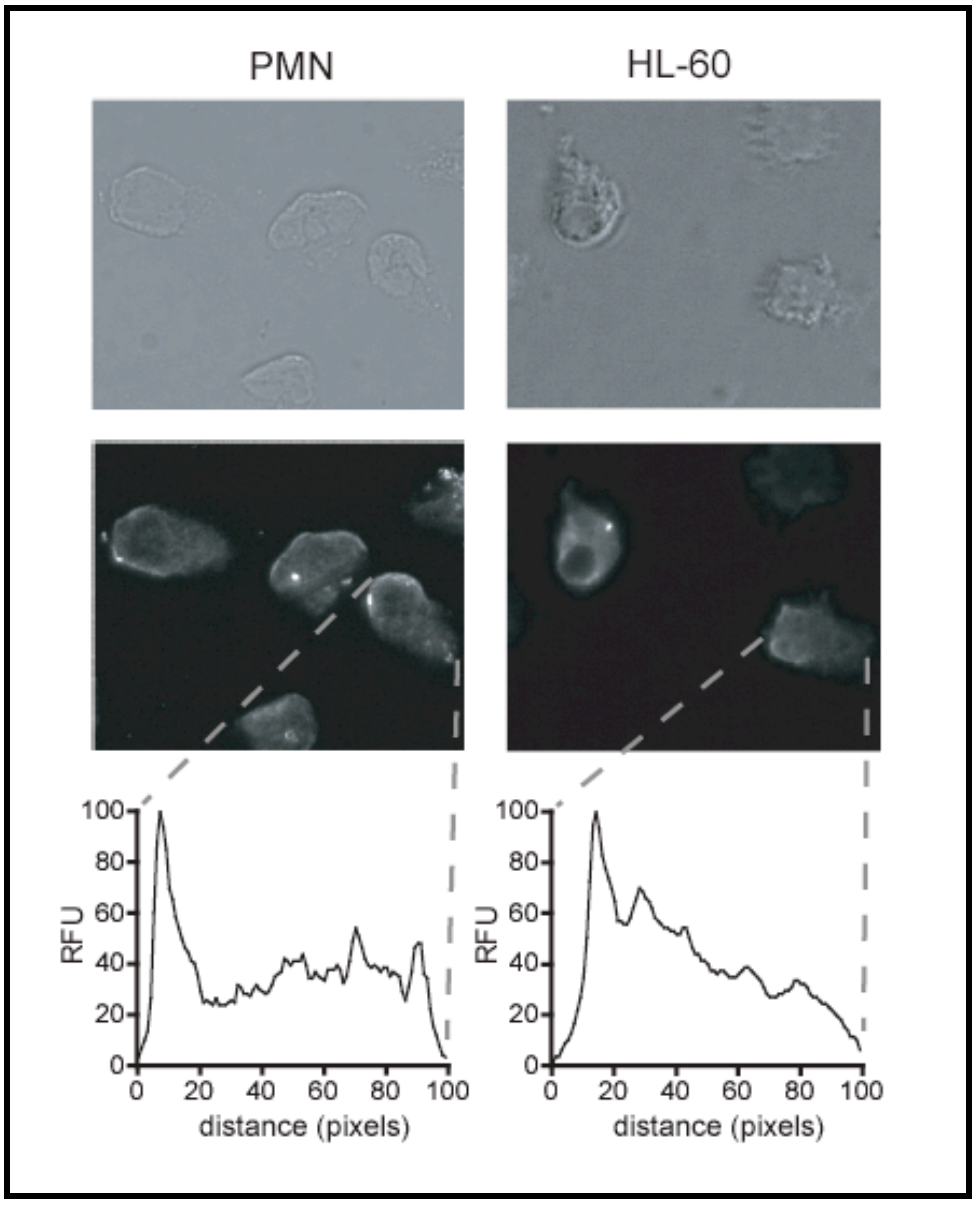

Figure 6: Localization of E-NTPDase1 in migrating PMN and HL-60 cells. PMN or differentiated HL-60 cells were plated on glass coverslips, stimulated with 10 nM fMLP, fixed with paraformaldehyde, and stained using a murine antibody to E-NTPDase1 followed by a fluorescent secondary goat anti-mouse antibody. The top and middle panels show bright field and fluorescent images, respectively. The bottom panels show pixel intensity diagrams of fluorescence along the length of cells. Grey dashed lines indicate the start and endpoints of the fluorescence intensity diagrams and represent the leading edge and uropod/back end of cells, respectively (RFU; relative fluorescence units). The results shown are representative of findings from three separate experiments obtained in at least 50 PMN or HL-60 cells and indicate that maximal fluorescence is present at the leading edge.

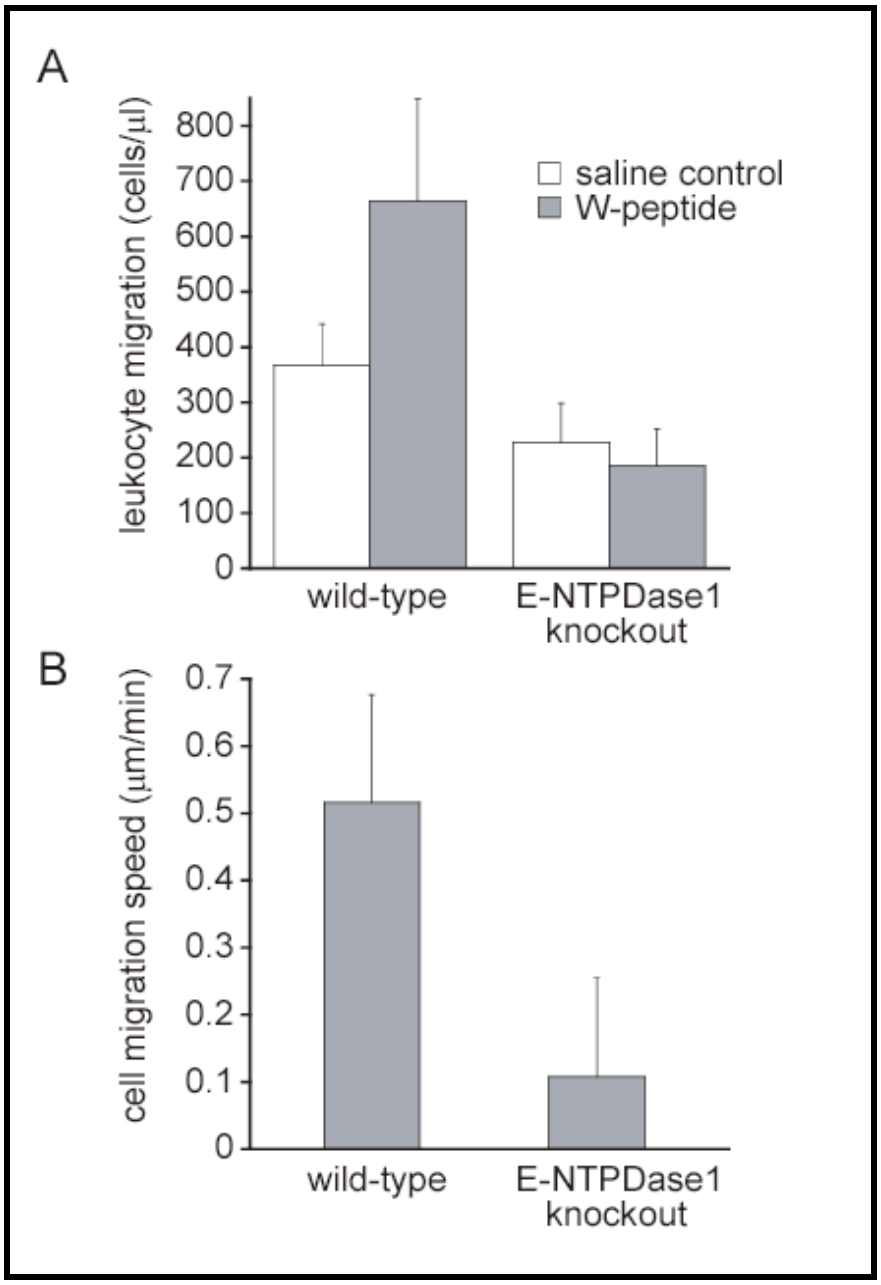

Figure 7: Migration of PMN from E-NTPDase1 knockout mice. (A) In vivo PMN migration was assessed by determining the influx of leukocytes in the abdominal cavity of WT and E-NTPDase1 knockout (KO) mice in response to intra-peritoneal injection of 1 nM W-peptide solution or normal saline as control. (B) The chemotactic properties of PMN from the bone marrow of WT or E-NTPDase1 KO mice in a gradient of W-peptide generated as described in Fig. 5 were assessed under the microscope using the methods described previously (8). The results shown are the mean ± SD of the results obtained with 3 to 6 different animals in each group.

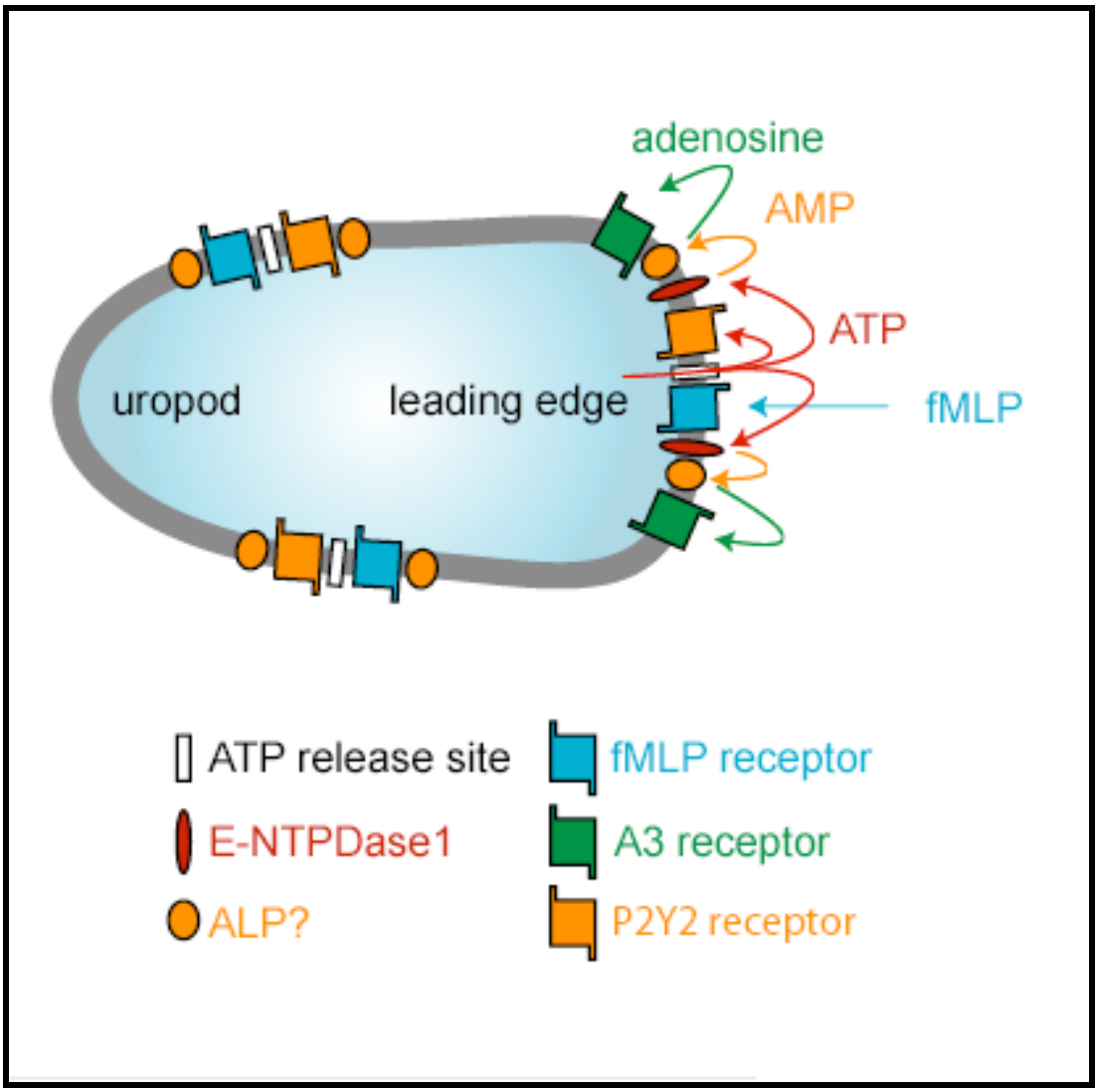

Figure 8: Proposed mechanism of ATP release, action and hydrolysis by PMN. Chemoattractant stimulation of PMN causes the release of ATP at the leading edge. Released ATP activates P2Y2 receptors, which stimulates chemokinesis, or is hydrolyzed to by E-NTPDase1, also localized at the leading edge. An additional enzyme, possibly ALP in human PMN, hydrolyzes extracellular AMP to adenosine, which activates A3 adenosine receptors at the leading edge and promotes cell migration towards the chemotactic source.

Acknowledgements for thesis:

Chapter 6, in full, is a reprint of the material as it appears in the Journal of Biological Chemistry, August 2008, Corriden, Ross; Chen, Yu; Inoue, Yoshiaki; Beldi, Guido; Robson, Simon; Insel, Paul A.; Junger, Wolfgang G. (Epub ahead of print) . The dissertation author was the primary investigator and author of this paper.

Chapter 7

Summary/Discussion

Summary

The observation that human neutrophils release ATP in response to stimulation with the chemoattractant fMLP led me to study the role of P1/P2 receptor signaling in chemotaxis. Extracellular ATP is a fast acting messenger that can be quickly degraded by ecto-ATPases to terminate its actions. For this reason it seemed to be an ideal signaling molecule to modulate cell polarity, a process that requires rapid adaptation to a changing environment. At the time I conducted my studies related to ATP, the idea that activation of chemoattractant receptors alone was enough to stimulate chemotaxis was dogma--one of the most frequently cited papers in the field explicitly stated that no extracellular modulators of chemotaxis are secreted by neutrophils (1). Evaluating the role of extracellular ATP in the process of neutrophil chemotaxis formed the basis for this thesis.

My initial hypothesis was that neutrophils released ATP at the leading edge during migration to establish polarity. Unfortunately, while there were methods available for studying polarized release of ATP, they were too unstable or cumbersome for studies of rapidly migrating neutrophils. My first goal was to develop an assay that would allow visualization of ATP release in real-time. The NADPH-based assay enabled this. The method is relatively easy to set up, much less expensive than others, and was the first method that allowed for visualization of ATP release with single-cell resolution.

Using the ATP visualization assay, I found that human neutrophils release ATP at the leading edge when exposed to a gradient of chemoattractant. Use of HPLC revealed that there was also extracellular accumulation of adenosine. Elimination of either the extracellular ATP or adenosine strongly inhibited migration, suggesting that both signaling molecules contributed to neutrophil chemotaxis. Further studies revealed that these effects were mediated by activation of P2Y2 receptors by ATP, which established cell polarity, and A3 receptors by adenosine, which promoted forward movement. The A3 receptor localized to the leading edge during chemotaxis, which allows cells to polarize their sensory machinery while maintaining a uniform distribution of plasma membrane chemoattractant receptors. This provided an explanation as to how neutrophils are able to orient and migrate in extremely shallow gradients of chemoattractant.

In the final set of studies presented in this thesis, I set out to identify which ecto-ATPases mediate the hydrolysis of extracellular ATP and identified E-NTPDase1 as the primary enzyme responsible for this hydrolysis of ATP. Inhibition of E-NTPDase1, which was localized on the leading edge of polarized cells, resulted in aberrant migration, which further supported the model of P1/P2 receptor mediated chemotaxis.

Future Directions

Though the findings presented in this thesis advance understanding of neutrophil chemotaxis, many unanswered questions remain, some of which I identify below.

The majority of the work presented in this thesis focused on extracellular events mediating P1/P2 receptor-driven chemotaxis. The precise intracellular mechanisms

linking the activation of these receptors to cytoskeletal rearrangement pathways still need to be identified. Determining if P1/P2 receptor signaling is responsible for polarized activation of PI3K and accumulation of PtdIns(3,4,5)P3 at the leading edge of cells is a particularly important "next step". Additionally, the results presented here suggest that the polarized activation of P2Y2 receptors is responsible for the recruitment of A3 receptors to the leading edge, though the mechanism of this recruitment is unknown and needs to be investigated. The exact role of the A3 receptors, which seem to facilitate forward movement, also needs to be explored in more detail. Specifically, it is important to determine if A3 receptors promote actin polymerization by activating Rho GTPases.

Although I identified E-NTPDase1 as a critical ecto-nucleotidase and mediator of chemotaxis, E-NTPDase1 only removes two phosphate groups from ATP and therefore is not capable of generating adenosine. Preliminary data suggest that tissue non-specific alkaline phosphatase performs this hydrolytic step, however a lack of specific inhibitors made this difficult to prove. Time did not allow for approaches using siRNA knockdown or neutrophils isolated from alkaline phosphate knockout mice, although such methods might reveal the mechanism by which adenosine is generated from extracellular ATP.

Another critical topic left unexplored is the role of P1/P2 receptor signaling in establishing 'backness' in migrating cells. Polarized release (and rapid hydrolysis) of ATP at the leading edge represents one way by which P1/P2 signaling can regulate cell polarity. Such polarized release could theoretically create a gradient of ATP and adenosine as cells migrate, with a higher concentration of ATP at the leading edge and adenosine at the trailing edge. Adenosine at the trailing edge could activate Gs-coupled A2a/A2b receptors, resulting in polarized increase of intracellular cAMP, which has been

implicated as an inhibitor of cell migration (3). Data presented in this thesis show that both A2a and A2b are expressed by neutrophils. The precise localization and role of these receptors in migrating cells is an important topic for future study.

The mechanism of ATP release from neutrophils and other non-excitatory cell types is unknown and represents another key,unanswered question. Recent evidence has suggested than pannexin channels might be sites for ATP release (3). Probenecid, a drug primarily used for the treatment of gout, can block pannexin channels (4). Gout is characterized by an accumulation of uric acid crystals in tissues, in particular in the intra-articular space of certain joints, and the subsequent inflammation caused by neutrophils that phagocytose the uric acid. In the treatment of gout, probenecid is thought to act primarily by increasing uric acid clearance, though recent evidence suggests it might also have an inhibitory effect on neutrophil function (5). The possibility that this could be due to the inhibition neutrophil ATP release is intriguing. Further studies could lead to a better understanding of ATP release mechanisms of neutrophils as well as insights into the molecular basis for probenecid action.

Finally, the NADPH-based ATP visualization assay presented in this thesis could be used to study ATP release mechanisms in other cell types. Currently, the most commonly used assay to study ATP release is the luciferase/luciferin-based system (6). While this system has facilitated the easy quantification of extracellular ATP, the luciferase enzyme itself is extremely sensitive and can be affected by channel blockers used to study ATP release, giving false positive/negative results (7). By comparison, the NAPDH-based ATP visualization assay is relatively robust. Further studies using this

system might facilitate the identification of ATP release mechanisms in a variety of cell types.

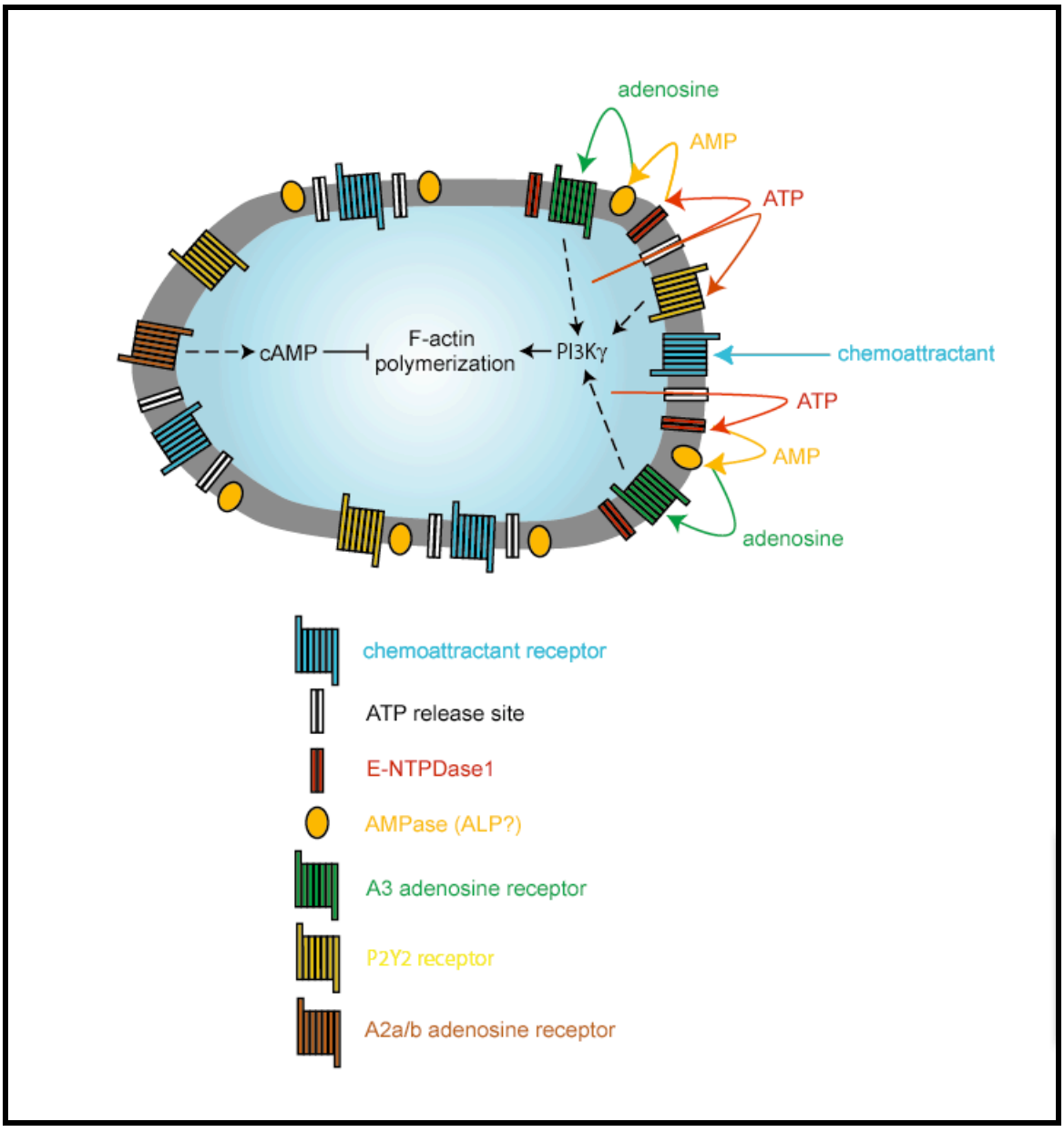

Figure 1: How P1/P2 receptor signaling and ATP release fit into our current understanding of neutrophil migration.

References: Chapter 1

1) Engelhardt B, Wolburg H. Mini-review: Transendothelial migration of leukocytes: through the front door or around the side of the house? *Eur J Immunol*. 2004 Nov;**34**(11):2955-63.

2) Zigmond SH. Ability of polymorphonuclear leukocytes to orient in gradients of chemotactic factors. *J Cell Biol.* 1977 Nov;**75**(2 Pt 1):606-16.

3) Meili R, Firtel RA. Two poles and a compass. *Cell*. 2003 Jul 25;**114**(2):153-6.

4) Chen Y, Shukla A, Namiki S, Insel PA, Junger WG. A putative osmoreceptor system that controls neutrophil function through the release of ATP, its conversion to adenosine, and activation of A2 adenosine and P2 receptors. *J Leukoc Biol*. 2004 Jul;**76**(1):245-53. Epub 2004 Apr 23.

5) Bours MJ, Swennen EL, Di Virgilio F, Cronstein BN, Dagnelie PC. Adenosine 5'-triphosphate and adenosine as endogenous signaling molecules in immunity and inflammation. *Pharmacol Ther.* 2006 Nov;**112**(2):358-404.

References: Chapter 2

1) Eisenbach M. 2004. Chemotaxis. London: *Imperial College Press*. 515 p.

2) McCutcheon, M. (1923) Studies on the locomotion of leukocytes. III The normal rate of locomotion of human neutrophilic leukocytes in vitro." *American Journal of Physiology*, **66**, 180-190.

3) Harris, A.K. (1973) Cell surface movements related to cell locomotion. *Ciba Foundation Symposium*, **14**, 3-26.

4) Zigmond SH. Ability of polymorphonuclear leukocytes to orient in gradients of chemotactic factors. *J Cell Biol.* 1977 Nov;**75**(2 Pt 1):606-16.

5) Comandon, J. (1919) Tactisme produit par l'amidon sur les leucocytes. Enrobement du charbon. *Comptes rendus hebdomadaires des séances et mémoires de la Société de Biologie*, **82**, 1171-1174.

6) Boyden, S. The chemotactic effect of mixtures of antibody and antigen on polymorphonuclear leucocytes. *J Exp Med.* 1962 Mar 1;**115**:453-66.

7) Ward PA, Lepow IH, Newman LJ. Bacterial factors chemotactic for polymorphonuclear leukocytes. *Am J Pathol.* 1968 Apr;**52**(4):725-36.

8) Schiffmann E, Corcoran BA, Wahl SM. N-formylmethionyl peptides as chemoattractants for leucocytes. *Proc Natl Acad Sci.* 1975 Mar;**72**(3):1059-62.

9) Schiffmann E, Showell HV, Corcoran BA, Ward PA, Smith E, Becker EL. The isolation and partial characterization of neutrophil chemotactic factors from Escherichia coli. *J Immunol.* 1975 Jun;**114**(6):1831-7.

10) Thomas KM, Pyun HY, Navarro J. Molecular cloning of the fMet-Leu-Phe receptor from neutrophils. *J Biol Chem.* 1990 Nov 25;**265**(33):20061-4.

11) Boulay F, Tardif M, Brouchon L, Vignais P. The human N-formylpeptide receptor. Characterization of two cDNA isolates and evidence for a new subfamily of G-protein-coupled receptors. *Biochemistry.* 1990 Dec 18;**29**(50):11123-33.

12) Boulay F, Mery L, Tardif M, Brouchon L, Vignais P. Expression cloning of a receptor for C5a anaphylatoxin on differentiated HL-60 cells. *Biochemistry.* 1991 Mar 26;**30**(12):2993-9.

13) Gerard NP, Gerard C. The chemotactic receptor for human C5a anaphylatoxin. *Nature.* 1991 Feb 14;**349**(6310):614-7.

14) Beckmann MP, Munger WE, Kozlosky C, VandenBos T, Price V, Lyman S, Gerard NP, Gerard C, Cerretti DP. Molecular characterization of the interleukin-8 receptor. *Biochem Biophys Res Commun.* 1991 Sep 16;**179**(2):784-9.

15) Holmes WE, Lee J, Kuang WJ, Rice GC, Wood WI. Structure and functional expression of a human interleukin-8 receptor. *Science.* 1991 Sep 13;**253**(5025):1278-80.

16) Murphy PM, Tiffany HL. Cloning of complementary DNA encoding a functional human interleukin-8 receptor. *Science.* 1991 Sep 13;**253**(5025):1280-3.

17) Bajno L, Grinstein S. Fluorescent proteins: powerful tools in phagocyte biology. *J Immunol Methods.* 1999 Dec 17;**232**(1-2):67-75.

18) Fontana JA, Wright DG, Schiffman E, Corcoran BA, Deisseroth AB. Development of chemotactic responsiveness in myeloid precursor cells: studies with a human leukemia cell line. *Proc Natl Acad Sci.* 1980 Jun;**77**(6):3664-8.

19) Devreotes PN, Zigmond SH. Chemotaxis in eukaryotic cells: a focus on leukocytes and Dictyostelium. *Annu Rev Cell Biol.* 1988;**4**:649-86.

20) Cassimeris L, Zigmond SH. Chemoattractant stimulation of polymorphonuclear leucocyte locomotion. *Semin Cell Biol.* 1990 Apr;**1**(2):125-34.

21) Caterina MJ, Devreotes PN. Molecular insights into eukaryotic chemotaxis. *FASEB J.* 1991 Dec;**5**(15):3078-85.

22) Downey GP. Mechanisms of leukocyte motility and chemotaxis. *Curr Opin Immunol.* 1994 Feb;**6**(1):113-24.

23) Fechheimer M, Zigmond SH. Changes in cytoskeletal proteins of polymorphonuclear leukocytes induced by chemotactic peptides. *Cell Motil.* 1983;**3**(4):349-61.

24) Weiner OD, Servant G, Welch MD, Mitchison TJ, Sedat JW, Bourne HR. Spatial control of actin polymerization during neutrophil chemotaxis. *Nat Cell Biol.* 1999 Jun;**1**(2):75-81.

25) Sasaki T, Irie-Sasaki J, Jones RG, Oliveira-dos-Santos AJ, Stanford WL, Bolon B, Wakeham A, Itie A, Bouchard D, Kozieradzki I, Joza N, Mak TW, Ohashi PS, Suzuki A, Penninger JM. Function of PI3Kgamma in thymocyte development, T cell activation, and neutrophil migration. *Science.* 2000 Feb 11;**287**(5455):1040-6.

26) Wang F, Herzmark P, Weiner OD, Srinivasan S, Servant G, Bourne HR. Lipid products of PI(3)Ks maintain persistent cell polarity and directed motility in neutrophils. *Nat Cell Biol.* 2002 Jul;**4**(7):513-8.

27) Haslam RJ, Koide HB, Hemmings BA. Pleckstrin domain homology. *Nature.* 1993 May 27;**363**(6427):309-10.

28) Harlan JE, Hajduk PJ, Yoon HS, Fesik SW. Pleckstrin homology domains bind to phosphatidylinositol-4,5-bisphosphate. *Nature.* 1994 Sep 8;**371**(6493):168-70.

29) Li Z, Hannigan M, Mo Z, Liu B, Lu W, Wu Y, Smrcka AV, Wu G, Li L, Liu M, Huang CK, Wu D. Directional sensing requires G beta gamma-mediated PAK1 and PIX alpha-dependent activation of Cdc42. *Cell.* 2003 Jul 25;**114**(2):215-27.

30) Machesky LM, Atkinson SJ, Ampe C, Vandekerckhove J, Pollard TD. Purification of a cortical complex containing two unconventional actins from Acanthamoeba by affinity chromatography on profilin-agarose. *J Cell Biol.* 1994 Oct;**127**(1):107-15.

31) Mullins RD, Heuser JA, Pollard TD. The interaction of Arp2/3 complex with actin: nucleation, high affinity pointed end capping, and formation of branching networks of filaments. *Proc Natl Acad Sci U S A.* 1998 May 26;**95**(11):6181-6.

32) Weiner OD, Servant G, Welch MD, Mitchison TJ, Sedat JW, Bourne HR. Spatial control of actin polymerization during neutrophil chemotaxis. *Nat Cell Biol.* 1999 Jun;**1**(2):75-81.

33) Rohatgi R, Ma L, Miki H, Lopez M, Kirchhausen T, Takenawa T, Kirschner MW. The interaction between N-WASP and the Arp2/3 complex links Cdc42-dependent signals to actin assembly. *Cell.* 1999 Apr 16;**97**(2):221-31.

34) Machesky LM, Insall RH. Scar1 and the related Wiskott-Aldrich syndrome protein, WASP, regulate the actin cytoskeleton through the Arp2/3 complex. *Curr Biol.* 1998 Dec 17-31;**8**(25):1347-56.

35) Keller HU, Niggli V. Colchicine-induced stimulation of PMN motility related to cytoskeletal changes in actin, alpha-actinin, and myosin. *Cell Motil Cytoskeleton.* 1993;**25**(1):10-8.

36) Eddy RJ, Pierini LM, Matsumura F, Maxfield FR. Ca2+-dependent myosin II activation is required for uropod retraction during neutrophil migration. *J Cell Sci.* 2000 Apr;**113** (Pt 7):1287-98.

37) Heit B, Robbins SM, Downey CM, Guan Z, Colarusso P, Miller BJ, Jirik FR, Kubes P. PTEN functions to 'prioritize' chemotactic cues and prevent 'distraction' in migrating neutrophils. *Nat Immunol.* 2008 Jul;**9**(7):743-52. Epub 2008 Jun 8.

38) Maehama T, Dixon JE. The tumor suppressor, PTEN/MMAC1, dephosphorylates the lipid second messenger, phosphatidylinositol 3,4,5-trisphosphate. *J Biol Chem.* 1998 May 29;**273**(22):13375-8.

39) Nishio M, Watanabe K, Sasaki J, Taya C, Takasuga S, Iizuka R, Balla T, Yamazaki M, Watanabe H, Itoh R, Kuroda S, Horie Y, Förster I, Mak TW, Yonekawa H, Penninger JM, Kanaho Y, Suzuki A, Sasaki T. Control of cell polarity and motility by the PtdIns(3,4,5)P3 phosphatase SHIP1. *Nat Cell Biol.* 2007 Jan;**9**(1):36-44. Epub 2006 Dec 17.

40) Xu J, Wang F, Van Keymeulen A, Herzmark P, Straight A, Kelly K, Takuwa Y, Sugimoto N, Mitchison T, Bourne HR. Divergent signals and cytoskeletal assemblies regulate self-organizing polarity in neutrophils. *Cell.* 2003 Jul 25;**114**(2):201-14.

41) Sharma VP, Desmarais V, Sumners C, Shaw G, Narang A. Immunostaining evidence for PI(4,5)P2 localization at the leading edge of chemoattractant-stimulated HL-60 cells. *J Leukoc Biol.* 2008 Aug;**84**(2):440-7.

42) Damen JE, Liu L, Rosten P, Humphries RK, Jefferson AB, Majerus PW, Krystal G. The 145-kDa protein induced to associate with Shc by multiple cytokines is an inositol tetraphosphate and phosphatidylinositol 3,4,5-triphosphate 5-phosphatase. *Proc Natl Acad Sci U S A.* 1996 Feb 20;**93**(4):1689-93.

43) Lioubin MN, Algate PA, Tsai S, Carlberg K, Aebersold A, Rohrschneider LR. p150Ship, a signal transduction molecule with inositol polyphosphate-5-phosphatase activity. *Genes Dev.* 1996 May 1;**10**(9):1084-95.

44) Scharenberg AM, El-Hillal O, Fruman DA, Beitz LO, Li Z, Lin S, Gout I, Cantley LC, Rawlings DJ, Kinet JP. Phosphatidylinositol-3,4,5-trisphosphate (PtdIns-3,4,5-P3)/Tec kinase-dependent calcium signaling pathway: a target for SHIP-mediated inhibitory signals. *EMBO J.* 1998 Apr 1;**17**(7):1961-72.

45) Aman MJ, Lamkin TD, Okada H, Kurosaki T, Ravichandran KS. The inositol phosphatase SHIP inhibits Akt/PKB activation in B cells. *J Biol Chem.* 1998 Dec 18;**273**(51):33922-8.

46) Ishizaki T, Naito M, Fujisawa K, Maekawa M, Watanabe N, Saito Y, Narumiya S. p160ROCK, a Rho-associated coiled-coil forming protein kinase, works downstream of Rho and induces focal adhesions. *FEBS Lett.* 1997 Mar 10;**404**(2-3):118-24.

47) Matsui T, Amano M, Yamamoto T, Chihara K, Nakafuku M, Ito M, Nakano T, Okawa K, Iwamatsu A, Kaibuchi K. Rho-associated kinase, a novel serine/threonine kinase, as a putative target for small GTP binding protein Rho. *EMBO J.* 1996 May 1;**15**(9):2208-16.

48) Hauert AB, Martinelli S, Marone C, Niggli V. Differentiated HL-60 cells are a valid model system for the analysis of human neutrophil migration and chemotaxis. *Int J Biochem Cell Biol.* 2002 Jul;**34**(7):838-54.

49) Majumdar M, Seasholtz TM, Buckmaster C, Toksoz D, Brown JH. A rho exchange factor mediates thrombin and Galpha(12)-induced cytoskeletal responses. *J Biol Chem.* 1999 Sep 17;*274*(38):26815-21.

50) Simchowitz L, Fischbein LC, Spilberg I, Atkinson JP. Induction of a transient elevation in intracellular levels of adenosine-3',5'-cyclic monophosphate by chemotactic factors: an early event in human neutrophil activation. *J Immunol.* 1980 Mar;**124**(3):1482-91.

51) Smolen JE, Korchak HM, Weissmann G. Increased levels of cyclic adenosine-3',5'-monophosphate in human polymorphonuclear leukocytes after surface stimulation. *J Clin Invest.* 1980 May;**65**(5):1077-85.

52) Spisani S, Pareschi MC, Buzzi M, Colamussi ML, Biondi C, Traniello S, Pagani Zecchini G, Paglialunga Paradisi M, Torrini I, Ferretti ME. Effect of cyclic AMP level reduction on human neutrophil responses to formylated peptides. *Cell Signal.* 1996 Jun;**8**(4):269-77.

53) Suzuki T, Hazeki O, Hazeki K, Ui M, Katada T. Involvement of the beta gamma subunits of inhibitory GTP-binding protein in chemoattractant receptor-mediated potentiation of cyclic AMP formation in guinea pig neutrophils. *Biochim Biophys Acta.* 1996 Aug 21;**1313**(1):72-8.

54) Ali H, Sozzani S, Fisher I, Barr AJ, Richardson RM, Haribabu B, Snyderman R. Differential regulation of formyl peptide and platelet-activating factor receptors. Role of phospholipase Cbeta3 phosphorylation by protein kinase *A*. *J Biol Chem.* 1998 May 1;**273**(18):11012-6.

55) Mahadeo DC, Janka-Junttila M, Smoot RL, Roselova P, Parent CA. A chemoattractant-mediated Gi-coupled pathway activates adenylyl cyclase in human neutrophils. *Mol Biol Cell.* 2007 Feb;**18**(2):512-22. Epub 2006 Nov 29.

56) Harvath L, Robbins JD, Russell AA, Seamon KB. cAMP and human neutrophil chemotaxis. Elevation of cAMP differentially affects chemotactic responsiveness. *J Immunol.* 1991 Jan 1;**146**(1):224-32.

57) VanUffelen BE, de Koster BM, Elferink JG. Interaction of cyclic GMP and cyclic AMP during neutrophil migration: involvement of phosphodiesterase type III. *Biochem Pharmacol.* 1998 Oct 15;**56**(8):1061-3.

58) Ariga M, Neitzert B, Nakae S, Mottin G, Bertrand C, Pruniaux MP, Jin SL, Conti M. Nonredundant function of phosphodiesterases 4D and 4B in neutrophil recruitment to the site of inflammation. *J Immunol.* 2004 Dec 15;**173**(12):7531-8.

59) Jones SL, Sharief Y. Asymmetrical protein kinase A activity establishes neutrophil cytoskeletal polarity and enables chemotaxis. *J Leukoc Biol.* 2005 Jul;**78**(1):248-58.

60) Servant G, Weiner OD, Neptune ER, Sedat JW, Bourne HR. Dynamics of a chemoattractant receptor in living neutrophils during chemotaxis. *Mol Biol Cell.* 1999 Apr;**10**(4):1163-78.

61) Zigmond SH, Levitsky HI, Kreel BJ. Cell polarity: an examination of its behavioral expression and its consequences for polymorphonuclear leukocyte chemotaxis. *J Cell Biol.* 1981 Jun;**89**(3):585-92.

References: Chapter 3

1) Burnstock G. Historical review: ATP as a neurotransmitter. *Trends Pharmacol Sci.* 2006 Mar;**27**(3):166-76.

2) Schwiebert EM, Zsembery A. Extracellular ATP as a signaling molecule for epithelial cells. *Biochim Biophys Acta.* 2003 Sep 2;**1615**(1-2):7-32.

3) Abbracchio MP, Burnstock G, Boeynaems JM, Barnard EA, Boyer JL, Kennedy C, Knight GE, Fumagalli M, Gachet C, Jacobson KA, Weisman GA. International Union of Pharmacology LVIII: update on the P2Y G protein-coupled nucleotide receptors: from molecular mechanisms and pathophysiology to therapy. *Pharmacol Rev.* 2006 Sep;**58**(3):281-341.

4) Khakh BS, Burnstock G, Kennedy C, King BF, North RA, Séguéla P, Voigt M, Humphrey PP. International union of pharmacology. XXIV. Current status of the nomenclature and properties of P2X receptors and their subunits. *Pharmacol Rev.* 2001 Mar;**53**(1):107-18.

5) Zimmermann H. (2006) Ectonucleotidases in the nervous system. *Novartis Found Symp*. **276**, 113-28.

6) Lazarowski ER, Boucher RC, Harden TK (2000) Constitutive release of ATP and evidence for major contribution of ecto-nucleotide pyrophosphatase and nucleoside diphosphokinase to extracellular nucleotide concentrations. *J. Biol. Chem*. **275**, 31061–31068.

7) Fredholm BB, IJzerman AP, Jacobson KA, Klotz KN, Linden J. International Union of Pharmacology. XXV. Nomenclature and classification of adenosine receptors. *Pharmacol Rev.* 2001 Dec;**53**(4):527-52.

8) Braunstein GM, Roman RM, Clancy JP, Kudlow BA, Taylor AL, Shylonsky VG, Jovov B, Peter K, Jilling T, Ismailov II, Benos DJ, Schwiebert LM, Fitz JG, Schwiebert EM. Cystic fibrosis transmembrane conductance regulator facilitates ATP release by stimulating a separate ATP release channel for autocrine control of cell volume regulation. *J Biol Chem.* 2001 Mar 2;**276**(9):6621-30.

9) Sugita M, Yue Y, Foskett JK. CFTR Cl- channel and CFTR-associated ATP channel: distinct pores regulated by common gates. *EMBO J.* 1998 Feb 16;**17**(4):898-908.

10) Watt WC, Lazarowski ER, Boucher RC. Cystic fibrosis transmembrane regulator-independent release of ATP. Its implications for the regulation of P2Y2 receptors in airway epithelia. *J Biol Chem.* 1998 May 29;**273**(22):14053-8.

11) Gatof D, Kilic G, Fitz JG. Vesicular exocytosis contributes to volume-sensitive ATP release in biliary cells. *Am J Physiol Gastrointest Liver Physiol.* 2004 Apr;**286**(4):G538-46.

12) Gatof D, Kilic G, Fitz JG. Vesicular exocytosis contributes to volume-sensitive ATP release in biliary cells. *Am J Physiol Gastrointest Liver Physiol.* 2004 Apr;**286**(4):G538-46.

13) Zhang Z, Chen G, Zhou W, Song A, Xu T, Luo Q, Wang W, Gu XS, Duan S. Regulated ATP release from astrocytes through lysosome exocytosis. *Nat Cell Biol.* 2007 Aug; **9**(8):945-53.

14) Kang J, Kang N, Lovatt D, Torres A, Zhao Z, Lin J, Nedergaard M. Connexin 43 hemichannels are permeable to ATP. *J Neurosci.* 2008 Apr 30;**28**(18):4702-11.

15) Huang YJ, Maruyama Y, Dvoryanchikov G, Pereira E, Chaudhari N, Roper SD. The role of pannexin 1 hemichannels in ATP release and cell-cell communication in mouse taste buds. *Proc Natl Acad Sci U S A.* 2007 Apr 10;**104**(15):6436-41.

16) Bell PD, Lapointe JY, Sabirov R, Hayashi S, Peti-Peterdi J, Manabe K, Kovacs G, Okada Y. Macula densa cell signaling involves ATP release through a maxi anion channel. *Proc Natl Acad Sci U S A.* 2003 Apr 1;**100**(7):4322-7.

17) Liu HT, Toychiev AH, Takahashi N, Sabirov RZ, Okada Y. Maxi-anion channel as a candidate pathway for osmosensitive ATP release from mouse astrocytes in primary culture. *Cell Res.* 2008 May;**18**(5):558-65.

18) Hisadome K, Koyama T, Kimura C, Droogmans G, Ito Y, Oike M. Volume-regulated anion channels serve as an auto/paracrine nucleotide release pathway in aortic endothelial cells. *J Gen Physiol.* 2002 Jun;**119**(6):511-20.

19) Koyama T, Kimura C, Hayashi M, Watanabe M, Karashima Y, Oike M. Hypergravity induces ATP release and actin reorganization via tyrosine phosphorylation and RhoA activation in bovine endothelial cells. *Pflugers Arch.* 2008 Jul 2. [Epub ahead of print]

20) Suadicani SO, Brosnan CF, Scemes E. P2X7 receptors mediate ATP release and amplification of astrocytic intercellular Ca2+ signaling. *J Neurosci.* 2006 Feb 1;**26**(5):1378-85.

21) Ostrom RS, Gregorian C, Insel PA. Cellular release of and response to ATP as key determinants of the set-point of signal transduction pathways. *J Biol Chem.* 2000 Apr 21;**275**(16):11735-9.

22) Shiga H, Tojima T, Ito E. Ca2+ signaling regulated by an ATP-dependent autocrine mechanism in astrocytes. *Neuroreport.* 2001 Aug 28;**12**(12):2619-22.

23) Scemes E, Suadicani SO, Spray DC. Intercellular communication in spinal cord astrocytes: fine tuning between gap junctions and P2 nucleotide receptors in calcium wave propagation. *J Neurosci.* 2000 Feb 15;**20**(4):1435-45.

24) Mongin AA, Kimelberg HK. ATP potently modulates anion channel-mediated excitatory amino acid release from cultured astrocytes. *Am J Physiol Cell Physiol.* 2002 Aug; **283**(2):C569-78.

25) Darby M, Kuzmiski JB, Panenka W, Feighan D, MacVicar BA. ATP released from astrocytes during swelling activates chloride channels. *J Neurophysiol.* 2003 Apr; **89**(4):1870-7.

26) Carabelli V, Carra I, Carbone E. Localized secretion of ATP and opioids revealed through single Ca2+ channel modulation in bovine chromaffin cells. *Neuron. 1998 Jun*; **20**(6):1255-68.

27) Ferrari D, Chiozzi P, Falzoni S, Dal Susino M, Collo G, Buell G, Di Virgilio F. ATP-mediated cytotoxicity in microglial cells. *Neuropharmacology.* 1997 Sep;**36**(9):1295-301.

28) Ferrari D, Chiozzi P, Falzoni S, Hanau S, Di Virgilio F. Purinergic modulation of interleukin-1 beta release from microglial cells stimulated with bacterial endotoxin. *J Exp Med.* 1997 Feb 3;**185**(3):579-82.

29) Seo DR, Kim KY, Lee YB. Interleukin-10 expression in lipopolysaccharide-activated microglia is mediated by extracellular ATP in an autocrine fashion. *Neuroreport.* 2004 May 19;**15**(7):1157-61.

30) Seo DR, Kim SY, Kim KY, Lee HG, Moon JH, Lee JS, Lee SH, Kim SU, Lee YB. Cross talk between P2 purinergic receptors modulates extracellular ATP-mediated interleukin-10 production in rat microglial cells. *Exp Mol Med.* 2008 Feb 29;**40**(1):19-26.

31) Kim SY, Moon JH, Lee HG, Kim SU, Lee YB. ATP released from beta-amyloid-stimulated microglia induces reactive oxygen species production in an autocrine fashion. *Exp Mol Med.* 2007 Dec 31;**39**(6):820-7.

32) Hussl S, Kubista H, Boehm S. Autoregulation in PC12 cells via P2Y receptors: Evidence for non-exocytotic nucleotide release from neuroendocrine cells. *Purinergic Signal.* 2007 Sep;**3**(4):367-75.

33) Scemes E, Duval N, Meda P. Reduced expression of P2Y1 receptors in connexin43-null mice alters calcium signaling and migration of neural progenitor cells. *J Neurosci.* 2003 Dec 10;**23**(36):11444-52.

34) Lin JH, Takano T, Arcuino G, Wang X, Hu F, Darzynkiewicz Z, Nunes M, Goldman SA, Nedergaard M. Purinergic signaling regulates neural progenitor cell expansion and neurogenesis. *Dev Biol.* 2007 Feb 1;**302**(1):356-66.

35) Chen ZP, Kratzmeier M, Levy A, McArdle CA, Poch A, Day A, Mukhopadhyay AK, Lightman SL. Evidence for a role of pituitary ATP receptors in the regulation of pituitary function. *Proc Natl Acad Sci U S A.* 1995 May 23;**92**(11):5219-23.

36) Tomi_ M, Jobin RM, Vergara LA, Stojilkovic SS. Expression of purinergic receptor channels and their role in calcium signaling and hormone release in pituitary gonadotrophs. Integration of P2 channels in plasma membrane- and endoplasmic reticulum-derived calcium oscillations. *J Biol Chem.* 1996 Aug 30;**271**(35):21200-8.

37) Stojilkovic SS, Tomic M, Van Goor F, Koshimizu T. Expression of purinergic P2X2 receptor-channels and their role in calcium signaling in pituitary cells. *Biochem Cell Biol.* 2000;**78**(3):393-404.

38) Nuñez L, Villalobos C, Frawley LS. Extracellular ATP as an autocrine/paracrine regulator of prolactin release. *Am J Physiol.* 1997 Jun;**272**(6 Pt 1):E1117-23.

39) Imai M, Goepfert C, Kaczmarek E, Robson SC. CD39 modulates IL-1 release from activated endothelial cells. *Biochem Biophys Res Commun.* 2000 Apr 2;**270**(1):272-8.

40) Hisadome K, Koyama T, Kimura C, Droogmans G, Ito Y, Oike M. Volume-regulated anion channels serve as an auto/paracrine nucleotide release pathway in aortic endothelial cells. *J Gen Physiol.* 2002 Jun;**119**(6):511-20.

41) Schwiebert LM, Rice WC, Kudlow BA, Taylor AL, Schwiebert EM. Extracellular ATP signaling and P2X nucleotide receptors in monolayers of primary human vascular endothelial cells. *Am J Physiol Cell Physiol.* 2002 Feb;**282**(2):C289-301.

42) Hong D, Barbee KA, Buerk DG, Jaron D. Heterogeneous cytoplasmic calcium response in microvascular endothelial cells. *Conf Proc IEEE Eng Med Biol Soc.* 2005;**7**:7493-6.

43) Gomes P, Srinivas SP, Vereecke J, Himpens B. ATP-dependent paracrine intercellular communication in cultured bovine corneal endothelial cells. *Invest Ophthalmol Vis Sci.* 2005 Jan;**46**(1):104-13.

44) Gerasimovskaya EV, Ahmad S, White CW, Jones PL, Carpenter TC, Stenmark KR. Extracellular ATP is an autocrine/paracrine regulator of hypoxia-induced adventitial fibroblast growth. Signaling through extracellular signal-regulated kinase-1/2 and the Egr-1 transcription factor. *J Biol Chem.* 2002 Nov 22;**277**(47):44638-50.

45) Kalinowski L, Dobrucki LW, Szczepanska-Konkel M, Jankowski M, Martyniec L, Angielski S, Malinski T. Third-generation beta-blockers stimulate nitric oxide release from endothelial cells through ATP efflux: a novel mechanism for antihypertensive action. *Circulation.* 2003 Jun 3;**107**(21):2747-52.

46) Hamada K, Takuwa N, Yokoyama K, Takuwa Y. Stretch activates Jun N-terminal kinase/stress-activated protein kinase in vascular smooth muscle cells through mechanisms involving autocrine ATP stimulation of purinoceptors. *J Biol Chem.* 1998 Mar 13;**273**(11):6334-40.

47) Tanneur V, Duranton C, Brand VB, Sandu CD, Akkaya C, Kasinathan RS, Gachet C, Sluyter R, Barden JA, Wiley JS, Lang F, Huber SM. Purinoceptors are involved in the induction of an osmolyte permeability in malaria-infected and oxidized human erythrocytes. *FASEB J.* 2006 Jan;**20**(1):133-5.

48) Baricordi OR, Melchiorri L, Adinolfi E, Falzoni S, Chiozzi P, Buell G, Di Virgilio F. Increased proliferation rate of lymphoid cells transfected with the P2X(7) ATP receptor. *J Biol Chem.* 1999 Nov 19;**274**(47):33206-8.

49) Placido R, Auricchio G, Falzoni S, Battistini L, Colizzi V, Brunetti E, Di Virgilio F, Mancino G. P2X(7) purinergic receptors and extracellular ATP mediate apoptosis of human monocytes/macrophages infected with Mycobacterium tuberculosis reducing the intracellular bacterial viability. *Cell Immunol.* 2006 Nov;**244**(1):10-8.

50) Tolhurst G, Vial C, Léon C, Gachet C, Evans RJ, Mahaut-Smith MP. Interplay between P2Y(1), P2Y(12), and P2X(1) receptors in the activation of megakaryocyte cation influx currents by ADP: evidence that the primary megakaryocyte represents a fully functional model of platelet P2 receptor signaling. *Blood.* 2005 Sep 1;**106**(5):1644-51.

51) Piccini A, Carta S, Tassi S, Lasiglié D, Fossati G, Rubartelli A. ATP is released by monocytes stimulated with pathogen-sensing receptor ligands and induces IL-1beta and IL-18 secretion in an autocrine way. *Proc Natl Acad Sci U S A.* 2008 Jun 10;**105**(23):8067-72.

52) Chen Y, Corriden R, Inoue Y, Yip L, Hashiguchi N, Zinkernagel A, Nizet V, Insel PA, Junger WG. ATP release guides neutrophil chemotaxis via P2Y2 and A3 receptors. *Science.* 2006 Dec 15;**314**(5806):1792-5.

53) Fung CY, Cendana C, Farndale RW, Mahaut-Smith MP. Primary and secondary agonists can use P2X(1) receptors as a major pathway to increase intracellular Ca(2+) in the human platelet. *J Thromb Haemost.* 2007 May;**5**(5):910-7.

54) Jorgensen NR, Geist ST, Civitelli R, Steinberg TH. ATP- and gap junction-dependent intercellular calcium signaling in osteoblastic cells. *J Cell Biol.* 1997 Oct 20;**139**(2):497-506.

55) Henriksen Z, Hiken JF, Steinberg TH, Jørgensen NR. The predominant mechanism of intercellular calcium wave propagation changes during long-term culture of human osteoblast-like cells. *Cell Calcium.* 2006 May;**39**(5):435-44.

56) Romanello M, Pani B, Bicego M, D'Andrea P. Mechanically induced ATP release from human osteoblastic cells. *Biochem Biophys Res Commun*. 2001 Dec 21;**289**(5):1275-81.

57) Romanello M, Codognotto A, Bicego M, Pines A, Tell G, D'Andrea P. Autocrine/paracrine stimulation of purinergic receptors in osteoblasts: contribution of vesicular ATP release. *Biochem Biophys Res Commun.* 2005 Jun 17;**331**(4):1429-38.

58) Grierson JP, Meldolesi J. Shear stress-induced [Ca2+]i transients and oscillations in mouse fibroblasts are mediated by endogenously released ATP. *J Biol Chem.* 1995 Mar 3;**270**(9):4451-6.

59) Solini A, Chiozzi P, Morelli A, Adinolfi E, Rizzo R, Baricordi OR, Di Virgilio F. Enhanced P2X7 activity in human fibroblasts from diabetic patients: a possible pathogenetic mechanism for vascular damage in diabetes. *Arterioscler Thromb Vasc Biol.* 2004 Jul;**24**(7):1240-5.

60) Riddle RC, Taylor AF, Rogers JR, Donahue HJ. ATP release mediates fluid flow-induced proliferation of human bone marrow stromal cells. *J Bone Miner Res.* 2007 Apr;**22**(4):589-600.

61) Kawano S, Otsu K, Kuruma A, Shoji S, Yanagida E, Muto Y, Yoshikawa F, Hirayama Y, Mikoshiba K, Furuichi T. ATP autocrine/paracrine signaling induces calcium oscillations and NFAT activation in human mesenchymal stem cells. *Cell Calcium.* 2006 Apr;**39**(4):313-24.

62) Tsuzaki M, Bynum D, Almekinders L, Yang X, Faber J, Banes AJ. ATP modulates load-inducible IL-1beta, COX 2, and MMP-3 gene expression in human tendon cells. *J Cell Biochem.* 2003 Jun 1;**89**(3):556-62.

63) Wurm A, Pannicke T, Wiedemann P, Reichenbach A, Bringmann A. Glial cell-derived glutamate mediates autocrine cell volume regulation in the retina: activation by VEGF. *J Neurochem.* 2008 Jan;**104**(2):386-99.

64) McNamara N, Khong A, McKemy D, Caterina M, Boyer J, Julius D, Basbaum C. ATP transduces signals from ASGM1, a glycolipid that functions as a bacterial receptor. *Proc Natl Acad Sci U S A.* 2001 Jul 31;**98**(16):9086-91.

65) Selzner N, Selzner M, Graf R, Ungethuem U, Fitz JG, Clavien PA. Water induces autocrine stimulation of tumor cell killing through ATP release and P2 receptor binding. *Cell Death Differ.* 2004 Dec;**11** Suppl 2:S172-80.

66) McNamara N, Khong A, McKemy D, Caterina M, Boyer J, Julius D, Basbaum C. ATP transduces signals from ASGM1, a glycolipid that functions as a bacterial receptor. *Proc Natl Acad Sci U S A.* 2001 Jul 31;*98*(16):9086-91.

67) Yamamoto T, Suzuki Y. Role of luminal ATP in regulating electrogenic Na(+) absorption in guinea pig distal colon. *Am J Physiol Gastrointest Liver Physiol.* 2002 Aug;**283**(2):G300-8.

68) Adinolfi E, Callegari MG, Ferrari D, Bolognesi C, Minelli M, Wieckowski MR, Pinton P, Rizzuto R, Di Virgilio F. Basal activation of the P2X7 ATP receptor elevates mitochondrial calcium and potential, increases cellular ATP levels, and promotes serum-independent growth. *Mol Biol Cell.* 2005 Jul;**16**(7):3260-72.

69) Hovater MB, Olteanu D, Welty EA, Schwiebert EM. Purinergic signaling in the lumen of a normal nephron and in remodeled PKD encapsulated cysts. *Purinergic Signal.* 2008 Jun;**4**(2):109-24.

70) Ma HP, Li L, Zhou ZH, Eaton DC, Warnock DG. ATP masks stretch activation of epithelial sodium channels in A6 distal nephron cells. *Am J Physiol Renal Physiol.* 2002 Mar;**282**(3):F501-5.

71) Gorelik J, Zhang Y, Sánchez D, Shevchuk A, Frolenkov G, Lab M, Klenerman D, Edwards C, Korchev Y. Aldosterone acts via an ATP autocrine/paracrine system: the Edelman ATP hypothesis revisited. *Proc Natl Acad Sci U S A.* 2005 Oct 18;**102**(42):15000-5.

72) Kempson SA, Edwards JM, Osborn A, Sturek M. Acute inhibition of the betaine transporter by ATP and adenosine in renal MDCK cells. *Am J Physiol Renal Physiol.* 2008 Jul;**295**(1):F108-17.

73) Iwata Y, Katanosaka Y, Hisamitsu T, Wakabayashi S. Enhanced Na+/H+ exchange activity contributes to the pathogenesis of muscular dystrophy via involvement of P2 receptors. *Am J Pathol.* 2007 Nov;**171**(5):1576-87.

74) Hellman B, Dansk H, Grapengiesser E. Pancreatic beta-cells communicate via intermittent release of ATP. *Am J Physiol Endocrinol Metab.* 2004 May;**286**(5):E759-65.

75) Wang Y, Roman R, Lidofsky SD, Fitz JG. Autocrine signaling through ATP release represents a novel mechanism for cell volume regulation. *Proc Natl Acad Sci U S A.* 1996 Oct 15;**93**(21):12020-5.

76) Roman RM, Wang Y, Lidofsky SD, Feranchak AP, Lomri N, Scharschmidt BF, Fitz JG. Hepatocellular ATP-binding cassette protein expression enhances ATP release and autocrine regulation of cell volume. *J Biol Chem.* 1997 Aug 29;**272**(35):21970-6.

77) Feranchak AP, Roman RM, Schwiebert EM, Fitz J.G. Phosphatidylinositol 3-kinase contributes to cell volume regulation through effects on ATP release. *J Biol Chem.* 1998 Jun 12;**273**(24):14906-11.

78) Feranchak AP, Fitz JG, Roman RM. Volume-sensitive purinergic signaling in human hepatocytes. *J Hepatol.* 2000 Aug;**33**(2):174-82.

79) Schlosser SF, Burgstahler AD, Nathanson MH. Isolated rat hepatocytes can signal to other hepatocytes and bile duct cells by release of nucleotides. *Proc Natl Acad Sci U S A.* 1996 Sep 3;**93**(18):9948-53.

80) Roman RM, Feranchak AP, Salter KD, Wang Y, Fitz JG. Endogenous ATP release regulates Cl- secretion in cultured human and rat biliary epithelial cells. *Am J Physiol.* 1999 Jun;**276**(6 Pt 1):G1391-400.

81) Minagawa N, Nagata J, Shibao K, Masyuk AI, Gomes DA, Rodrigues MA, Lesage G, Akiba Y, Kaunitz JD, Ehrlich BE, Larusso NF, Nathanson MH. Cyclic AMP regulates bicarbonate secretion in cholangiocytes through release of ATP into bile. *Gastroenterology.* 2007 Nov;**133**(5):1592-602.

82) Wang Q, Wang L, Feng YH, Li X, Zeng R, Gorodeski GI. P2X7 receptor-mediated apoptosis of human cervical epithelial cells. *Am J Physiol Cell Physiol.* 2004 Nov;**287**(5):C1349-58.

83) Sauer H, Hescheler J, Wartenberg M. Mechanical strain-induced Ca(2+) waves are propagated via ATP release and purinergic receptor activation. *Am J Physiol Cell Physiol.* 2000 Aug;**279**(2):C295-307.

84) Sauer H, Stanelle R, Hescheler J, Wartenberg M. The DC electrical-field-induced Ca(2+) response and growth stimulation of multicellular tumor spheroids are mediated by ATP release and purinergic receptor stimulation. *J Cell Sci.* 2002 Aug 15;**115**(Pt 16):3265-73.

85) Schwiebert EM, Egan ME, Hwang TH, Fulmer SB, Allen SS, Cutting GR, Guggino WB. CFTR regulates outwardly rectifying chloride channels through an autocrine mechanism involving ATP. *Cell.* 1995 Jun 30;**81**(7):1063-73.

86) Watt WC, Lazarowski ER, Boucher RC. Cystic fibrosis transmembrane regulator-independent release of ATP. Its implications for the regulation of P2Y2 receptors in airway epithelia. *J Biol Chem.* 1998 May 29;**273**(22):14053-8.

87) Braunstein GM, Roman RM, Clancy JP, Kudlow BA, Taylor AL, Shylonsky VG, Jovov B, Peter K, Jilling T, Ismailov II, Benos DJ, Schwiebert LM, Fitz JG, Schwiebert EM. Cystic fibrosis transmembrane conductance regulator facilitates ATP release by stimulating a separate ATP release channel for autocrine control of cell volume regulation. *J Biol Chem.* 2001 Mar 2;**276**(9):6621-30.

88) Braunstein GM, Zsembery A, Tucker TA, Schwiebert EM. Purinergic signaling underlies CFTR control of human airway epithelial cell volume. *J Cyst Fibros.* 2004 Jun;**3**(2):99-117.

89) Ito Y, Son M, Sato S, Ishikawa T, Kondo M, Nakayama S, Shimokata K, Kume H. ATP release triggered by activation of the Ca2+-activated K+ channel in human airway Calu-3 cells. *Am J Respir Cell Mol Biol.* 2004 Mar;**30**(3):388-95.

90) Tatur S, Groulx N, Orlov SN, Grygorczyk R. Ca2+-dependent ATP release from A549 cells involves synergistic autocrine stimulation by coreleased uridine nucleotides. *J Physiol.* 2007 Oct 15;**584**(Pt 2):419-35.

91) Yoshida H, Kobayashi D, Ohkubo S, Nakahata N. ATP stimulates interleukin-6 production via P2Y receptors in human HaCaT keratinocytes. *Eur J Pharmacol.* 2006 Jul 1;**540**(1-3):1-9.

92) Caraccio N, Monzani F, Santini E, Cuccato S, Ferrari D, Callegari MG, Gulinelli S, Pizzirani C, Di Virgilio F, Ferrannini E, Solini A. Extracellular adenosine 5'-triphosphate modulates interleukin-6 production by human thyrocytes through functional purinergic P2 receptors. *Endocrinology.* 2005 Jul;**146**(7):3172-8.

93) Pines A, Bivi N, Vascotto C, Romanello M, D'Ambrosio C, Scaloni A, Damante G, Morisi R, Filetti S, Ferretti E, Quadrifoglio F, Tell G. Nucleotide receptors stimulation by extracellular ATP controls Hsp90 expression through APE1/Ref-1 in thyroid cancer cells: a novel tumorigenic pathway. *J Cell Physiol.* 2006 Oct;**209**(1):44-55.

94) Boyer JL, Graf J, Meier PJ. Hepatic transport systems regulating pHi, cell volume, and bile secretion. *Annu Rev Physiol.* 1992;**54**:415-38.

References: Chapter 4:

1) Alund M, Olson L. (1979) Depolarization-induced decreases in fluroescence intensity of gastro-intestinal quinacrine-binding nerves. *Brain Res.* 166(1), 121-37.

2) Bodin P, Burnstock G. (2001) Purinergic signalling: ATP release. *Neurochem Res*. 26, 959-69.

3) Beigi R, Kobatake E, Aizawa M, Dubyak GR (1999) Detection of local ATP release from activated platelets using cell surface-attached firefly luciferase. *Am J Physiol*. 276, C267-78.

4) Bell PD, Lapointe JY, Sabirov R, Hayashi S, Peti-Peterdi J, Manabe K, Kovacs G, Okada Y. (2003) Macula densa cell signaling involves ATP release through a maxi anion channel. *Proc Natl Acad Sci*. 4322-7.

5) Burnstock, G. (2006) Purinergic signalling. *Br. J Pharmacol*. 147 (Suppl 1), S172-81.

6) Burnstock G. (2007) Physiology and pathophysiology of purinergic neurotransmission. *Physiol Rev.* 87(2), 659-797.

7) Chen, Y., Corriden, R., Inoue, I., Yip, L., Hashiguchi, N., Zinkernagel, A., Nizet, V., Insel, P.A., Junger, W. (2006) ATP Release Guides Neutrophil Chemotaxis via P2Y2 and A3 Receptors. *Science* 314, 1792-1795.

8) Chen Y, Shukla A, Namiki S, Insel PA, Junger WG. (2004) A putative osmoreceptor system that controls neutrophil function through the release of ATP, its conversion to adenosine, and activation of A2 adenosine and P2 receptors. *J Leukoc Biol.* 76, 245-53.

9) Dubyak GR. (2000) Purinergic signaling at immunological synapses. *J Auton Nerv Syst*. 81(1-3), 64-8.

10) Dutta AK, Sabirov RZ, Uramoto H, Okada Y. (2004) Role of ATP-conductive anion channel in ATP release from neonatal rat cardiomyocytes in ischaemic or hypoxic conditions. *J Physiol.* 559(Pt 3), 799-812.

11) Eltzschig HK, Eckle T, Mager A, Küper N, Karcher C, Weissmüller T, Boengler K, Schulz R, Robson SC, Colgan SP. (2006) ATP release from activated neutrophils occurs via connexin 43 and modulates adenosine-dependent endothelial cell function. *Circ Res*. 99(10), 1100-8.

12) Fredholm BB. (1997) Purines and neutrophil leukocytes. *Gen Pharmacol.* 28, 345-50.

13) Hazama A, Hayashi S, Okada Y. (1998) Cell surface measurements of ATP release from single pancreatic beta cells using a novel biosensor technique. *Pfluegers Arch*. 437, 31–35.

14) Hayashi S, Hazama A, Dutta AK, Sabirov RZ, Okada Y. (2004) Detecting ATP release by a biosensor method. *Sci STKE*. 258, pl14.

15) Ito Y, Son M, Sato S, Ishikawa T, Kondo M, Nakayama S, Shimokata K, Kume H. (2004) ATP release triggered by activation of the Ca2+-activated K+ channel in human airway Calu-3 cells. *Am J Respir Cell Mol Biol*. 30(3), 388-95.

16) Junger W, Hoyt D, Davis RE, Herdon-Remelius C, Namiki S, Junger H, Loomis W, Altman A (1998) Hypertonicity Regulates the Function of Human Neutrophils by Modulating Chemoattractant Receptor Signaling and Activating Mitogen-activated Protein Kinase p38. *J. Clin. Invest*. 101, 2768-2779.

17) Lazarowski ER, Boucher RC, Harden TK (2000) Constitutive release of ATP and evidence for major contribution of ecto-nucleotide pyrophosphatase and nucleoside diphosphokinase to extracellular nucleotide concentrations. *J. Biol. Chem*. 275, 31061–31068.

18) Lee SC, Vielhauer NS, Leaver EV, Pappone PA. (2005) Differential regulation of Ca(2+) signaling and membrane trafficking by multiple P2 receptors in brown adipocytes. *J Membr Biol*. 207(3),131-42.

19) Llaudet E, Hatz S, Droniou M, Dale N. (2005) Microelectrode biosensor for real-time measurement of ATP in biological tissue. *Anal Chem*. 77, 3267-73.

20) Loomis WH, Namiki S, Ostrom RS, Insel PA, Junger WG. (2003) Hypertonic stress increases T cell interleukin-2 expression through a mechanism that involves ATP release, P2 receptor, and p38 MAPK activation. *J Biol Chem*. 278, 4590-6.

21) Nakamura M, Mie M, Funabashi H, Yamamoto K, Ando J, Kobatake E. (2006) Cell-surface-localized ATP detection with immobilized firefly luciferase. Anal Biochem. 352(1), 61-7.

22) Neeley, WE (1972) Simple automated determination of serum or plasma glucose by a hexokinase-glucose-6-phosphate dehydrogenase method. *Clin Chem.* 18, 509-15.

23) North RA, Verkhratsky A. (2006) Purinergic transmission in the central nervous system. *Pflugers Arch*. 452, 479-85.

24) Olson L, Alund M, Norberg KA. (1976) Fluorescence-microscopical demonstration

of a population of gastro-intestinal nerve fibres with a selective affinity for quinacrine. *Cell Tissue Res*. 171(4), 407-23.

25) Ostrom RS, Gregorian C, Insel PA. (2000) Cellular release of and response to ATP as key determinants of the set-point of signal transduction pathways. *J Biol Chem.* 275(16), 11735-9.

26) Ostrom RS, Gregorian C, Drenan RM, Gabot K, Rana BK, Insel PA. (2001) Key role for constitutive cyclooxygenase-2 of MDCK cells in basal signaling and response to released ATP. *Am J Physiol Cell Physiol*. 281(2):C524-31.

27) Pellegatti P, Falzoni S, Pinton P, Rizzuto R, Di Virgilio F. (2005) A novel recombinant plasma membrane-targeted luciferase reveals a new pathway for ATP secretion. *Mol Biol Cell*. 16(8), 3659-65.

28) Piston D.W., Knobel S.M. (1999) Real-time analysis of glucose metabolism by microscopy. *Trends Endocrinol. Metab*. 10, 413-4177.

29) Purich DL, Fromm HJ, Rudolph FB. (1973) The hexokinases: kinetic, physical, and regulatory properties. Adv Enzymol Relat Areas Mol Biol. 39, 249-326.

30) Schwiebert EM, Zsembery A. (2003) Extracellular ATP as a signaling molecule for epithelial cells. *Biochim Biophys Acta*. 1615, 7-32.

40) Sorensen CE, Novak I. (2001) Visualization of ATP release in pancreatic acini in response to cholinergic stimulus. Use of fluorescent probes and confocal microscopy. *J Biol Chem*. 276, 32925-32

41) Stout CE, Costantin JL, Naus CC, Charles AC. (2002) Intercellular calcium signaling in astrocytes via ATP release through connexin hemichannels. *J Biol Chem*. 277(12),10482-8.

42) Tsai CS, Chen Q. (1998) Purification and kinetic characterization of hexokinase and glucose-6-phosphate dehydrogenase from Schizosaccharomyces pombe. *Biochem Cell Biol.* 76, 107-13

43) Yegutkin G, Bodin P, Burnstock G. (2000) Effect of shear stress on the release of soluble ecto-enzymes ATPase and 5'-nucleotidase along with endogenous ATP from vascular endothelial cells. *Br J Pharmacol*. 129, 921-6.

44) Yip L, Cheung CW, Corriden R, Chen Y, Insel PA, Junger WG. (2007) Hypertonic stress regulates T-cell function by the opposing actions of extracellular adenosine triphosphate and adenosine. *Shock* 27, 242-250.

45) Zimmermann H. (2000) Extracellular metabolism of ATP and other nucleotides.

References: Chapter 5

1) Weiss SJ. Tissue destruction by neutrophils. *N Engl J Med.* 1989 Feb 9;**320**(6):365-76.

2) Zigmond SH. Ability of polymorphonuclear leukocytes to orient in gradients of chemotactic factors. *J Cell Biol.* 1977 Nov;**75**(2 Pt 1):606-16.

3) Ridley AJ, Schwartz MA, Burridge K, Firtel RA, Ginsberg MH, Borisy G, Parsons JT, Horwitz AR. Cell migration: integrating signals from front to back. *Science.* 2003 Dec 5;**302**(5651):1704-9.

4) Van Haastert PJ, Devreotes PN. Chemotaxis: signalling the wayforward. *Nat Rev Mol Cell Biol.* 2004 Aug;**5**(8):626-34.

5) Bodin P, Burnstock G. Purinergic signalling: ATP release. Neurochem Res. 2001 Sep;**26**(8-9):959-69.

6) Yegutkin G, Bodin P, Burnstock G. Effect of shear stress on the release of soluble ecto-enzymes ATPase and 5'-nucleotidase along with endogenous ATP from vascular endothelial cells. *Br J Pharmacol.* 2000 Mar;**129**(5):921-6.

7) Zimmermann H. Extracellular metabolism of ATP and other nucleotides. Naunyn Schmiedebergs Arch Pharmacol. 2000 Nov;**362**(4-5):299-309.

8) Fredholm BB. Purines and neutrophil leukocytes. *Gen Pharmacol.* 1997 Mar;**28**(3):345-50.

9) Chen Y, Shukla A, Namiki S, Insel PA, Junger WG. A putative osmoreceptor system that controls neutrophil function through the release of ATP, its conversion to adenosine, and activation of A2 adenosine and P2 receptors. *J Leukoc Biol.* 2004 Jul;**76**(1):245-53. Epub 2004 Apr 23.

10) Burnstock G, Knight GE. Cellular distribution and functions of P2 receptor subtypes in different systems. *Int Rev Cytol.* 2004;**240**:31-304.

11) Fredholm BB, IJzerman AP, Jacobson KA, Klotz KN, Linden J. International Union of Pharmacology. XXV. Nomenclature and classification of adenosine receptors. *Pharmacol Rev.* 2001 Dec;**53**(4):527-52.

12) Zhang Y, Palmblad J, Fredholm BB. Biphasic effect of ATP on neutrophil functions mediated by P2U and adenosine A2A receptors. *Biochem Pharmacol.* 1996 Apr

12;**51**(7):957-65.

13) Hauert AB, Martinelli S, Marone C, Niggli V. Differentiated HL-60 cells are a valid model system for the analysis of human neutrophil migration and chemotaxis. *Int J Biochem Cell Biol.* 2002 Jul;**34**(7):838-54.

14) Servant G, Weiner OD, Herzmark P, Balla T, Sedat JW, Bourne HR. Polarization of chemoattractant receptor signaling during neutrophil chemotaxis. *Science.* 2000 Feb 11;**287**(5455):1037-40.

15) Downey GP. Mechanisms of leukocyte motility and chemotaxis. *Curr Opin Immunol.* 1994 Feb;**6**(1):113-24.

16) Seo JK, Choi SY, Kim Y, Baek SH, Kim KT, Chae CB, Lambeth JD, Suh PG, Ryu SH. A peptide with unique receptor specificity: stimulation of phosphoinositide hydrolysis and induction of superoxide generation in human neutrophils. *J Immunol.* 1997 Feb 15;**158**(4):1895-901.

17) la Sala A, Ferrari D, Di Virgilio F, Idzko M, Norgauer J, Girolomoni G. Alerting and tuning the immune response by extracellular nucleotides. *J Leukoc Biol.* 2003 Mar;**73**(3):339-43.

18) Knight D, Zheng X, Rocchini C, Jacobson M, Bai T, Walker B. Adenosine A3 receptor stimulation inhibits migration of human eosinophils. *J Leukoc Biol.* 1997 Oct;**62**(4):465-8.

19) Walker BA, Jacobson MA, Knight DA, Salvatore CA, Weir T, Zhou D, Bai TR. Adenosine A3 receptor expression and function in eosinophils. *Am J Respir Cell Mol Biol.* 1997 May;**16**(5):531-7.

20) Kimmel AR, Firtel RA. Breaking symmetries: regulation of Dictyostelium development through chemoattractant and morphogen signal-response. *Curr Opin Genet Dev.* 2004 Oct;**14**(5):540-9.

21) Ridley AJ, Schwartz MA, Burridge K, Firtel RA, Ginsberg MH, Borisy G, Parsons JT, Horwitz AR. Cell migration: integrating signals from front to back. *Science.* 2003 Dec 5;**302**(5651):1704-9.

22) Maeda M, Lu S, Shaulsky G, Miyazaki Y, Kuwayama H, Tanaka Y, Kuspa A, Loomis WF. Periodic signaling controlled by an oscillatory circuit that includes protein kinases ERK2 and PKA. *Science.* 2004 May 7;**304**(5672):875-8.

23) Junger WG, Hoyt DB, Davis RE, Herdon-Remelius C, Namiki S, Junger H, Loomis W, Altman A. Hypertonicity regulates the function of human neutrophils by modulating chemoattractant receptor signaling and activating mitogen-activated protein kinase p38. *J Clin Invest.* 1998 Jun 15;**101**(12):2768-79.

24) Hestdal K, Ruscetti FW, Ihle JN, Jacobsen SE, Dubois CM, Kopp WC, Longo DL, Keller JR. Characterization and regulation of RB6-8C5 antigen expression on murine bone marrow cells. *J Immunol.* 1991 Jul 1;**147**(1):22-8.

25) Wang L, Karlsson L, Moses S, Hultgårdh-Nilsson A, Andersson M, Borna C, Gudbjartsson T, Jern S, Erlinge D. P2 receptor expression profiles in human vascular smooth muscle and endothelial cells. *J Cardiovasc Pharmacol.* 2002 Dec;**40**(6):841-53.

References: Chapter 6

1) Burnstock, G. (2006) Purinergic signalling. *Br. J Pharmacol*. **147** (Suppl 1), S172-81.

2) North RA, Verkhratsky A. (2006) Purinergic transmission in the central nervous system. *Pflugers Arch*. **452**, 479-85.

3) Schwiebert EM, Zsembery A. (2003) Extracellular ATP as a signaling molecule for epithelial cells. *Biochim Biophys Acta*. **1615**, 7-32.

4) Fredholm BB. (1997) Purines and neutrophil leukocytes. *Gen Pharmacol*. **28**, 345-50.

5) Eltzschig HK, Weissmüller T, Mager A, Eckle T. (2006) Nucleotide metabolism and cell-cell interactions. *Methods Mol Biol*. **341**, 73-87.

6) Zimmermann H. (2006) Ectonucleotidases in the nervous system. *Novartis Found Symp*. **276**, 113-28.

7) Lazarowski ER, Boucher RC, Harden TK (2000) Constitutive release of ATP and evidence for major contribution of ecto-nucleotide pyrophosphatase and nucleoside diphosphokinase to extracellular nucleotide concentrations. J. Biol. Chem. **275**, 31061–31068.

8) Chen, Y., Corriden, R., Inoue, I., Yip, L., Hashiguchi, N., Zinkernagel, A., Nizet, V., Insel, P.A., Junger, W. (2006) ATP Release Guides Neutrophil Chemotaxis via P2Y2 and A3 Receptors. *Science* **314**, 1792-1795.

9) Chen Y, Shukla A, Namiki S, Insel PA, Junger WG. (2004) A putative osmoreceptor system that controls neutrophil function through the release of ATP, its conversion to adenosine, and activation of A2 adenosine and P2 receptors. *J Leukoc Biol*. **76**, 245-53.

10) Zimmermann H. (2000) Ecto-nucleotidases. *Handbook of experimental pharmacology*. Abbracchio MP, Williams M. Springer, Berlin Heidelberg New York, 209-250.

11) Goding JW, Grobben B, Slegers H. (2003) Physiological and pathophysiological functions of the ecto-nucleotide pyrophosphatase/phosphodiesterase family. *Biochim Biophys Acta*. **1638**, 1-19.

12) Hunsucker SA, Mitchell BS, Spychala J. (2005) The 5'-nucleotidases as regulators of nucleotide and drug metabolism. *Pharmacol Ther*. **107**, 1-30.

13) Junger WG, Hoyt D, Davis RE, Herdon-Remelius C, Namiki S, Junger H, Loomis W, Altman A (1998) Hypertonicity Regulates the Function of Human Neutrophils by Modulating Chemoattractant Receptor Signaling and Activating Mitogen-activated Protein Kinase p38. *J. Clin. Invest.* **101**, 2768-2779.

14) Hohenwallner W, Wimmer E. (1973) The Malachite green micromethod for the determination of inorganic phosphate. *Clin Chim Acta*. **45**, 169-75.

15) Bodin P, Burnstock G. (2001) Purinergic signalling: ATP release. *Neurochem Res*. **26**, 959-69.

16) Yegutkin G, Bodin P, Burnstock G. (2000) Effect of shear stress on the release of soluble ecto-enzymes ATPase and 5'-nucleotidase along with endogenous ATP from vascular endothelial cells. *Br J Pharmacol*. **129**, 921-6.

17) Roman RM, Feranchak AP, Davison AK, Schwiebert EM, Fitz JG. (1999) Evidence for Gd(3+) inhibition of membrane ATP permeability and purinergic signaling. *Am J Physiol*. **277**, G1222-30.

18) Kaczmarek E, Koziak K, Sevigny J, Siegel JB, Anrather J, Beaudoin AR, Bach FH, Robson SC. (1996) Identification and characterization of CD39/vascular ATP diphosphohydrolase. *J Biol Chem*. **271**, 33116-22.

19) Wang TF, Guidotti G. (1998) Golgi localization and functional expression of human uridine diphosphatase. *J Biol Chem*. **273**,11392-9.

20) Heine P, Braun N, Heilbronn A, Zimmermann H. (1999) Functional characterization of rat ecto-ATPase and ecto-ATP diphosphohydrolase after heterologous expression in CHO cells. *Eur J Biochem*. **262**,102-7.

21) Kegel B, Braun N, Heine P, Maliszewski CR, Zimmermann H. (1997) An ecto-ATPase and an ecto-ATP diphosphohydrolase are expressed in rat brain. *Neuropharmacology*. **36**,1189-200.

22) Kirley TL. (1997) Complementary DNA cloning and sequencing of the chicken muscle ecto-ATPase. Homology with the lymphoid cell activation antigen CD39. *J Biol Chem*. **272**(2), 1076-81.

23) Mateo J, Harden TK, Boyer JL. (1999) Functional expression of a cDNA encoding a human ecto-ATPase. *Br J Pharmacol*. **128**, 396-402.

24) Vlajkovic SM, Thorne PR, Housley GD, Muñoz DJ, Kendrick IS. (1998) The pharmacology and kinetics of ecto-nucleotidases in the perilymphatic compartment of the guinea-pig cochlea. *Hear Res*. **117,** 71-80.

25) Crack BE, Pollard CE, Beukers MW, Roberts SM, Hunt SF, Ingall AH, McKechnie KC, IJzerman AP, Leff P. (1995) Pharmacological and biochemical analysis of FPL 67156, a novel, selective inhibitor of ecto-ATPase. *Br J Pharmacol*. **114**, 475-81.

26) Shinozaki T, Watanabe H, Arita S, Chigira M. (1995) Amino acid phosphatase activity of alkaline phosphatase. A possible role of protein phosphatase. *Eur J Biochem*. **227**, 367-71.

27) Fallon MD, Whyte MP, Teitelbaum SL. (1980) Stereospecific inhibition of alkaline phosphatase by L-tetramisole prevents in vitro cartilage calcification. *Lab Invest*. **43**, 489-94.

28) Jin RC, Voetsch B, Loscalzo J. (2005) Endogenous mechanisms of inhibition of platelet function. *Microcirculation* **12**, 247-58.

29) Eltzschig HK, Weissmüller T, Mager A, Eckle T. (2006) Nucleotide metabolism and cell-cell interactions. *Methods Mol Biol*. **341**:73-87.

30) Eltzschig HK, Eckle T, Mager A, Küper N, Karcher C, Weissmüller T, Boengler K, Schulz R, Robson SC, Colgan SP. (2006) ATP release from activated neutrophils occurs via connexin 43 and modulates adenosine-dependent endothelial cell function. *Circ Res*. **99**, 1100-8.

31) Okun DB, Tanaka KR. (1978) Leukocyte alkaline phosphatase. *Am J Hematol*. **4**, 293-9.

References: Chapter 7

1) Zigmond SH. Ability of polymorphonuclear leukocytes to orient in gradients of chemotactic factors. *J Cell Biol.* 1977 Nov;**75**(2 Pt 1):606-16.

2) Elferink JG, VanUffelen BE. The role of cyclic nucleotides in neutrophil migration. *Gen Pharmacol.* 1996 Mar;**27**(2):387-93.

3) Huang YJ, Maruyama Y, Dvoryanchikov G, Pereira E, Chaudhari N, Roper SD. The role of pannexin 1 hemichannels in ATP release and cell-cell communication in mouse taste buds. *Proc Natl Acad Sci U S A.* 2007 Apr 10;**104**(15):6436-41.

4) Silverman W, Locovei S, Dahl GP. PROBENECID, A GOUT REMEDY, INHIBITS PANNEXIN 1 CHANNELS. *Am J Physiol Cell Physiol.* 2008 Jul 2. [Epub ahead of print]

5) Leite DF, Echevarria-Lima J, Ferreira SC, Calixto JB, Rumjanek VM. ABCC transporter inhibition reduces zymosan-induced peritonitis. *J Leukoc Biol.* 2007 Sep;**82**(3):630-7.

6) Schwiebert EM, Zsembery A. Extracellular ATP as a signaling molecule for epithelial cells. *Biochim Biophys Acta.* 2003 Sep 2;**1615**(1-2):7-32.

7) Boudreault F, Grygorczyk R. Cell swelling-induced ATP release and gadolinium-sensitive channels. *Am J Physiol Cell Physiol.* 2002 Jan;**282**(1):C219-26.